National Défense
Defence nationale

# THEORETICAL ASSESSMENT OF A NON-DESTRUCTIVE ETHANE GAS TEST FOR PRODUCTION CONTROL OF MILITARY CANISTERS (U)

by

**Shankar B. Narayan and Brain H. Harrison**







**DEFENCE RESEARCH ESTABLISHMENT OTTAWA**
REPORT NO. 1231

Canada



January 1994
Ottawa

National Defence / Défense nationale

# THEORETICAL ASSESSMENT OF A NON-DESTRUCTIVE ETHANE GAS TEST FOR PRODUCTION CONTROL OF MILITARY CANISTERS (U)

by

**Brain H. Harrison**
*Protective Sciences Division*

and

**Shankar B. Narayan**
*Adsorption Technology Consultant*
*Kanata, Ontario*



**DEFENCE RESEARCH ESTABLISHMENT OTTAWA**
REPORT N0. 1231

PCN
0511B

January 1994
Ottawa

## ABSTRACT

A non-destructive vapour test, involving an ethane pulse challenge, that measures the integrity of the activated carbon bed in military canisters is presently under development at the Defence Research Establishment Ottawa. The effectiveness of the test has been theoretically assessed in this report by modelling the effect of the presence of defects in the carbon bed on its performance. The model has been modified to successfully predict the adsorption behaviour of a dry ethane pulse- or a dry n-octane step-challenge on uneven, non-uniform or short beds. It has been found that the behaviour for the non-uniform beds is different from uneven beds and that care must be taken in selecting the breakthrough concentration for the ethane test. Whilst the sensitivity of the ethane pulse test to identify the defects is not as good as the n-octane step test, the time required for the ethane test is much shorter. It has been shown that this reduced sensitivity is more than compensated for by the ability to test 100% of the canisters with the ethane pulse challenge test.



## RESUME

Un test de vapeur non-destructif, qui fait intervenir le challenge de l'impulsion de l'éthane, qui mesure l'integrité du lit du charbon de bois activé dans les cartouches militaire est présentement en développement à la Division de la Protection des Sciences. L'efficacité du test a été théoriquement évalué dans ce rapport en modellant l'influence de la présence de défaults dans le lit du charbon sur ses performances. Le model a été modifié de façon à prédire avec succès le comportement de l'adsorption de l'éthane sec ou du n-octane sec lors du challenge sur les lits irréguliers, inégaux ou de peu de durée. Il a été trouvé que le comportement pour les lits irréguliers diffère des lits inégaux et que le plus grand soin doit être apporté pour la sélection de la percée de concentration pour le test d'éthane. Quoique la sensitivité du test d'éthane pour identifier les défaults ne soit pas aussi bon que le test avec le n-octane, il a été montré que la perte de sensitivité est plus que compensée par l'habilité a tester 100% les cartouches avec le test de l'impulsion de l'éthane.

## EXECUTIVE SUMMARY

In the manufacture of military canisters it would be extremely valuable to have a non-destructive gas test that can be used on every canister to measure the performance of the charcoal bed against vapours and assure its integrity. A non-destructive gas test employing an ethane pulse has been proposed for this quality control test. The purpose of this report is to establish whether the new non-destructive gas test can identify defects in the charcoal bed and is as sensitive as the normal gas tests that are employed but are destructive in nature. The analysis showed that whilst the sensitivity of the ethane pulse test to identify the defects is not as good as the destructive test, the reduced sensitivity is more than compensated for by the ability to test every canister.

TABLE OF CONTENTS

## 1.0 BACKGROUND

During the manufacture of both the C1 and C2 canisters, the protection against both aerosols and vapours had to be assured. Every canister was therefore challenged with a DOP aerosol and its filtration efficiency measured to estimate the ability of the canister to protect against aerosols. The canisters, which did not meet the required standards of filtration efficiency, were rejected. For protection against the vapours, a test, that measured the integrity of the activated carbon bed, was used. The test involved challenging the canister continuously with air containing a certain concentration of a gas such as phosgene or dimethyl-methylphosphonate (DMMP) and measuring the time until the effluent concentration of the gas reached a specific value. This time is called the "breaktime" of the gas and such a test is called a "step" or a "constant" challenge test. Since this test is destructive in nature (i.e. the canister cannot be reused after being contaminated with phosgene or DMMP), only a small number of canisters, randomly selected from the whole lot of canisters, are tested. It is assumed that the selected canisters are the true representatives of the whole lot of canisters being manufactured. However, because only a small number of canisters are tested with vapours, it is possible for defective canisters to unknowingly enter service. The above tests ensure that every canister, which enters the service, will provide protection against the toxic aerosols but the same guarantee cannot be provided for protection against the vapours.

Recently, effort at the Defence Research Establishment Ottawa has been devoted to finding a non-destructive vapour test that can be used on every canister during its manufacture to measure its performance for protecting against vapours. The research has identified a gas test, which involves challenging the canister with a pulse of dry ethane and measuring its concentration at the exit of the canister. The time until the effluent from the canister reaches a certain concentration is termed the "ethane gas time". Follow-on activities have resulted in the development of test equipment that can be used on the production line to measure ethane gas times. Whilst this equipment has been used to provide qualitative data during the development of the new high performance plastic C7 canister, sufficient data were not available to make direct comparisons with the phosgene or DMMP 'breaktimes' for defective canisters.

In order to provide a lot more basic information on the validity of the ethane gas times for detecting defective canisters, a theoretical study was undertaken, using a recently developed simulation model. The objectives were to determine how the defects, that are normally encountered during the manufacture of the canisters, would affect the ethane gas times; and whether the ethane gas test is as sensitive as the other gas tests particularly considering that the temperature at which the test is carried out

as phosgene or DMMP) than to the boiling point of ethane. For simplicity, in this report, n-octane has been used as the adsorbate vapour to simulate the adsorption behaviour of DMMP. It should be noted that the tests involving ethane and n-octane are different because in the case of ethane a short pulse of dry ethane is introduced into the canister and the time until ethane elutes from the bed is measured. In the case of the test involving n-octane, the canister is challenged with a constant concentration of n-octane and the time until n-octane saturates the bed and elutes from the canister is measured.

The present report has been divided into three main sections. The first section describes the model used to simulate the adsorption behaviour of ethane and presents the comparison between the simulation results and the experimental data for the adsorption behaviour of ethane on the C2 canisters filled with ASC carbon. The second section deals with different types of production problems such as uneven bed, non-uniform packing and insufficient amount of the activated carbon in the bed. The effect of the presence of these defects on the concentration responses of the ethane and n-octane challenges to the ASC carbon-filled C2 canisters has been modelled and the results have also been analyzed in the second section. The remaining part of the report discusses the results from the first two sections to calculate the probability of detecting faulty canisters by either of the two test methods; and makes recommendations for further studies.

## 2.0 THEORETICAL CONSIDERATIONS

The theoretical assessment of the non-destructive ethane gas test was carried out by prediction of the performance of the canisters when subjected to a pulse of dry ethane. In order to theoretically predict the response of the canisters a simple model, based on the mass and heat balance equations, was developed **[1]**. The model assumed plug flow of the carrier gas, pseudo-equilibrium at the adsorption site and a linearized rate equation to represent the mass transfer of the adsorbate from the bulk gas phase to the adsorption site. The adsorption equilibrium for the organic adsorbate-activated carbon system was represented by the Dubinin-Radushkevich (D-R) **[2]** equation, given below.

$$n^*_o = w_o \rho_o Exp\left[-\frac{BT^2}{\beta_o} Log^2\left(\frac{C_{so}}{C_o}\right)\right] \qquad (1)$$

where $n^*_o$, in g/g, and $c_o$, in g/cm$^3$, represent the concentrations of the adsorbate in the adsorbed and the gas phases respectively. $w_o$ and B represent the micropore volume, in cm$^3$/g, and the structural parameter of the activated carbon in $^\circ K^{-2}$ respectively. $\rho_o$ and $\beta_o$ represent the liquid density in g/cm$^3$ and the affinity coefficient of the adsorbate respectively. $c_{so}$ represents the concentration of

the adsorbate, in $g/cm^3$, corresponding to its saturation vapour pressure at the temperature T, in °K.

The overall mass transfer coefficient, $k_{co}$, in $s^{-1}$, of the adsorbate was the only adjustable parameter in the solution of the model equations for a given organic adsorbate-activated carbon system. The validity of the model and its solution was confirmed by successfully comparing the experimental and simulation results. The experimental data, in terms of the concentration and the temperature of the adsorbate in the gas phase at the exit of the canister, were obtained by DND for a range of operating variables and system parameters. A parametric sensitivity analysis was also carried out to study the effect of the operating variables and the parameters of the D-R equation on the breakthrough behaviour of some organic adsorbates through the activated carbon-filled canisters.

The same model has been used to predict the response of the ASC carbon-filled C2 canisters, subjected to a pulse of dry ethane. In order to calculate the parameters $w_o$ and B of the ASC carbon, the adsorption isotherm for the dry ethane-ASC carbon system was measured experimentally at 298 °K. The experimental data points were converted into the coordinates of the D-R plot [$Ln(n^*_o)$ and $Log^2(c_{so}/c_o)$] and a linear regression analysis was carried out to calculate the values of the parameters which provide the best fit.

The values of $w_o$ and B can be calculated from the slope and the intercept of the D-R plot only if the values of $\rho_o$ and $\beta_o$ for ethane are known. The liquid density of ethane at 298 °K was calculated, from the Rackett's equation **[3]**, as 0.31284 $g/cm^3$. The value of $\beta_o$ for ethane was calculated as 0.5412 by taking the ratio of the parachor values of ethane and benzene, which was taken as the reference adsorbate. The values of $w_o$ and B, calculated from the slope and the intercept of the D-R plot, are given in Table 1, which also shows the values of the same parameters for BPL, ASC/3T and PPC (Penetrant Protective Carbon recently developed at DREO) carbons.

**TABLE 1:** "$w_o$" and "B" Values for Different Carbons

| Carbon | $w_o$ ($cm^3/g$) | B ($°K^{-2}$) |
|---|---|---|
| BPL | 0.6490 | 7.67E-7 |
| PPC | 0.5789 | 1.18E-6 |
| ASC | 0.4597 | 7.37E-7 |
| ASC/3T | 0.4054 | 8.41E-7 |

The adsorption isotherm, calculated from the D-R equation, for the dry ethane-ASC carbon system is compared with the experimental

data in Fig. 1. It is obvious that the D-R equation represents the adsorption equilibrium for the dry ethane-ASC carbon system satisfactorily in the concentration range of experimental measurements of the isotherm.

## 3.0 IDEAL CASE

### 3.1 COMPARISON BETWEEN THE EXPERIMENTAL AND SIMULATION RESULTS

The first step was to compare the pulse response, in terms of the concentration of ethane in the gas phase at the exit of the canister, predicted by the simulation with the experimental data. The pulse response data for dry ethane through the C2 canisters filled with the ASC-carbon was measured by Racal Filter Technologies Limited (RFTL). It is important to point out that the challenge concentration was measured experimentally as the maximum value (2.1E-6 $g/cm^3$) of a pulse of dry ethane introduced in the chuck from a sample loop of 2.0 $cm^3$ volume. In the simulation, the challenge concentration to the canister was considered to be the concentration response from the chuck, assumed to be a perfectly-mixed vessel, subjected to a pulse of dry ethane of concentration 2.1E-06 $g/cm^3$. The simulation runs were carried out with the set of values of the operating variables and system parameters given in the Table 2. The value of the mass transfer coefficient, $k_{co}$, for ethane was selected based on the comparison between the experimental and simulation results for the breakthrough of ethane through a BPL carbon-filled C2 canister.

**TABLE 2:** Operating Variables and Parameters for Simulation

| Variable | Symbol | Unit | Value |
|---|---|---|---|
| Structural Parameter | B | $°K^{-2}$ | 7.3664E-07 |
| Micropore Volume | $w_o$ | $cm^3/g$ | 4.5966E-07 |
| Apparent Density | $\rho_{app}$ | $g/cm^3$ | 8.4377E-01 |
| Bed Diameter | $D_{ia}$ | cm | 1.0500E+01 |
| Bed Volume | V | $cm^3$ | 1.7000E+02 |
| Bed Bulk Density | $\rho_b$ | $g/cm^3$ | 5.8740E-01 |
| Chuck Volume | $V_{ch}$ | $cm^3$ | 6.9000E+02 |
| Temperature | T | °K | 2.9800E+02 |
| Flow Rate of Air | q | $cm^3/s$ | 5.0000E+02 |
| Pre-Challenge Conc. | $O_{cci}$ | $g/cm^3$ | 0.0000E-00 |
| Challenge Concentration | $O_{cc}$ | $g/cm^3$ | 2.1000E-06 |
| Affinity Coefficient | $\beta_o$ | - | 5.4120E-01 |
| Mass Transfer Coeff. | $k_{co}$ | $s^{-1}$ | 2.5000E-01 |
| Density of Ethane | $\rho_o$ | $g/cm^3$ | 3.1284E-01 |
| Heat of Adsorption | $Q_{ads}$ | cal/mol | 2.3766E-03 |
| Heat of Immersion | $Q_{imm}$ | cal/g(C) | 8.4776E-00 |

The comparison between the simulation and the experimental results, in terms of the concentration of ethane in the exit gas stream, is shown in the Fig. 2. The shapes of the two curves are similar till about 1.5 minutes though they are offset in time. The peak maxima of the two curves, though different in magnitudes, are reached around the same time. The complete elution of the predicted peak occurs very fast whereas the experimental response curve shows a long tail after reaching its maximum. The probable causes for the difference between the simulation and the experimental results are explained below.

## 3.2 REASONS FOR THE DIFFERENCE BETWEEN THE EXPERIMENTAL AND SIMULATION RESULTS

### 3.2.1 Concentration Measurement System

#### 3.2.1.1 'Contamination' of the Detection System

The signal from the FID detector, used by RFTL to measure the concentration of ethane, was found to take a long time to return to the baseline (i.e. zero concentration). This was observed even in the case of an experiment, without a canister, wherein no adsorption of ethane was occurring. This indicated that the detection system was getting 'contaminated' even at fairly low concentrations of ethane, which were measured in the presence of the ASC carbon-filled C2 canisters. Considering the facts that the shapes of the initial portions of the simulation and experimental pulse response curves are similar and only the experimental response curve shows a long tail, the slow recovery of the detector can be considered a primary reason for the differences between the simulation and the experimental results.

#### 3.2.1.2 Discrepancy Between the Amount Injected and the Amount Eluted

As mentioned earlier, ethane from a sampling loop of volume 2.0 $cm^3$ was introduced in the carrier gas stream. Assuming that the pressure of ethane in the sampling loop was 101.303 kPa (1.0 atm) at 298 °K, the total amount of ethane injected was theoretically calculated, from ideal gas law, to be 2.46 mg. The total amount of ethane eluted from the system was determined by multiplying the volumetric flow rate of the carrier gas with the calculated area under the experimentally measured concentration response curve of ethane. The amount of ethane eluted from the system was calculated as 1.526 mg.

The apparent 'contamination' of the detector and the discrepancy between the amount of ethane injected into and that eluted from the system indicate a strong possibility that the

concentration measurement system is probably not very accurate and reliable.

### 3.2.2 Input Signal

In the equipment developed at RFTL the sharp concentration pulse of ethane is not injected directly into the canister, instead the pulse is introduced into a large volume (chuck) before it enters the canister as shown schematically in Fig.3. Therefore the input concentration signal to the canister has to be considered as the concentration response from the chuck. Like any other vessel, the concentration response from the chuck depends on the nature of flow distribution within the chuck and its volume for a fixed flow rate of the carrier gas.

In this study, the chuck has been assumed to be a perfectly-mixed vessel, subjected to a pulse challenge of dry ethane. For simulation purposes, the predicted concentration response from the chuck, assuming perfect mixing, to an ideal pulse challenge of ethane has been used as the input concentration challenge to the canister. If this assumption is not valid then the actual concentration challenge to the canister will be different than the challenge signal used in the simulation. This could cause differences between the simulation results and the experimental data for the adsorption behaviour of ethane.

In order to characterize the effect of the chuck on the shape of the pulse, an experiment was carried out in which a pulse challenge of ethane was introduced into the chuck, which did not contain any canister. The concentration of ethane at the exit end of the chuck was measured. Based on the empty chuck volume of 1140 $cm^3$ and a peak concentration of 1.107E-6 $g/cm^3$ (as reported by RFTL), the concentration of ethane at the exit of the chuck was predicted assuming a perfectly-mixed chuck. The experimental data are compared with the theoretically predicted response from the chuck in Fig.4. It is important to note that the experimental measurement of the concentration was stopped after a certain time when the concentration was still greater than zero. Therefore the predicted response curve can be compared with only the limited experimental data. Based on a fairly good match between the predicted and the limited experimental response curves, as shown in Fig.4, the empty chuck can be considered a perfectly-mixed vessel for the volumetric flow rate used in this study.

Though the empty chuck can be considered a perfectly-mixed vessel the concentration response of the chuck is also dependent on its volume, which was not measured accurately. A series of runs were carried out to study the effect of the chuck volume on the concentration response of the ASC carbon-filled canister keeping the challenge concentration constant. As shown in Fig.5, the effect of the chuck volume is not significant when varied between

690 and 740 $cm^3$ assuming that the volume of the canister is approximately 450 $cm^3$. However, it can be used as a variable to match the simulation results with the experimental pulse response data of ethane as shown in Fig.5 when a chuck volume of 290 $cm^3$ was used in the model.

The experimentally measured concentration signal includes the concentration response from the canister and the rest of the system. In order to compare the simulation results with the experimental data it is important to subtract the concentration response of the rest of the system from the measured concentration signal. This is particularly important because the overall breakthrough time of ethane is fairly small (in the range of 20-30 s). Experiments, run without the presence of the canister, provided breakthrough times of 6-7 s indicating thereby that the effect of the rest of the system on the concentration response of ethane cannot be neglected.

### 3.2.3 Suitability of the D-R Equation

Though the D-R equation seems to represent the overall adsorption equilibrium for the ethane-ASC carbon system fairly well it is important to check its suitability in the concentration range of the experiments. The lowest pressure, at which the adsorption equilibrium for this system was measured, was 2.76 mm Hg whereas the concentration of 2.1E-6 $g/cm^3$ for ethane at 298 °K corresponds to a pressure of 1.3 mm Hg.

The shape of the initial part of the experimental pulse response curve indicates a constant-pattern behaviour **[4]**, which is usually exhibited by an adsorbate-adsorbent system having an isotherm of the Type I. In contrast, the initial part of the predicted response curve indicates a continuously expanding wave (called proportionate-pattern **[4]**). This type of behaviour is usually exhibited by an adsorbate-adsorbent system having an adsorption isotherm of the Type II. However, as shown in Fig.1, the D-R equation indicates an overall isotherm of the Type I for the ethane-ASC carbon system. This implied that the adsorption isotherm predicted by the D-R equation changed from one of Type II to one of Type I at concentrations of ethane in the gas phase at which the adsorption equilibrium data were measured. To theoretically verify it, the slopes of the adsorption isotherm predicted by the D-R equation were calculated at different concentrations of ethane in the gas phase. A plot of the slope of the adsorption isotherm for the ethane-ASC carbon system predicted by the D-R equation in the concentration range 1.0E-8-5.0E-7 $g/cm^3$ is shown in Fig.6. The change in the direction of the slope of

the adsorption isotherm in Fig.6 indicates a change in the adsorption isotherm behaviour from Type II to Type I. Since the shape of the predicted response curve is significantly dependent on the shape of the adsorption isotherm it is important to verify the applicability of the D-R equation to predict the adsorption equilibrium for the ethane-ASC carbon system for the concentration range in which the experiments have been carried out.

### 3.2.4 Presence of Other Adsorbates

The partial pressure of ethane in the carrier gas stream is so small that the effect of the presence of other adsorbates such as methane (an impurity in the ethane sample), $N_2$ and $O_2$ (from the air used as the carrier gas) on the adsorption of ethane can not be considered negligible unless verified experimentally.

## 3.3 DISCUSSION OF THE COMPARISON BETWEEN THE EXPERIMENTAL AND SIMULATION RESULTS

From the above discussion of the reasons, which explain the difference between the simulation and experimental pulse response data, it can be concluded that the accuracy and reliability of the concentration measurement system needs significant improvement; and it is important to characterize the response of the rest of the system in terms of the flow distribution and the dead time. Moreover the suitability of the D-R equation at such low concentrations of ethane, and the effect of the presence of other adsorbates also need to be studied. Since the time needed for the 'recovery' of the detection system is fairly long, it was considered important to try and match the simulation results with the experimental data in the initial part of the breakthrough curve of ethane.

The parametric sensitivity analysis in the earlier work **[5]** had shown that the breakthrough behaviour of the low molecular weight organic adsorbates is significantly affected by the values of $\beta_o$ and $k_{co}$ used in the simulation. Wood **[6]** has compiled a list of sources of adsorption isotherm data for various adsorbates and calculated the values of their affinity coefficients which provide the best fit to the experimental data. The values of $\beta_o$ for ethane range from 0.56 to 0.67 in his review paper. The predicted breakthrough behaviour for a number of values of $\beta_o$ (between 0.5 and 0.575) and $k_{co}$ (between 0.1 and 2.5 $s^{-1}$) is shown in Fig.7. The comparison between the experimental and the simulation results in the initial part of the breakthrough curve for dry ethane-dry ASC carbon-filled C2 canister is shown in Fig.8. It is obvious that the initial part of the experimental breakthrough curve for dry ethane pulse challenge can be successfully matched with the

simulation results when the values of $\beta_o$ and $k_{co}$ are 0.56 and 2.5 $s^{-1}$ respectively.

The simulation results, based on the use of the D-R equation, show that the slope of the breakthrough curve increases with time to a maximum at around 150 s before it starts reducing as shown in the Fig.9. Similar trend is shown by the experimental data also though the slope reaches its maximum value much earlier. In principle, the threshold value, in terms of the concentration in the gas phase, of the breakthrough point should be the one at which the slope of the breakthrough curve is maximum.

Keeping in mind the limitations of the experimental system, it can be concluded that the simulation provides a good representation of the experimental data. The simulation can therefore be used to predict the effect of the presence of defects in the activated carbon bed on the concentration response to the ethane pulse or n-octane step challenge tests.

## 4.0 PRODUCTION PROBLEMS

### 4.1 UNEVEN BED

One of the probable causes of variability in the breakthrough times of dry ethane, injected as a pulse challenge, through the activated carbon filters is the "non-uniformity" of the bed. This can be caused by the "unevenness" of the bed generated due to improper filling of the activated carbon particles in the canister. The non-uniformity of the bed due to its improper filling, as shown schematically in Fig.10, will result in the non-uniform distribution of the flow of the carrier gas through the activated carbon bed. This will result in variation of the breakthrough time and the adsorption behaviour of dry ethane through different parts of the bed. The overall concentration response of the bed will be the sum of the concentration responses in each section multiplied by the ratio of the volumetric flow rate through that section to the total flow rate through the bed. Because of the non-uniformity of flow of the carrier gas through different sections of the bed the overall concentration response from such an uneven bed will be different from the response from an even, uniform bed.

With the existing computer system, to facilitate easy simulation of the pulse response from an uneven bed, the activated carbon bed was divided in three sections of different cross-sectional areas and bed depths. As shown schematically in Fig.11, the overall radius of the C2 canister was divided in three equal parts. This divided the total cross-sectional area of the bed, corresponding to an internal diameter of 10.5 cm, in three sections I, II and III of cross-sectional areas 48.106, 28.263 and 9.621 $cm^2$ respectively. The length of each section was assumed to vary from the section next to it by a step of length $\Delta L$. Keeping the overall

diameter (10.5 cm) and the total volume of the C2 canister (170 $cm^3$) fixed, the lengths of each section were calculated by the procedure outlined in Appendix A. For values of $\Delta L$ ranging between 0 and 0.25 cm the calculated values of the length and volume of each section are given in Table 3.

**TABLE 3:** Length and Volume of Sections I, II and III

| $\Delta L$ (cm) | $L_1$ (cm) | $L_2$ (cm) | $L_3$ (cm) | $V_1$ ($cm^3$) | $V_2$ ($cm^3$) | $V_3$ ($cm^3$) |
|---|---|---|---|---|---|---|
| 0.00 | 1.963 | 1.963 | 1.963 | 94.4445 | 56.667 | 18.889 |
| 0.05 | 1.908 | 2.008 | 2.108 | 91.772 | 57.949 | 20.279 |
| 0.10 | 1.852 | 2.052 | 2.252 | 89.099 | 59.232 | 21.668 |
| 0.15 | 1.797 | 2.097 | 2.397 | 86.427 | 60.515 | 23.058 |
| 0.20 | 1.741 | 2.141 | 2.541 | 83.754 | 61.798 | 24.448 |
| 0.25 | 1.685 | 2.185 | 2.685 | 81.082 | 63.081 | 25.837 |

In order to calculate the distribution of the superficial velocity and the volumetric flow rate of the carrier gas through each section the following assumptions were made.

a. Ergun's equation **[7]**, which is used to calculate the pressure drop for the axial flow of a fluid through a packed bed, can also be used to calculate the pressure drop for the axial flow of a fluid through an annular packed bed.

b. The contribution of the pressure drop, due to the turbulent flow of the carrier gas, is negligible in comparison to the overall pressure drop across the bed.

c. The parameters such as the bed voidage ($\epsilon$), the particle diameter ($d_p$), the viscosity ($\mu$) and the density ($\rho$) of the carrier gas are the same for each section of the bed.

d. The pressure drop across each section of the bed is the same.

Based on the above assumptions the superficial velocity and the volumetric flow rates through each section were calculated by the procedure described in Appendix A. Keeping the total volumetric flow rate through the C2 canister fixed at 500.0 $cm^3/s$ (30 lpm), the calculated values of the velocities and the flow rates through each section are given in Table 4.

**TABLE 4:** Superficial Velocity and Volumetric Flow Rates through Sections I, II and III

| $\Delta L$ (cm) | $V_{pb1}$ (cm/s) | $V_{pb2}$ (cm/s) | $V_{pb3}$ (cm/s) | $q_{31}$ ($cm^3$/s) | $q_{32}$ ($cm^3$/s) | $q_{33}$ ($cm^3$/s) |
|---|---|---|---|---|---|---|
| 0.00 | 5.774 | 5.774 | 5.774 | 277.778 | 166.667 | 55.556 |
| 0.05 | 5.935 | 5.640 | 5.372 | 285.529 | 162.784 | 51.687 |
| 0.10 | 6.092 | 5.499 | 5.010 | 293.083 | 158.712 | 48.206 |
| 0.15 | 6.246 | 5.352 | 4.682 | 300.467 | 154.484 | 45.049 |
| 0.20 | 6.396 | 5.201 | 4.383 | 307.704 | 150.130 | 42.166 |
| 0.25 | 6.544 | 5.047 | 4.107 | 314.810 | 145.673 | 39.517 |

For each value of $\Delta L$, the superficial velocity of the carrier gas in the section I is greater than its value for an even bed (i.e. when $\Delta L$=0.0 cm). The superficial velocities of the carrier gas in the sections II and III are lower than the value for an even bed as shown in Table 4. As $\Delta L$ increases the superficial velocity and the corresponding volumetric flow rate of the carrier gas in section I increases whereas those in sections II and III decrease.

The model, described in Section "Theoretical Considerations", was modified to incorporate the calculation of the superficial velocity and the pulse response, in terms of the concentration of ethane in the gas phase, at the exit of each section of the bed. The overall concentration response from the bed was then calculated by combining the concentration responses from each section multiplied by the ratio of the volumetric flow rate of the carrier gas through the section to the total volumetric flow rate through the bed.

A single run was carried out with this modified model using $\Delta L$=0.0 cm, which represents an even bed, and the set of values of the operating variables and the system parameters given in Table 2. A run was also carried out with the old model, which assumed a single even bed, using the same set of values of the operating variables and system parameters. The results from the two models are compared in Fig.12. Since the results from the two models are identical, it is concluded that the solution of the model and its implementation on the personal computer for the uneven bed is correct.

The predicted concentration response from each section and the overall bed for three values (namely 0.1, 0.2 and 0.25 cm) of $\Delta L$ are shown in Fig. 13-15 for a challenge concentration of 2.1 E-6

$g/cm^3$ (2100 $mg/m^3$). Since the overall bed has been divided in three sections, of different lengths and cross-sectional areas, subjected to different flow rates of the carrier gas, the response of each section is expected to be different. For a pulse challenge of ethane in the gas phase, three different peaks, corresponding to the responses from the three sections I, II and III, are predicted as shown in Fig. 13-15.

For each value of $\Delta L$, the predicted breakthrough of ethane through the section I occurs before the breakthrough of ethane through the overall bed. This is expected because the superficial velocity of the carrier gas through the section I in an uneven bed is greater than the superficial velocity for an even bed as given in Table 4. The predicted breakthrough of ethane through the sections II and III occur later than the breakthrough of ethane through the overall bed. Secondly the concentration of ethane in the gas phase at the exit of at least one of the sections is always greater than the concentration of ethane in the gas phase at the exit of the overall bed. This is understandable considering that the concentration at the exit of the overall bed is calculated by combining the concentrations and flow rates at the exit of each section.

The predicted effect of the degree of unevenness of the bed is shown in Fig. 16, wherein the concentration of ethane at the exit of the overall bed for different values of $\Delta L$ is plotted along with the predicted response from an even bed ($\Delta L$=0.0 cm). As the degree of unevenness increases the effect of each section on the overall response behaviour also increases as shown by the increased distinctness of the three peaks with increasing $\Delta L$ in Fig. 16. The overall response curves show the same number of peaks as the number of steps in the activated carbon bed. If the length of the bed varies continuously from the edge of the canister to its centre then it is quite likely that the overall response curve will be fairly wide.

The predicted breakthrough times, for the concentration of ethane in the exit gas stream to reach values of 0.05, 0.25, 0.5, 1.0, 5.0 and 20.0 $mg/m^3$, for different values of $\Delta L$ are given in Table 5. As expected the breakthrough time of ethane decreases as the degree of unevenness, as denoted by $\Delta L$, increases. To quantitatively represent the effect of the degree of unevenness, the ratio of the breakthrough time for an uneven bed to its corresponding value for an even bed ($\Delta L$=0.0 cm), for each value of the breakthrough concentration, was calculated. The values of these ratios are also given in Table 5.

After studying the effect of the unevenness of the bed on the concentration response to a pulse challenge of dry ethane to the ASC carbon-filled C2 canister, the next step was to study the effect of the same on the concentration response to a step challenge of dry n-octane. The model, which was used to predict

**TABLE 5:** Predicted Breakthrough Times of Ethane for Different Values of ΔL

| Organic | ΔL (cm) | BTC ($mg/m^3$) | T (min) | $[T/T_{nb}]$ |
|---|---|---|---|---|
| $C_2H_6$ | 0.00 | 0.05 | 0.130 | 1.0000 |
| | | 0.25 | 0.415 | 1.0000 |
| | | 0.50 | 0.620 | 1.0000 |
| | | 1.00 | 0.875 | 1.0000 |
| | | 5.00 | 1.635 | 1.0000 |
| | | 20.0 | 2.505 | 1.0000 |
| | 0.10 | 0.05 | 0.125 | 0.9615 |
| | | 0.25 | 0.405 | 0.9759 |
| | | 0.50 | 0.600 | 0.9677 |
| | | 1.00 | 0.845 | 0.9657 |
| | | 5.00 | 1.570 | 0.9602 |
| | | 20.0 | 2.415 | 0.9641 |
| | 0.20 | 0.05 | 0.120 | 0.9231 |
| | | 0.25 | 0.375 | 0.9036 |
| | | 0.50 | 0.555 | 0.8952 |
| | | 1.00 | 0.780 | 0.8914 |
| | | 5.00 | 1.430 | 0.8746 |
| | | 20.0 | 2.200 | 0.8782 |
| | 0.25 | 0.05 | 0.110 | 0.8461 |
| | | 0.25 | 0.355 | 0.8554 |
| | | 0.50 | 0.530 | 0.8548 |
| | | 1.00 | 0.740 | 0.8457 |
| | | 5.00 | 1.355 | 0.8287 |
| | | 20.0 | 2.075 | 0.8283 |

the concentration response of dry ethane pulse challenge to an uneven bed, was also used to predict the adsorption behaviour of a dry n-octane step challenge to the same bed. The values of the operating variables and the system parameters used in the dry n-octane step challenge studies are given in Table 6.

**TABLE 6:** Operating Variables and Parameters for n-Octane Studies

| Variable | Symbol | Unit | Value |
|---|---|---|---|
| Challenge Concentration | $O_{cc}$ | $g/cm^3$ | 2.1000E-06 |
| Affinity Coefficient | $\beta_o$ | - | 1.7047E+00 |
| Mass Transfer Coeff. | $k_{co}$ | $s^{-1}$ | 7.5000E-04 |
| Density of n-Octane | $\rho_o$ | $g/cm^3$ | 7.0300E-01 |
| Heat of Adsorption | $Q_{ads}$ | cal/mol | 9.9153E+03 |
| Heat of Immersion | $Q_{imm}$ | cal/g(C) | 1.5796E+01 |

The predicted concentration responses from each section and the overall bed for three values (namely 0.1, 0.2 and 0.25cm) of $\Delta L$ are shown in Fig. 17-19. Similar to the adsorption behaviour of dry ethane, for a step challenge in the concentration of n-octane, three step responses, each corresponding to the response from a different section, are predicted by the model. The concentration response of the overall bed also shows three plateaux corresponding to the response of each section as shown in Fig. 17-19. It is important to note that, unlike the concentration responses of dry ethane pulse, the breakthrough of n-octane from the overall bed occurs almost at the same time as the breakthrough of n-octane from the section I.

The predicted effect of the degree of unevenness of the activated carbon bed on the adsorption behaviour of n-octane is shown in Fig. 20. The responses from the overall bed, in terms of the concentration of n-octane in the exit gas stream, for different values of $\Delta L$, denoting the degree of unevenness, are compared with the response from an even bed ($\Delta L$=0.0 cm) in Fig. 20. Similar to the behaviour of dry ethane, the breakthrough time of n-octane decreases as the degree of unevenness of the bed increases. The time required for the concentration of n-octane in the gas phase at the outlet of the bed to reach the final steady state increases as the value of $\Delta L$ increases. The overall response curves show the same number of plateaux as the number of steps in the activated carbon bed. If the length of the bed varies continuously from the edge of the canister to its centre then it is likely that the overall response curve, in terms of the concentration of n-octane in the gas phase, will be quite wide.

The predicted breakthrough times, for the concentration of n-octane in the exit gas stream to reach values of 0.05, 0.25, 0.5, 1.0, 5.0 and 20.0 $mg/m^3$, for different values of $\Delta L$ are given in Table 7. As expected the breakthrough time of n-octane decreases as the degree of unevenness of the bed, as denoted by $\Delta L$, increases. Similar to Table 5, the ratios of breakthrough times for an uneven bed to its value for an even bed are also given in Table 7.

**TABLE 7:** Predicted Breakthrough Times of n-Octane as a Function of $\Delta L$

| Organic | $\Delta L$ (cm) | BTC ($mg/m^3$) | T (min) | $[T/T_o]$ |
|---|---|---|---|---|
| $n\text{-}C_8H_{18}$ | 0.00 | 0.05 | 453 | 1.0000 |
| | | 0.25 | 454 | 1.0000 |
| | | 0.50 | 455 | 1.0000 |
| | | 1.00 | 456 | 1.0000 |
| | | 5.00 | 457 | 1.0000 |
| | | 20.0 | 458 | 1.0000 |
| | 0.10 | 0.05 | 403 | 0.8896 |
| | | 0.25 | 404 | 0.8899 |
| | | 0.50 | 405 | 0.8901 |
| | | 1.00 | 405 | 0.8881 |
| | | 5.00 | 407 | 0.8906 |
| | | 20.0 | 408 | 0.8908 |
| | 0.20 | 0.05 | 359 | 0.7925 |
| | | 0.25 | 360 | 0.7929 |
| | | 0.50 | 360 | 0.7878 |
| | | 1.00 | 360 | 0.7895 |
| | | 5.00 | 362 | 0.7921 |
| | | 20.0 | 363 | 0.7926 |
| | 0.25 | 0.05 | 339 | 0.7483 |
| | | 0.25 | 339 | 0.7467 |
| | | 0.50 | 339 | 0.7450 |
| | | 1.00 | 340.5 | 0.7467 |
| | | 5.00 | 340.5 | 0.7450 |
| | | 20.0 | 342 | 0.7467 |

The next step was to compare the sensitivities of the responses from the ethane pulse challenge test with the n-octane step challenge test as a function of the degree of unevenness of the bed. The ratio of the breakthrough time of ethane for a particular value of $\Delta L$ to the breakthrough time for an even bed is

compared with a corresponding ratio of the breakthrough times for n-octane in Fig. 21. For a specific value of $\Delta L$, the ratio of the breakthrough times for n-octane step challenge remains almost constant in comparison with the variation of the ratio of the breakthrough times for ethane pulse challenge. This can be understood by comparing the response curves from Fig. 13-15 and Fig. 17-19. The concentration of n-octane changes sharply as soon as its breakthrough occurs which means that the breakthrough times of n-octane for different values of its breakthrough concentrations do not change significantly. In contrast the concentration of ethane changes slowly once its breakthrough occurs which means that the breakthrough time of ethane is dependent on its breakthrough concentration.

It is important to note that all the values of the ratios of the breakthrough times for ethane pulse and n-octane step challenges for all values of the breakthrough concentrations are less than 1.0. This means that the breakthrough times of both of these adsorbates are always less than their respective breakthrough times for even beds for any value of the breakthrough concentration irrespective of the degree of unevenness.

## 4.2 CHANNELS OR VOIDS IN THE BED

One of the other probable causes of variability in the breakthrough times of dry ethane through activated carbon filters is the "non-uniformity" of the bed. This can be caused by the presence of sections of different voidages in the bed generated due to improper filling of the activated carbon particles in the canister. The presence of sections of different voidages will result in the channelling or preferential flow of the carrier gas through sections with voidages greater than those in the other sections as shown schematically in Fig. 22. This will result in the variation of the breakthrough times of dry ethane through different sections of the bed. The overall concentration response from the bed is obtained by summing the concentration responses from each section multiplied by the ratio of the volumetric flow rate in that section to the total volumetric flow rate of the carrier gas through the bed. Therefore the overall concentration response will also be affected by the presence of sections of different voidages in the bed.

Keeping in mind the limitation of the computing facility the presence of sections of different voidages in the bed was simulated as an overall bed made up of two sections one of which had a voidage higher than the one obtained by uniform packing of the activated carbon particles in the canister. As shown in Fig. 23 the canister was divided in two sections of different voidages. The voidage of the bed in the section I, $\epsilon_1$, was varied from its normal value (0.3) to 0.4. Keeping the internal diameter of the

overall bed same as that of the C2 canister (=10.5 cm), the voidage of section II was calculated by a mass balance from the total amount of the activated carbon filled in the normal canister and its normal bulk density (Appendix B). The voidage of the section II, $\epsilon_2$, for different values of the diameter, $D_1$, and the voidage, $\epsilon_1$, of the section I were calculated and are shown in Table 8.

**TABLE 8:** $\epsilon_2$ as a Function of $D_1$ and $\epsilon_1$

| $\epsilon_1$ | $D_1$ | $\epsilon_2$ |
|---|---|---|
| 0.35 | 0.00 | 0.30384 |
| | 0.25 | 0.30381 |
| | 0.50 | 0.30373 |
| | 1.00 | 0.30342 |
| | 1.50 | 0.30288 |
| | 2.00 | 0.30210 |
| | 2.50 | 0.30106 |
| 0.40 | 0.00 | 0.30384 |
| | 0.25 | 0.30378 |
| | 0.50 | 0.30362 |
| | 1.00 | 0.30396 |
| | 1.50 | 0.30184 |
| | 2.00 | 0.30022 |
| | 2.50 | 0.29806 |

The superficial velocity and the volumetric flow rates of the carrier gas through sections I and II were calculated based on a procedure similar to the one used for uneven beds (See Appendix B). The results for a total carrier gas flow rate of 500 $cm^3/s$ through the C2 canister (10.5 cm diameter) are given in Table 9.

**TABLE 9:** Superficial Velocity and Flow Rate through Sections I and II

| $\epsilon_1$ | $D_1$ (cm) | $v_{pb1}$ (cm/s) | $v_{pb2}$ (cm/s) | $Q_{pb1}$ ($cm^3/s$) | $Q_{pb2}$ ($cm^3/s$) |
|---|---|---|---|---|---|
| 0.35 | 0.25 | 9.6649 | 5.7721 | 0.4744 | 499.5256 |
| 0.35 | 0.50 | 9.6630 | 5.7655 | 1.8973 | 498.1027 |
| 0.35 | 1.00 | 9.6552 | 5.7388 | 7.5831 | 492.4169 |
| 0.35 | 1.50 | 9.6419 | 5.6938 | 17.0387 | 482.9613 |
| 0.35 | 2.00 | 9.6230 | 5.6294 | 30.2315 | 469.7685 |
| 0.35 | 2.50 | 9.5978 | 5.5446 | 47.1132 | 452.8868 |
| 0.40 | 0.25 | 15.7036 | 5.7687 | 0.7708 | 499.2292 |
| 0.40 | 0.50 | 15.6897 | 5.7518 | 3.0807 | 496.9193 |
| 0.40 | 1.00 | 15.6339 | 5.6841 | 12.2789 | 487.7211 |
| 0.40 | 1.50 | 15.5401 | 5.5709 | 27.4616 | 472.5384 |
| 0.40 | 2.00 | 15.4069 | 5.4117 | 48.4021 | 451.5979 |
| 0.40 | 2.50 | 15.2324 | 5.2059 | 74.7721 | 425.2279 |

For all values of $D_1>0.0$ and $\epsilon_1>0.3$ the superficial velocity of the carrier gas in section I, denoted by $v_{pb1}$ in cm/s, is greater than the superficial velocity in the normal bed with $\epsilon=0.3$. For any fixed value of $D_1$, $v_{pb1}$ increases as $\epsilon_1$ increases because of the decreased flow resistance. It is important to note that though the superficial velocity in section I is greater than its corresponding value in section II, the volumetric flow rate through section I, denoted by $Q_{pb1}$ in $cm^3/s$, is smaller than the flow rate through section II for the selected range of values of $D_1$ and $\epsilon_1$.

The model, described in Section "Theoretical Considerations", was modified to incorporate the calculation of the concentration response, in terms of the concentration of ethane in the gas phase at the exit of each section of the bed. The solution of the model equations in this case was based on the assumption that there is no interaction between the two sections having different voidages. The overall concentration response from the bed was calculated by adding the concentration response from each section multiplied by the ratio of the volumetric flow rate of the carrier gas through that section to the total volumetric flow rate of the carrier gas through the bed.

A number of simulation runs were done to predict the concentration response at the exit of each section as well as the bed, subjected to a pulse challenge of dry ethane in the carrier gas at the inlet. The overall concentration responses at the exit of the bed for three values of $D_1$ (0.5, 1.5 and 2.5 cm) and two values of $\epsilon_1$ (0.35 and 0.4) are shown in Fig. 24-26. The predicted concentration response from the normal, uniform bed (with $\epsilon=0.3$) is also shown in Fig. 24-26 for comparison.

For $D_1$=0.5 cm, the overall concentration profiles of ethane for $\epsilon_1$=0.35 and $\epsilon_1$=0.4 are fairly similar to that of the normal bed though the initial breakthrough profiles are different. The initial parts of the curves, given in Fig. 24, show that the increase in $\epsilon_1$ from 0.3 to 0.35 does not make a noticeable difference in the initial breakthrough behaviour of ethane for $D_1$=0.5 cm. However the increase in $\epsilon_1$ from 0.35 to 0.4 makes a considerable difference in the initial breakthrough behaviour of ethane even at $D_1$=0.5 cm. From Fig. 24 it can be concluded that the effect of increasing $\epsilon_1$ from 0.3 to 0.4 is negligible on the overall concentration response of ethane except in the initial breakthrough period.

As $D_1$ increases the effect of $\epsilon_1$ on the adsorption behaviour of ethane increases as shown by the increasing presence of two distinct peaks in Fig. 25 and Fig. 26. The two distinct peaks represent the concentration responses from the two sections of the bed with different voidages. The first peak corresponds to the concentration response from section I, which has a voidage greater than that of the normal bed. The first peak becomes sharper and higher as $D_1$ increases and correspondingly the second peak becomes broader and shorter. This is because of the increased flow rate of the carrier gas and the increased amount of ethane introduced in the section I as its diameter increases.

The effect of $\epsilon_1$ and $D_1$ on the breakthrough times of ethane, which was introduced as a pulse challenge to the bed, is shown in Table 10. The breakthrough times for different breakthrough concentrations of ethane for three values of $D_1$ and two values of $\epsilon_1$ are shown in Table 10. The ratios of the breakthrough times for different values of $D_1$ and $\epsilon_1$ to its value for a normal bed are also shown in Table 10. In general as $D_1$ increases for any value of $\epsilon_1$ the ratio of breakthrough times decreases indicating thereby an increasing effect of $D_1$ on the breakthrough behaviour of ethane. For the same value of $D_1$ the ratio decreases as the value of $\epsilon_1$ increases. This also shows an increasing effect of $\epsilon_1$ on the breakthrough behaviour of ethane.

Similar to the study of the adsorption behaviour of ethane on the ASC carbon-filled C2 canisters, subjected to a pulse challenge, simulation runs were made to study the adsorption behaviour of dry n-octane on the same canisters, subjected to a step challenge. The operating variables and the system parameters used in the dry n-octane step challenge studies were the same as those given in Table 7.

The predicted responses, in terms of the concentration of n-octane in the exit gas stream, for three values of $D_1$ and two values of $\epsilon_1$ are shown in Fig. 27-29. The predicted response from a normal, uniform bed is also shown in Fig. 27-29 for comparison.

**TABLE 10:** Ratio of Breakthrough Times of Ethane for a Non-Uniform Bed

| $D_1$ (cm) | BTC ($mg/m^3$) | $T_{nb}$ A (min) | [A/A] | $T_{0.35}$ B (min) | [B/A] | $T_{0.4}$ C (min) | [C/A] |
|---|---|---|---|---|---|---|---|
| 0.5 | 0.05 | 0.130 | 1.00 | 0.130 | 1.0000 | 0.100 | 0.7690 |
| | 0.25 | 0.415 | 1.00 | 0.410 | 0.9880 | 0.230 | 0.5542 |
| | 0.50 | 0.615 | 1.00 | 0.600 | 0.9756 | 0.290 | 0.4715 |
| | 1.00 | 0.875 | 1.00 | 0.830 | 0.9486 | 0.360 | 0.4114 |
| | 5.00 | 1.630 | 1.00 | 1.640 | 1.0060 | 1.650 | 1.0122 |
| | 20.0 | 2.505 | 1.00 | 2.520 | 1.0060 | 2.535 | 1.0120 |
| 1.5 | 0.05 | 0.130 | 1.00 | 0.130 | 0.9230 | 0.055 | 0.4230 |
| | 0.25 | 0.415 | 1.00 | 0.360 | 0.8675 | 0.140 | 0.3373 |
| | 0.50 | 0.615 | 1.00 | 0.510 | 0.8293 | 0.180 | 0.2927 |
| | 1.00 | 0.875 | 1.00 | 0.670 | 0.7657 | 0.220 | 0.2514 |
| | 5.00 | 1.630 | 1.00 | 1.705 | 1.0460 | 0.330 | 0.2024 |
| | 20.0 | 2.505 | 1.00 | 2.620 | 1.0459 | 2.780 | 1.1099 |
| 2.5 | 0.05 | 0.130 | 1.00 | 0.105 | 0.8077 | 0.035 | 0.2692 |
| | 0.25 | 0.415 | 1.00 | 0.305 | 0.7349 | 0.100 | 0.2410 |
| | 0.50 | 0.615 | 1.00 | 0.430 | 0.6992 | 0.135 | 0.2195 |
| | 1.00 | 0.875 | 1.00 | 0.565 | 0.6457 | 0.175 | 0.2000 |
| | 5.00 | 1.630 | 1.00 | 0.925 | 0.5675 | 0.270 | 0.1656 |
| | 20.0 | 2.505 | 1.00 | 2.860 | 1.1417 | 0.390 | 0.1557 |

In general the breakthrough time of n-octane decreases as $\epsilon_1$ increases for a particular value of $D_1$. The concentration of n-octane corresponding to the first plateau increases as $\epsilon_1$ increases for any value of $D_1$; and also the concentration corresponding to the first plateau increases as $D_1$ increases for any value of $\epsilon_1$. This is expected because as $\epsilon_1$ increases the volumetric flow rates of the carrier gas and the n-octane through the section with higher $\epsilon_1$ or $D_1$ also increase. Since the volumetric flow rate of the carrier gas varies as $D_1^2$, the increase in the concentration of n-octane corresponding to the first plateau for an increase in the value of $D_1$ is more than the corresponding increase for an increase in the value of $\epsilon_1$. Since the breakthrough time of n-octane decreases as $\epsilon_1$ increases for any value of $D_1$ the breakthrough time from the second bed increases as shown in Fig. 27-29.

The effect of $D_1$ and $\epsilon_1$ on the breakthrough times for various values of the breakthrough concentrations of n-octane in the exit gas stream is shown in Table 11. In general the breakthrough time of n-octane decreases as $\epsilon_1$ increases for a particular value of $D_1$. However the breakthrough time of n-octane remains more or less constant as $D_1$ increases from 0.5 to 2.5 cm for any particular value of $\epsilon_1$. The ratios of breakthrough times of n-octane through a bed with certain values of $\epsilon_1$ and $D_1$ to its value through a normal bed are also shown in Table 11. It is interesting to note that only for $D_1$=0.5 cm and a breakthrough concentration of n-octane as 20 $mg/m^3$ is predicted breakthrough time almost the same as the breakthrough time from a normal, uniform bed. This means that only if the values of $D_1$ and $\epsilon_1$ are less than 0.5 cm and 0.4 respectively will the concentration response of the bed for a step challenge in the concentration of n-octane be the same as that from a normal, uniform bed.

The next step was to compare the sensitivity of the response of the bed to a pulse concentration challenge of dry ethane with the one to a step challenge of dry n-octane. For different values of the breakthrough concentrations, the ratios of the breakthrough times of ethane for different values of $D_1$ and $\epsilon_1$ to its value for a normal bed are compared with the corresponding ratios for n-octane in Fig. 30. For a particular value of $\epsilon_1$, the ratio of the breakthrough times for n-octane remains constant irrespective of the variation in the ratio for ethane so long as the breakthrough concentration is $< 5.0$ $mg/m^3$. This can be understood by comparing the response curves from Fig. 24-26 and Fig. 27-29. The concentration of the n-octane changes sharply as soon as its breakthrough occurs which means that the breakthrough times of n-octane for different values of its breakthrough concentrations does not change significantly. In contrast the concentration of ethane changes slowly once its breakthrough occurs which means that the breakthrough time of ethane is dependent on its breakthrough concentration.

**Table 11: Ratio of Breakthrough Times of n-Octane for a Non-Uniform Bed**

| $D_1$ | BTC | $T_{nb}$ A | [A/A] | $T_{0.35}$ B | [B/A] | $T_{0.4}$ C | [C/A] |
|---|---|---|---|---|---|---|---|
| cm | $mg/m^3$ | min | - | min | - | min | - |
| 0.5 | 0.05 | 453.0 | 1.00 | 147.0 | 0.3245 | 48.00 | 0.1060 |
| | 0.25 | 453.0 | 1.00 | 147.0 | 0.3245 | 48.00 | 0.1060 |
| | 0.50 | 455.0 | 1.00 | 148.0 | 0.3253 | 48.00 | 0.1055 |
| | 1.00 | 456.0 | 1.00 | 149.0 | 0.3268 | 49.00 | 0.1075 |
| | 5.00 | 457.0 | 1.00 | 162.0 | 0.3544 | 53.00 | 0.1160 |
| | 20.0 | 458.0 | 1.00 | 459.0 | 1.0022 | 461.0 | 1.0066 |
| 1.5 | 0.05 | 453.0 | 1.00 | 147.0 | 0.3245 | 49.00 | 0.1082 |
| | 0.25 | 453.0 | 1.00 | 147.0 | 0.3245 | 49.00 | 0.1082 |
| | 0.50 | 455.0 | 1.00 | 147.0 | 0.3231 | 49.00 | 0.1077 |
| | 1.00 | 456.0 | 1.00 | 148.0 | 0.3246 | 49.00 | 0.1075 |
| | 5.00 | 457.0 | 1.00 | 149.0 | 0.3260 | 50.00 | 0.1094 |
| | 20.0 | 458.0 | 1.00 | 153.0 | 0.3341 | 51.00 | 0.1113 |
| 2.5 | 0.05 | 453.0 | 1.00 | 148.0 | 0.3267 | 51.00 | 0.1126 |
| | 0.25 | 453.0 | 1.00 | 148.0 | 0.3267 | 51.00 | 0.1126 |
| | 0.50 | 455.0 | 1.00 | 149.0 | 0.3275 | 51.00 | 0.1121 |
| | 1.00 | 456.0 | 1.00 | 149.0 | 0.3268 | 51.00 | 0.1118 |
| | 5.00 | 457.0 | 1.00 | 150.0 | 0.3282 | 51.00 | 0.1116 |
| | 20.0 | 458.0 | 1.00 | 151.0 | 0.3297 | 52.00 | 0.1135 |

For different values of the breakthrough concentrations, the ratios of the breakthrough times of ethane and n-octane for different values of $D_1$ and $\epsilon_1$ to their respective values for a normal bed are plotted as shown in Fig. 31 and Fig. 32. In general the ratio of the breakthrough times of ethane decreases with increasing values of the breakthrough concentration till 1.0 $mg/m^3$ for all values of $D_1$. The general trend indicates that as the breakthrough concentration approaches 1.0 $mg/m^3$ the breakthrough time ratio for ethane reaches a plateau. Compared to the behaviour of ethane, the ratio of the breakthrough times for n-octane remains almost constant.

It is important to note that except for the case of $D_1$=2.5 cm and $\epsilon_1$= 0.4 the values of the ratios of breakthrough times of ethane, for a breakthrough concentration of 20 $mg/m^3$, are greater than 1.0. This means that the time for the ethane concentration to reach a value of 20 $mg/m^3$ from a bed, with two sections of different voidages, is more than the time needed to reach the same value of the concentration in a normal, uniform bed. This behaviour is opposite of what is observed in the case of an uneven bed where the breakthrough time for ethane to reach a concentration of 20 $mg/m^3$ is always less than the time to reach the same value for an even, uniform bed. If the concentration response of ethane is followed till it reaches a value of 20 $mg/m^3$ then, depending on whether the time to reach that concentration is greater or less than that for a normal bed, the type of fault in the canister can be confirmed.

### 4.3 SHORT BED

It is possible that less than the normal volume (170 $cm^3$) of the activated carbon particles is used to fill the C2 canister. This would result in a shorter than normal depth of the bed assuming the diameter of the canister is the same as the one for a normal bed. To study the effect of the bed depth on the response of the C2 canister to the ethane pulse or the n-octane step challenge, it was assumed that the volumetric flow rate of the carrier gas remained the same as the one (500 $cm^3/s$ [30 lpm]) in a normal bed.

The model described in Section "Theoretical Considerations" was used to calculate the responses of the C2 canister, as a function of the bed depth, subjected to a pulse challenge in the concentration of dry ethane. Three simulation runs were done, with the bed depth 100%, 95% and 90% of the normal bed depth, to predict the concentration response from the C2 canister using the values of the operating variables and the parameters given in Table 2. The simulation results, in terms of the concentration of ethane in the exit gas stream, are shown in Fig. 33. The same model was used to study the effect of the bed depth on the concentration response of the C2 canister subjected to a step challenge in the concentration of n-octane. The simulation results, based on the values of the

operating variables and the parameters given in Table 6, for the breakthrough behaviour of n-octane are shown in Fig. 34.

The breakthrough times of ethane and n-octane for different values of the breakthrough concentration decrease with decreasing bed depth as given in the Tables 12 and 13. This is because of the reduced adsorption capacity of the bed due to reduction in its depth.

**Table 12: Breakthrough Times of Ethane as a Function of Bed Depth**

| ORGANIC<br>- | L<br>cm | BTC<br>$mg/m^3$ | T<br>min | $[T/T_{nb}]$<br>- |
|---|---|---|---|---|
| $C_2H_6$ | 2.00 | 0.05 | 0.130 | 1.0000 |
| | | 0.25 | 0.415 | 1.0000 |
| | | 0.50 | 0.620 | 1.0000 |
| | | 1.00 | 0.875 | 1.0000 |
| | | 5.00 | 1.635 | 1.0000 |
| | | 20.0 | 2.505 | 1.0000 |
| | 1.90 | 0.05 | 0.120 | 0.9231 |
| | | 0.25 | 0.380 | 0.9157 |
| | | 0.50 | 0.571 | 0.9193 |
| | | 1.00 | 0.810 | 0.9257 |
| | | 5.00 | 1.540 | 0.9419 |
| | | 20.0 | 2.400 | 0.9581 |
| | 1.80 | 0.05 | 0.110 | 0.8461 |
| | | 0.25 | 0.362 | 0.8674 |
| | | 0.50 | 0.540 | 0.8710 |
| | | 1.00 | 0.770 | 0.8800 |
| | | 5.00 | 1.450 | 0.8868 |
| | | 20.0 | 2.260 | 0.9022 |

Table 13: Breakthrough Times of n-Octane for Various Bed Sizes

| ORGANIC<br>- | L<br>cm | BTC<br>$mg/m^3$ | T<br>min | $[T/T_0]$<br>- |
|---|---|---|---|---|
| $n-C_8H_{18}$ | 2.00 | 0.05 | 453 | 1.0000 |
| | | 0.25 | 454 | 1.0000 |
| | | 0.50 | 455 | 1.0000 |
| | | 1.00 | 456 | 1.0000 |
| | | 5.00 | 457 | 1.0000 |
| | | 20.0 | 458 | 1.0000 |
| | 1.90 | 0.05 | 429 | 0.9470 |
| | | 0.25 | 431 | 0.9493 |
| | | 0.50 | 431 | 0.9472 |
| | | 1.00 | 432 | 0.9473 |
| | | 5.00 | 433 | 0.9474 |
| | | 20.0 | 434 | 0.9476 |
| | 1.80 | 0.05 | 406 | 0.8963 |
| | | 0.25 | 407 | 0.8965 |
| | | 0.50 | 407 | 0.8945 |
| | | 1.00 | 408 | 0.8947 |
| | | 5.00 | 409 | 0.8950 |
| | | 20.0 | 410 | 0.8952 |

## 5.0 DISCUSSION OF RESULTS

The aim of the present study is to theoretically assess the feasibility of replacing a destructive testing procedure by a non-destructive one carried out on every canister. The destructive test, involving a constant challenge of DMMP or phosgene and simulated by the step concentration challenge of n-octane in this report, is carried out on a few randomly selected C2 military canisters from the production line. The non-destructive test, by a pulse concentration challenge of dry ethane, would be carried out

on every canister in the production line. The most important criterion in this regard is to determine whether the probability of detecting a "faulty" canaster by the non-destructive pulse test is greater than its value for detection by the destructive step test.

The other important criterion to confirm the validity of the replacing the n-octane step test by the ethane pulse test is to ensure that during the production of the canisters at least all the "faults", which are detected by the step test are also detected by the pulse test. A "pass/fail (P/F)" criterion has to be developed to ensure that the presence of a fault is detected by either of the tests. The development of such a P/F criterion depends significantly on the confidence level and the standard deviation of the breakthrough times of either of these adsorbates measured experimentally. In this study the uncertainty in the accuracy of the experimental measurement of the breakthrough times of ethane and n-octane was arbitrarily fixed at 10%, 20%, 25% and 30% of the predicted breakthrough times of the same adsorbates for an even, uniform bed, denoted by $T_{nb}$. In the presence of any fault, if the predicted breakthrough time from either of the tests was less than 90%, 80%, 75% or 70% of $T_{nb}$ for the same test then the test method was assumed to have successfully detected the fault or "passed" the detection criterion.

Two commonly present faults in the canisters are the "unevenness" and "non-uniformity" of the activated carbon bed. The breakthrough time data for the ethane pulse and the n-octane step concentration challenge tests, as a function of the degree of unevenness, as given in Tables 5 and 7 respectively, were subjected to the above P/F criterion. The results for ethane and n-octane are given in Tables 14 and 15 respectively.

The ethane pulse test fails to detect any fault of size $\Delta L \leq 0.1$ cm for all values of the breakthrough concentration and $(f.T_{nb})$, where f is 0.9, 0.8, 0.75 or 0.7, chosen for its detection (Table 14). For faults of size $\Delta L \geq 0.2$ cm, the ethane pulse test passes in their detection for all values of the breakthrough concentration only if $f \geq 0.9$. On the other hand, the n-octane step test detects all the faults of size $\Delta L \geq 0.1$ cm for all values of the breakthrough concentration of n-octane so long as $f \geq 0.9$ (Table 15).

The breakthrough time data for the ethane pulse and the n-octane step concentration challenge tests, as a function of the non-uniformity of the bed, in terms of $D_1$ and $\epsilon_1$, as given in Tables 10 and 11 respectively, were also subjected to the P/F criterion. The results for ethane and n-octane are given in Tables 16 and 17 respectively.

The ethane pulse test fails to detect any fault of size $D_1 \leq 0.5$ cm and $0.3 < \epsilon_1 \leq 0.35$ for all values of the breakthrough concentration and $(f.T_{nb})$ chosen for its detection (Table 16). For $0.3 < \epsilon_1 \leq 0.35$ and

**Table 14 : Application of the P/F Criterion to the Ethane Pulse Response Data for the Uneven C2 Canister**

| ΔL<br>cm | BTC<br>$mg/m^3$ | $0.9T_{nb}$<br>- | $0.8T_{nb}$<br>- | $0.75T_{nb}$<br>- | $0.7T_{nb}$<br>- |
|---|---|---|---|---|---|
| 0.10 | 0.05 | F | F | F | F |
| | 0.25 | F | F | F | F |
| | 0.50 | F | F | F | F |
| | 1.00 | F | F | F | F |
| | 5.00 | F | F | F | F |
| | 20.0 | F | F | F | F |
| 0.20 | 0.05 | F-P | F | F | F |
| | 0.25 | F-P | F | F | F |
| | 0.50 | F-P | F | F | F |
| | 1.00 | F-P | F | F | F |
| | 5.00 | P | F | F | F |
| | 20.0 | P | F | F | F |
| 0.25 | 0.05 | P | F | F | F |
| | 0.25 | P | F | F | F |
| | 0.50 | P | F | F | F |
| | 1.00 | P | F | F | F |
| | 5.00 | P | F | F | F |
| | 20.0 | P | F | F | F |

**Table 15: Application of the P/F Criterion to the n-Octane Pulse Response Data for an Uneven C2 Canister**

| ΔL<br>cm | BTC<br>$mg/m^3$ | $0.9T_{nb}$<br>- | $0.8T_{nb}$<br>- | $0.75T_{nb}$<br>- | $0.7T_{nb}$<br>- |
|---|---|---|---|---|---|
| 0.10 | 0.05 | P-F | F | F | F |
| | 0.25 | P-F | F | F | F |
| | 0.50 | P-F | F | F | F |
| | 1.00 | P-F | F | F | F |
| | 5.00 | P-F | F | F | F |
| | 20.0 | P-F | F | F | F |
| 0.20 | 0.05 | P | P-F | F | F |
| | 0.25 | P | P-F | F | F |
| | 0.50 | P | P-F | F | F |
| | 1.00 | P | P-F | F | F |
| | 5.00 | P | P-F | F | F |
| | 20.0 | P | P-F | F | F |
| 0.25 | 0.05 | P | P | P-F | F |
| | 0.25 | P | P | P-F | F |
| | 0.50 | P | P | P-F | F |
| | 1.00 | P | P | P-F | F |
| | 5.00 | P | P | P-F | F |
| | 20.0 | P | P | P-F | F |

**Table 16: Application of the P/F Criterion to the Ethane Pulse Test for a Non-uniform C2 Canister**

| $\epsilon_1$ - | $D_1$ cm | BTC $mg/m^3$ | $0.9T_b$ - | $0.8T_b$ - | $0.75T_b$ - | $0.7T_b$ - |
|---|---|---|---|---|---|---|
| 0.35 | 0.5 | 0.05 | F | F | F | F |
| | | 0.25 | F | F | F | F |
| | | 0.50 | F | F | F | F |
| | | 1.00 | F | F | F | F |
| | | 5.00 | F | F | F | F |
| | | 20.0 | F | F | F | F |
| | 1.5 | 0.05 | F | F | F | F |
| | | 0.25 | P | F | F | F |
| | | 0.50 | P | F | F | F |
| | | 1.00 | P | P | F | F |
| | | 5.00 | F | F | F | F |
| | | 20.0 | F | F | F | F |
| | 2.5 | 0.05 | P | F-P | F | F |
| | | 0.25 | P | P | P | F |
| | | 0.50 | P | P | P | F-P |
| | | 1.00 | P | P | P | P |
| | | 5.00 | P | P | P | P |
| | | 20.0 | F | F | F | F |
| 0.4 | 0.5 | 0.05 | P | P-F | F | F |
| | | 0.25 | P | P | P | P |
| | | 0.50 | P | P | P | P |
| | | 1.00 | P | P | P | P |
| | | 5.00 | F | F | F | F |
| | | 20.0 | F | F | F | F |
| | 1.5 | 0.05 | P | P | P | P |
| | | 0.25 | P | P | P | P |
| | | 0.50 | P | P | P | P |
| | | 1.00 | P | P | P | P |
| | | 5.00 | P | P | P | P |
| | | 20.0 | F | F | F | F |
| | 2.5 | 0.05 | P | P | P | P |
| | | 0.25 | P | P | P | P |
| | | 0.50 | P | P | P | P |
| | | 1.00 | P | P | P | P |
| | | 5.00 | P | P | P | P |
| | | 20.0 | P | P | P | P |

**Table 17: Application of the P/F Criterion to the n-Octane Step Test for a Non-uniform C2 Canister**

| $\epsilon_1$ - | $D_1$ cm | BTC $mg/m^3$ | $0.9T_b$ - | $0.8T_b$ - | $0.75T_b$ - | $0.7T_b$ - |
|---|---|---|---|---|---|---|
| 0.35 | 0.5 | 0.05 | P | P | P | P |
| | | 0.25 | P | P | P | P |
| | | 0.50 | P | P | P | P |
| | | 1.00 | P | P | P | P |
| | | 5.00 | P | P | P | P |
| | | 20.0 | F | F | F | F |
| | 1.5 | 0.05 | P | P | P | P |
| | | 0.25 | P | P | P | P |
| | | 0.50 | P | P | P | P |
| | | 1.00 | P | P | P | P |
| | | 5.00 | P | P | P | P |
| | | 20.0 | P | P | P | P |
| | 2.5 | 0.05 | P | P | P | P |
| | | 0.25 | P | P | P | P |
| | | 0.50 | P | P | P | P |
| | | 1.00 | P | P | P | P |
| | | 5.00 | P | P | P | P |
| | | 20.0 | P | P | P | P |
| 0.4 | 0.5 | 0.05 | P | P | P | P |
| | | 0.25 | P | P | P | P |
| | | 0.50 | P | P | P | P |
| | | 1.00 | P | P | P | P |
| | | 5.00 | P | P | P | P |
| | | 20.0 | F | F | F | F |
| | 1.5 | 0.05 | P | P | P | P |
| | | 0.25 | P | P | P | P |
| | | 0.50 | P | P | P | P |
| | | 1.00 | P | P | P | P |
| | | 5.00 | P | P | P | P |
| | | 20.0 | P | P | P | P |
| | 2.5 | 0.05 | P | P | P | P |
| | | 0.25 | P | P | P | P |
| | | 0.50 | P | P | P | P |
| | | 1.00 | P | P | P | P |
| | | 5.00 | P | P | P | P |
| | | 20.0 | P | P | P | P |

$D_1 \geq 1.5$ cm, the ethane pulse test detects the presence of the fault only if the values of the breakthrough concentration and $(f.T_{nb})$ are within a narrow range. For $\epsilon_1 \geq 0.4$, the ethane pulse test successfully detects the presence of the fault only if the breakthrough concentration of ethane is not greater than 1.0 $mg/m^3$ and $f \geq 0.8$. On the other hand, the n-octane step challenge test detects all the faults for all values of breakthrough concentration less than 20 $mg/m^3$ and $(f.T_{nb})$.

The breakthrough time data for the ethane pulse and the n-octane step concentration challenge tests, as a function of the bed depth (Tables 12 and 13 respectively), were also subjected to the P/F criterion. The results for ethane and n-octane are given in the Tables 18 and 19 respectively. The results show that both the ethane pulse and the n-octane step challenge tests fail to detect the presence of a bed of depth ≥1.90 cm.

**Table 18: Application of the P/F Criterion to the Ethane Pulse Response Data for Various Bed Depths**

| L<br>cm | BTC<br>$mg/m^3$ | $0.9T_{nb}$<br>- | $0.8T_{nb}$<br>- | $0.75T_{nb}$<br>- | $0.7T_{nb}$<br>- |
|---|---|---|---|---|---|
| 1.90 | 0.05 | F | F | F | F |
| | 0.25 | F | F | F | F |
| | 0.50 | F | F | F | F |
| | 1.00 | F | F | F | F |
| | 5.00 | F | F | F | F |
| | 20.0 | F | F | F | F |
| 1.80 | 0.05 | P-F | F | F | F |
| | 0.25 | P-F | F | F | F |
| | 0.50 | P-F | F | F | F |
| | 1.00 | P-F | F | F | F |
| | 5.00 | P-F | F | F | F |
| | 20.0 | F | F | F | F |

**Table 19: Application of the P/F Criterion to the n-Octane Step Response Data for Various Bed Depths**

| L<br>cm | BTC<br>$mg/m^3$ | $0.9T_{nb}$<br>- | $0.8T_{nb}$<br>- | $0.75T_{nb}$<br>- | $0.7T_{nb}$<br>- |
|---|---|---|---|---|---|
| 1.90 | 0.05 | F | F | F | F |
| | 0.25 | F | F | F | F |
| | 0.50 | F | F | F | F |
| | 1.00 | F | F | F | F |
| | 5.00 | F | F | F | F |
| | 20.0 | F | F | F | F |
| 1.80 | 0.05 | P-F | F | F | F |
| | 0.25 | P-F | F | F | F |
| | 0.50 | P-F | F | F | F |
| | 1.00 | P-F | F | F | F |
| | 5.00 | P-F | F | F | F |
| | 20.0 | P-F | F | F | F |

The above analysis clearly indicates that the ethane pulse challenge test is not able to detect all the faults, which are successfully detected by the n-octane step challenge test. However it is important to keep in mind the following points.

a The n-octane step test, which is destructive in nature, is carried out on a few randomly selected canisters only.
b The ethane pulse test, which is non-destructive in nature, would be carried out on every canister in the production line.

It is therefore important to calculate the probability of detecting the faulty canisters based on

- the total number of canisters produced,
- the ratio of the number of canisters tested by the n-octane step test to the total number of canisters produced,
- the fraction of the total canisters, which have a fault of a certain type,
- the experimental accuracy, in the measurement of the breakthrough times of ethane or n-octane for a normal bed.

A brief statistical analysis was carried out based on the following assumptions.

- Lot size of the canisters produced = 10000,
- number of the canisters tested by n-octane test = 100,
- number of faulty canisters = 90,
- the uncertainty in the accuracy of the measurement of the breakthrough times of ethane or n-octane, for breakthrough concentrations between 0.25 and 1.0 $mg/m^3$, is within 10% of the breakthrough times of the same adsorbates for an even, uniform bed.

The basis of the selected number of faulty canisters is as follows. In this report, 6 (3 diameters x 2 voidages) sizes of faults for the non-uniform bed and 3 sizes of the faults for the uneven bed have been considered. It is assumed that the number of canisters with each type of fault is 0.1% of the total number of the canisters produced. Therefore for a total of 9 sizes of the faults, the total number of faulty canisters is 9*0.001*10000=90.

Using the results, given in the Tables 14-17, of the application of the P/F criterion developed earlier, it is found that the ethane pulse test is unable to detect the faults of 2 sizes whereas the n-octane test is able to detect all the faults. Hence the ethane pulse test fails to detect only 20 out of the 90 faulty canisters in a lot of 10000 canisters. Were the n-octane test carried out on all the 10000 canisters it would have detected all the 90 faulty canisters. However the n-octane test is carried out only on a sample of randomly selected 100 canisters. It is therefore important to calculate the number of the faulty canisters which are likely to be found in the sample of 100 canisters. The probability of finding no faulty canister in a sample of 100 canisters from a lot of 10000 canisters, containing 90 faulty canisters, was calculated as 0.4049 from the following formula based on the binomial distribution.

$$P_{(x=0)} = \frac{n!}{x!\,(n-x)!}\pi^{x}(1-\pi)^{n-x} \qquad (2)$$

where x denotes the number of successes, n denotes the sample size; and $\pi$ denotes the probability of success based on the population (or lot) size. This means that there is approximately 40.5% chance that not a single faulty canister would be detected by the n-octane step test because there is a 40.5% chance that it would not be present in the sample of 100 canisters.

The above analysis clearly indicates that though the ethane pulse test is unable to detect all the faults of all the sizes present in the canisters, it is definitely better than the n-octane step test in terms of the number of faulty canisters detected.

## 6.0 CONCLUSIONS AND RECOMMENDATIONS

Based on the results and their discussion, presented in the above sections, the following conclusions can be drawn.

6.1.1 The D-R equation represents the adsorption equilibrium for the dry ethane-activated carbon system for BPL, ASC, ASC/3T and PPC carbons satisfactorily in the range of concentrations for which the experimental measurements were made.

6.1.2 The theoretical model, developed in the earlier work, has been utilized to predict the adsorption behaviour of a pulse challenge in the concentration of dry ethane in the inlet gas stream to an ASC activated carbon-filled C2 military canaster.

6.1.3 The simulation results match fairly well with the experimental ethane pulse response data in the initial part of the breakthrough curve. However, the simulation results do not match the size and shape of the experimentally measured overall pulse response curve. A number of possible reasons for the discrepancy between the experimental and the simulation results have been described.

6.1.4 The model has been successfully modified to predict the adsorption behaviour of dry ethane pulse or dry n-octane step challenge to an unevenly packed ASC activated carbon-filled C2 canister. The actual uneven bed, having its length vary continuously from the edge to the centre of the canister, has been simulated as a bed with three sections of different lengths, varying in step sizes ($\Delta L$) from 0.05 to 0.25 cm, and cross-sectional areas. The distribution of the superficial velocities and the volumetric flow rates through the uneven bed have also been calculated.

6.1.5 The effect of the degree of unevenness of the bed on the breakthrough times of dry ethane and n-octane for different breakthrough concentrations has been studied. The ethane concentration response curve from the overall uneven bed is found to show three peaks corresponding to the different responses from each section. Similarly the n-octane concentration response curve from the overall bed is found to show three plateaux corresponding to the responses from each section.

6.1.6 The ratios of the breakthrough times of ethane for an uneven bed to their corresponding values for an even bed were compared with similar ratios for n-octane in order to compare the responses from the ethane pulse with the n-octane step challenges. For any value of $\Delta L$, the ratio of the breakthrough times for n-octane remains almost constant for different values of the breakthrough concentrations whereas the ratio for ethane varies significantly.

6.1.7 The model has been successfully modified to predict the adsorption behaviour of dry ethane pulse or dry n-octane step challenge to a non-uniformly packed ASC activated carbon-filled C2 canaster. The actual non-uniform bed, containing sections of varying voidages, has been simulated as a bed made up of two sections of different sizes and voidages. The distribution of the superficial velocities and the volumetric flow rates for beds, containing one section with diameter varying from 0.5 to 2.5 cm and voidage varying from 0.3 to 0.4, has been calculated.

6.1.8 The effect of the non-uniformity of the bed on the breakthrough times of ethane and n-octane for different breakthrough concentrations has been studied. The ethane concentration response from the overall non-uniform bed is found to show two distinct peaks corresponding to the responses from the two sections of the bed, similar to concentration responses from an uneven bed. The n-octane concentration response is also found to show two plateaux corresponding to the responses from the two sections.

6.1.9 The ratios of the breakthrough times of ethane for a non-uniform bed to their corresponding values for a uniform bed were compared with similar ratios for n-octane in order to compare the responses from the ethane pulse with the n-octane step challenges. For any particular value of voidage ($\epsilon_1$) of the section I, the ratio of the breakthrough times for n-octane remains almost constant for different values of the breakthrough concentrations whereas the ratio for ethane varies significantly.

6.1.10 For a breakthrough concentration of 20 $mg/m^3$, the ratios of the breakthrough times of n-ethane for an uneven bed to its value for an even bed, for different values of $\Delta L$, are less than 1.0. Similar ratios for a breakthrough concentration of 20 $mg/m^3$ of ethane for a non-uniform bed are found to be greater than 1.0. This can be used as a means of detecting the type of fault if the concentration of dry ethane in the exit gas stream is measured till it reaches a value of 20 $mg/m^3$.

6.1.11 The effect of bed depth on the concentration response to the ethane pulse and the n-octane step challenge tests was also studied. Understandably the breakthrough time of both the adsorbates decreases as the bed depth decreases.

6.1.12 A Pass/Fail (P/F) criterion has been developed assuming an uncertainty of 10%, 20%, 25% or 30% in the experimental measurement of the breakthrough times of either ethane or n-octane through a C2 canister. It has been found that, for an uncertainty of 10% in the measurement of the breakthrough time, the n-octane step challenge test successfully detects all the faults caused by the unevenness and the non-uniformity of the bed. Whereas, for the same uncertainty, the ethane pulse challenge test fails to detect any fault in an uneven bed of $\Delta L \leq 0.1$ cm and in a non-uniform bed for $D_1 \leq 0.5$ cm and $\epsilon_1 \leq 0.35$.

6.1.13 Considering that the destructive test, simulated by the n-octane step challenge test, is carried out on a small sample of the C2 canisters, randomly selected from a large lot during the production process; and the non-destructive ethane pulse test is to be carried out on all the canisters in the production line, the ethane pulse test is better than the n-octane step test in terms of the number of faulty canisters detected.

Keeping in view the conclusions of the analysis carried out in this report, the following recommendations are made.

6.2.1 The experimental set-up and the procedure of ethane pulse testing should be carefully evaluated to:

1. characterize the input concentration signal,
2. characterize the concentration response of the chuck,
3. measure the nature and amount of the dead-volume and dead-time,
4. measure and set specific limits on the uncertainty in the experimental measurement of the breakthrough time of either ethane or n-octane through the C2 canister,
5. and to carry out step 4 as a function of the breakthrough concentration.

6.2.2 The suitability of the D-R equation, to represent the adsorption equilibrium for the dry ethane-ASC carbon system in the concentration range of the pulse response experiments, has to be verified experimentally. It may not be possible to experimentally measure the adsorption equilibrium data accurately for the above system at such low concentrations. It is probably easier to carry out experimental measurements of the pulse response data at higher concentrations than to measure the adsorption isotherm data at low concentrations. Therefore a detailed study of the effect of the challenge concentration of ethane on the adsorption behaviour of the C2 canaster bed should be carried out.

6.2.3 Assuming that the D-R equation is not probably the most suitable one for the above system at very low concentrations, the model should be modified to use the Langmuir equation or a linear equation to represent the adsorption equilibrium for this system.

6.2.4 The effect of the presence of other adsorbates such as $N_2$, $O_2$ and $CH_4$ should be taken into account in the model. This can be done by modifying the model for a single adsorbate system to a multi-adsorbate system. Experimentally the effect of the presence of $N_2$, $O_2$ and $CH_4$ can be confirmed by using He instead of air as the carrier gas and also studying the response of pure methane separately.

6.2.5 A detailed statistical analysis should be carried out based on the experimental measurement of the numbers of canisters containing different types and sizes of faults. The analysis would also help in establishing the size of the sample, to be used for destructive testing.

6.2.6 This study has been carried out assuming a dry-dry system. The relative humidity of the carrier gas and the pre-conditioning of the activated carbon significantly affect the adsorption of ethane on the carbon particularly at low concentrations of ethane in the gas phase. It is therefore important to study experimentally and theoretically the effect of humidity of the carrier gas and the pre-conditioning of activated carbon on the breakthrough behaviour of ethane.

6.2.7 The adsorption behaviour of the adsorbate varies significantly with the nature of the activated carbon and the size and shape of the bed used in the canaster. It is therefore important to extend the study to single- and dual-bed C7 canisters containing BPL, ASC, ASC/3T and PPC carbons and any combination of these carbons.

## 7.0 REFERENCES


1. **Harrison B. H. and Narayan S. B.;** "Prediction of the Performance of a Charcoal Filter", Proceedings of the U.S. Army Scientific Conference on Chemical Defence and Research held in November, 1990 at Aberdeen Proving Ground, Maryland (DSIS AD-P200 902).

2. **Dubinin M. M.;** "The Potential Theory of Adsorption of Gases and Vapours for Adsorbents with Energetically Nonuniform Surfaces", Chem. Rev., 60, 235 (1960).

3. **Smith J. M. and Van Ness H. C.;** "Introduction to Chemical Engineering Thermodynamics", Third edition, McGraw-Hill, 1975.

4. **Ruthven D. M.;**"Principles of Adsorption and Adsorption Processes", John Wiley & Sons, New York, 1984.

5. **Narayan S. B.;** "Breakthrough Curve Simulation: Final Report" submitted to DREO, Ottawa, December 1989.

6. **Wood G. O.;** "Activated Carbon Adsorption Capacities for Vapors", Carbon, 30 (4), 593-599 (1992).

7. **Bird R. B., Stewart W. E. and Lightfoot E. N.;** "Transport Phenomena", John Wiley and Sons, New York, p.200 (1960).

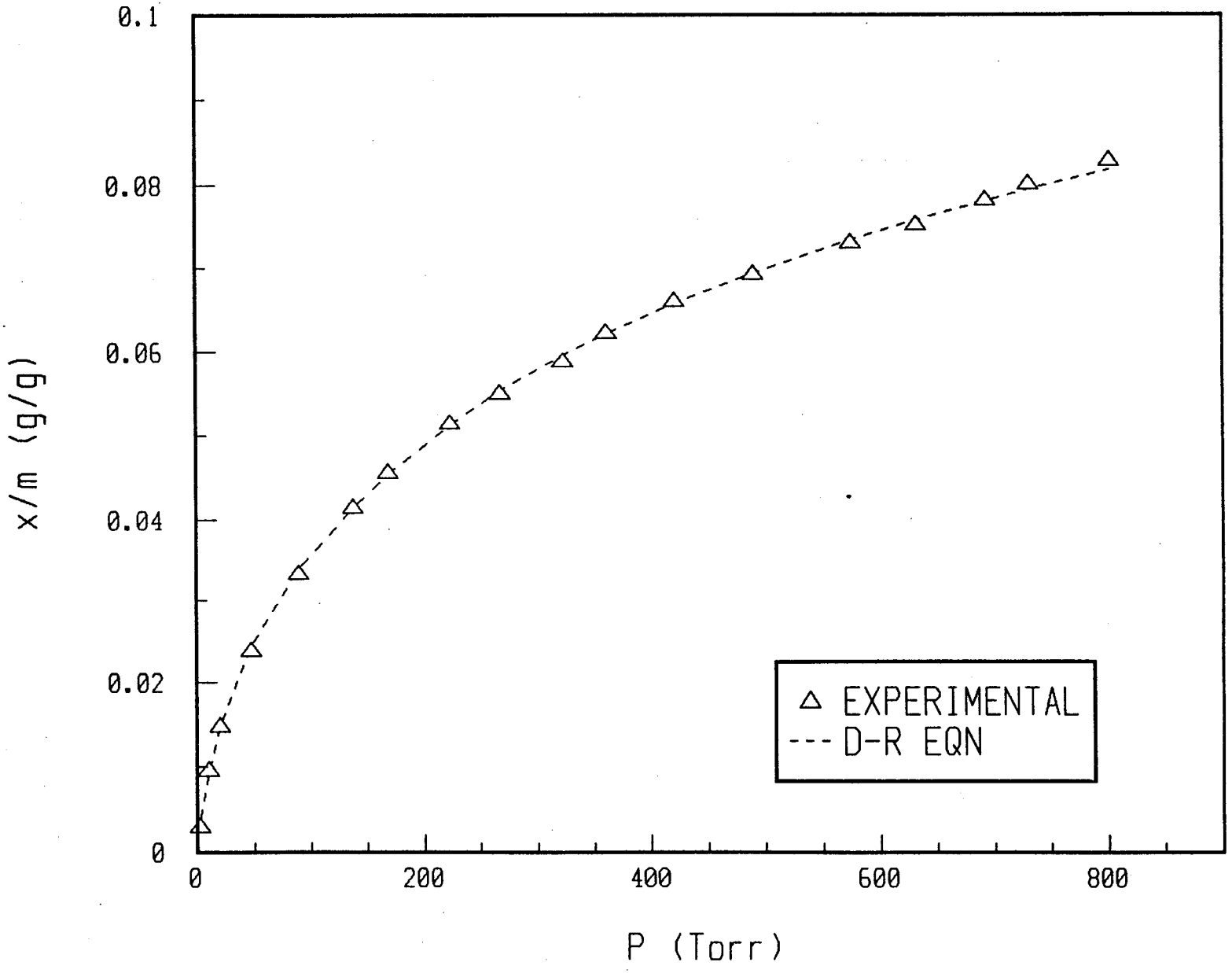


Fig.1: Experimental and the D-R isotherms for ethane-ASC carbon

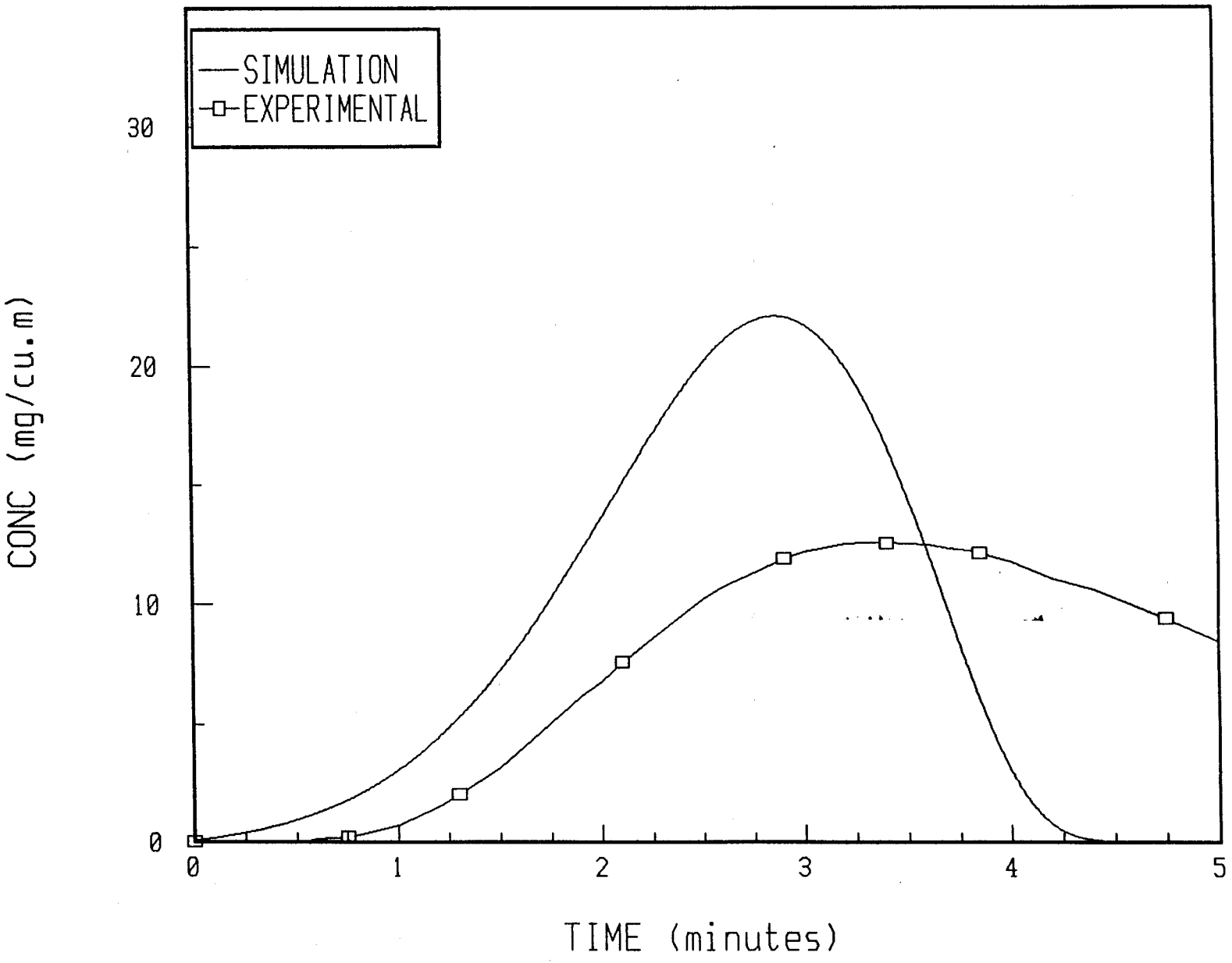


Fig.2: Experimental and simulation ethane pulse response curves for ASC carbon-filled C2 canister

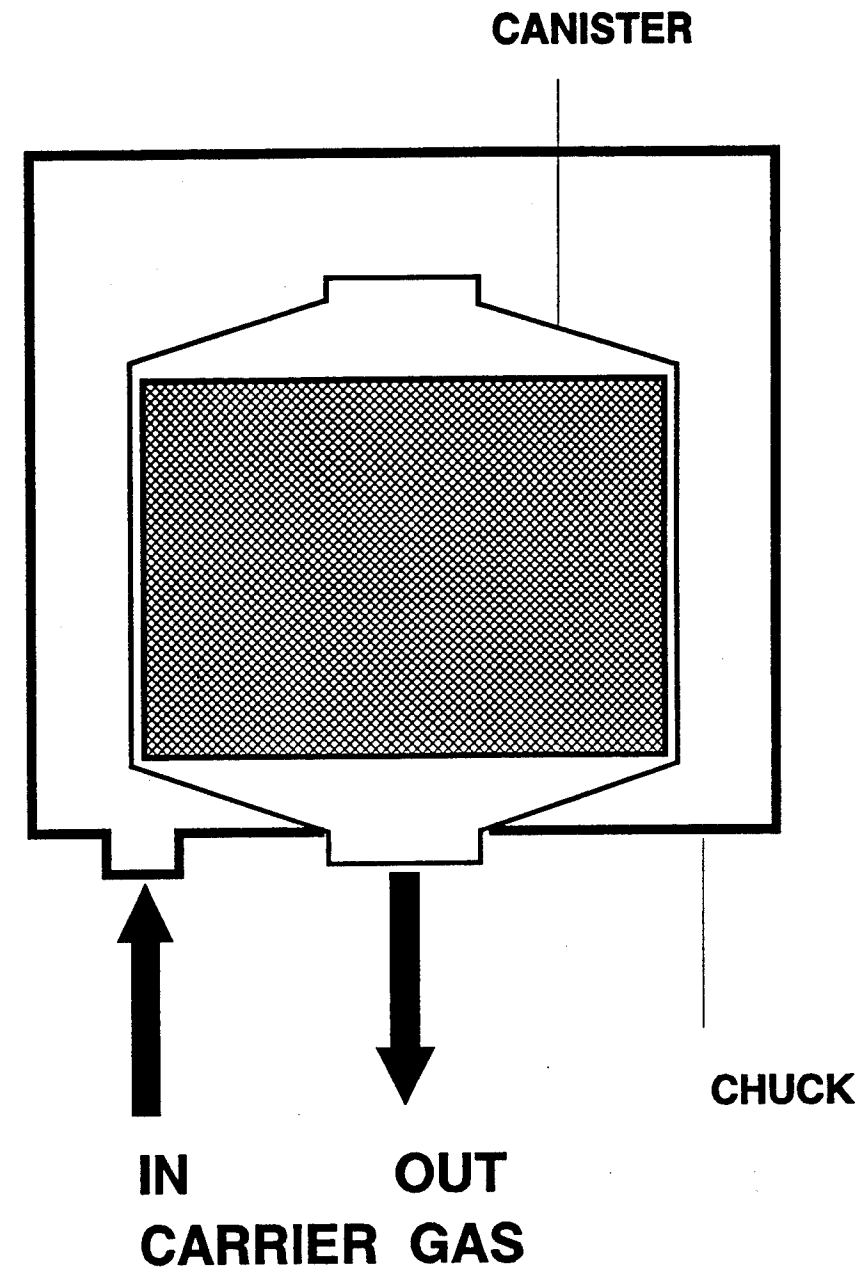


Fig. 3: Schematic of the Chuck - Canister flow assembly

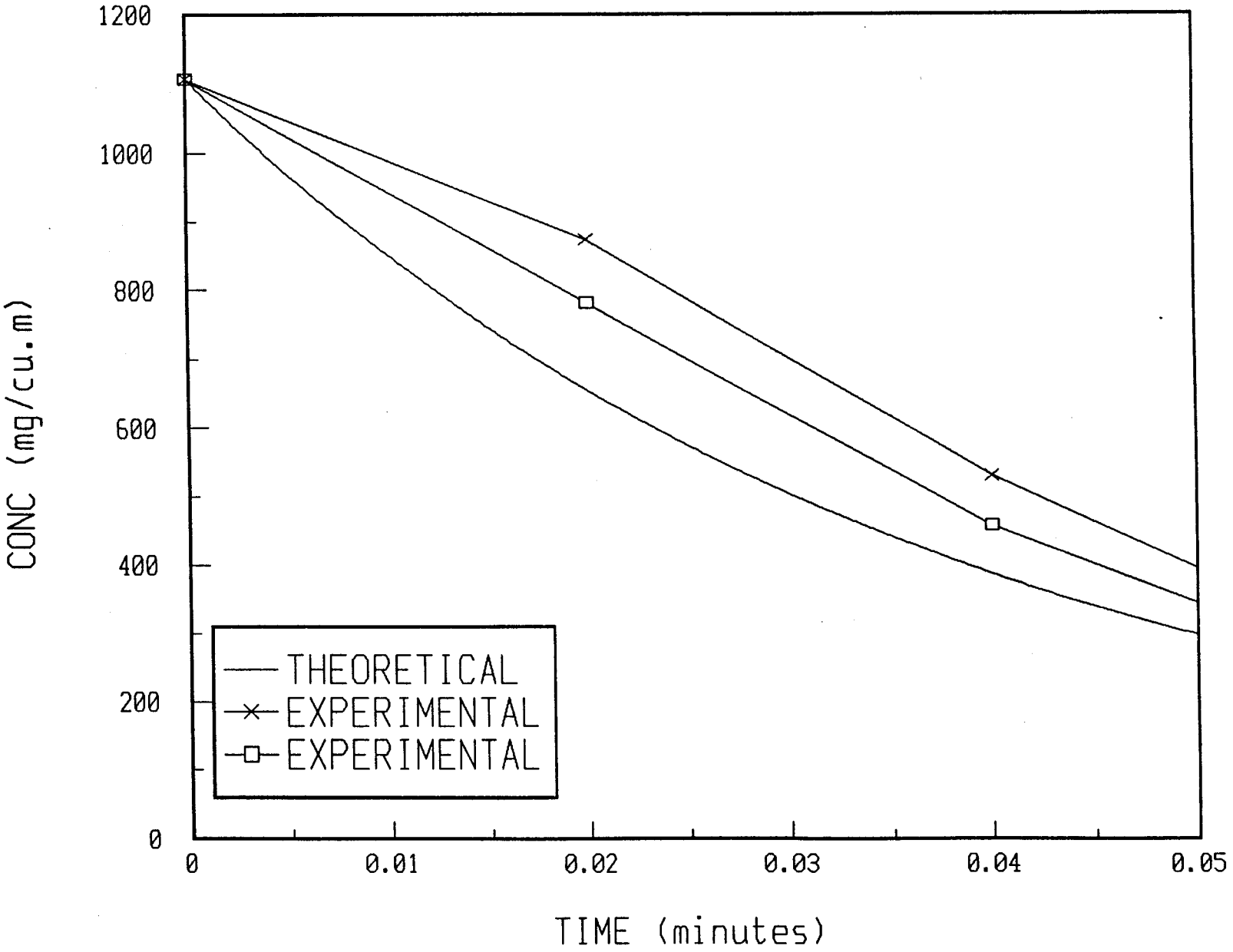


Fig.4: Experimental and theoretical response curves of the chuck
Occ:1107 mg/cu.m; Q: 500 cc/s; V: 1140 cc

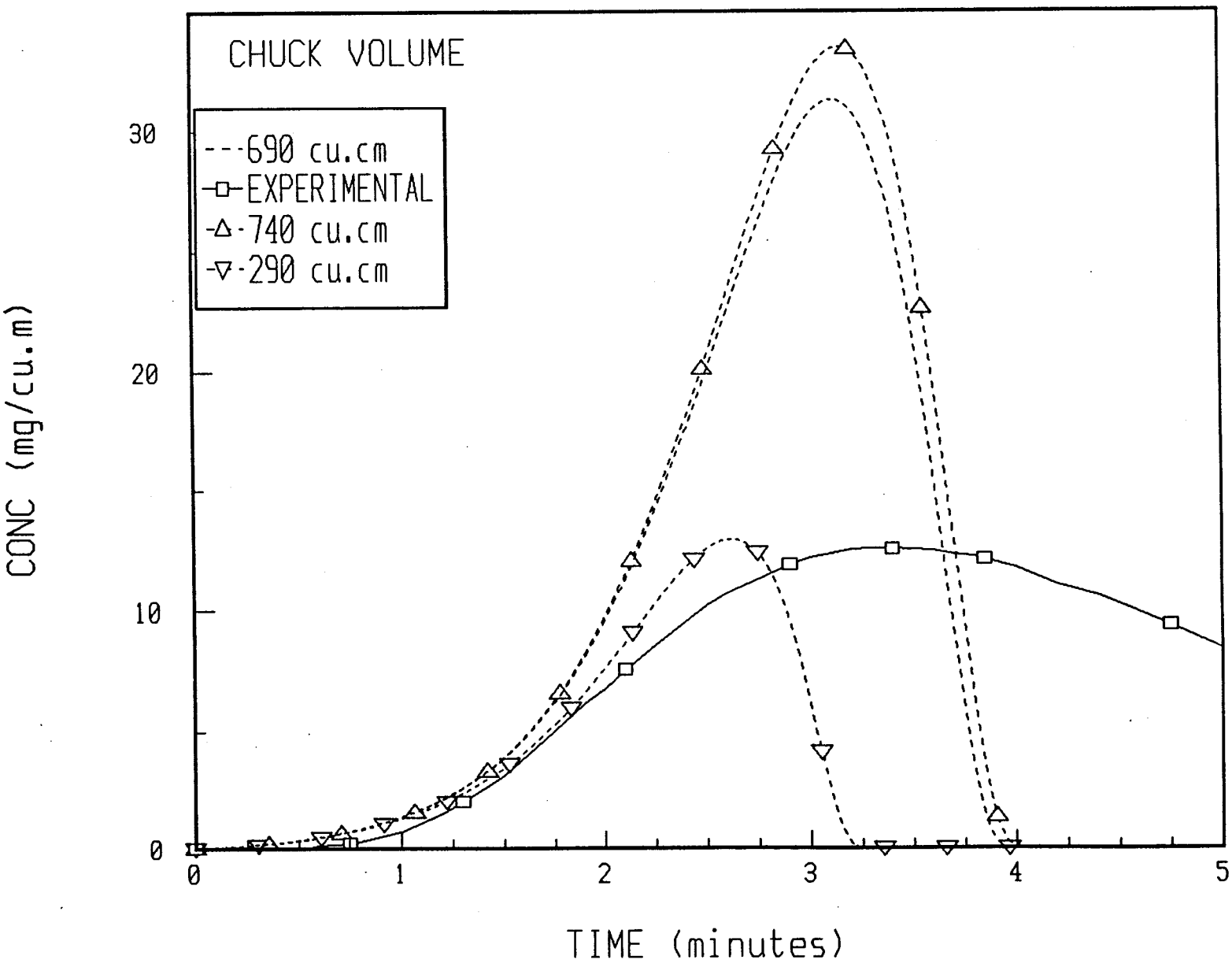


Fig.5: Effect of the chuck volume on the predicted ethane pulse response through an ASC carbon-filled C2 canister

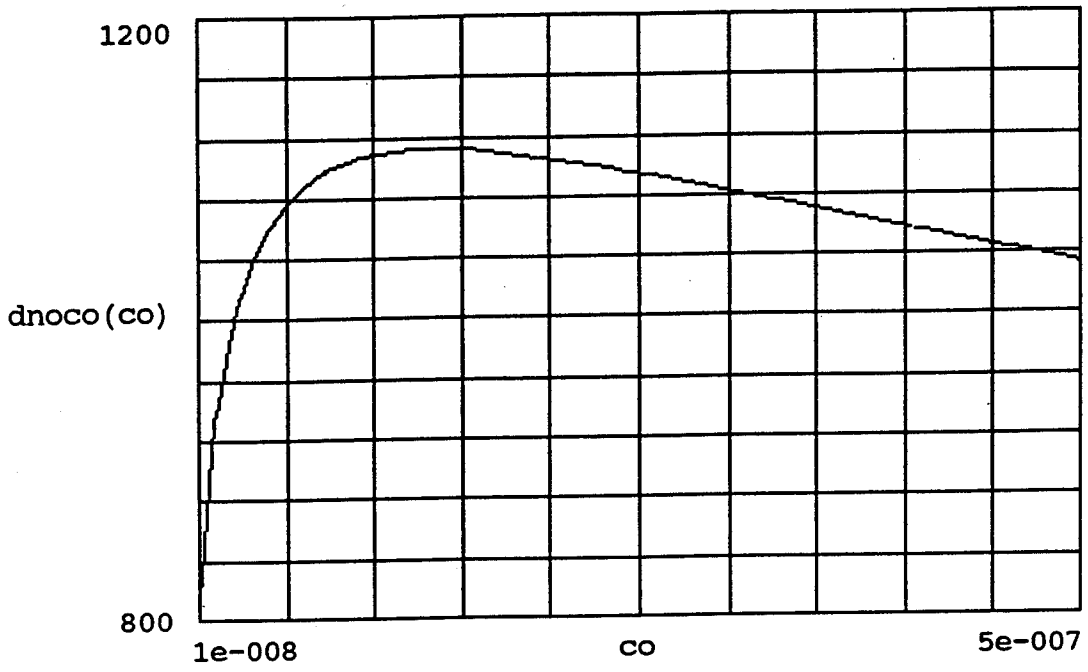


Fig.6: Slope of the D-R equation for the ethane-ASC carbon system

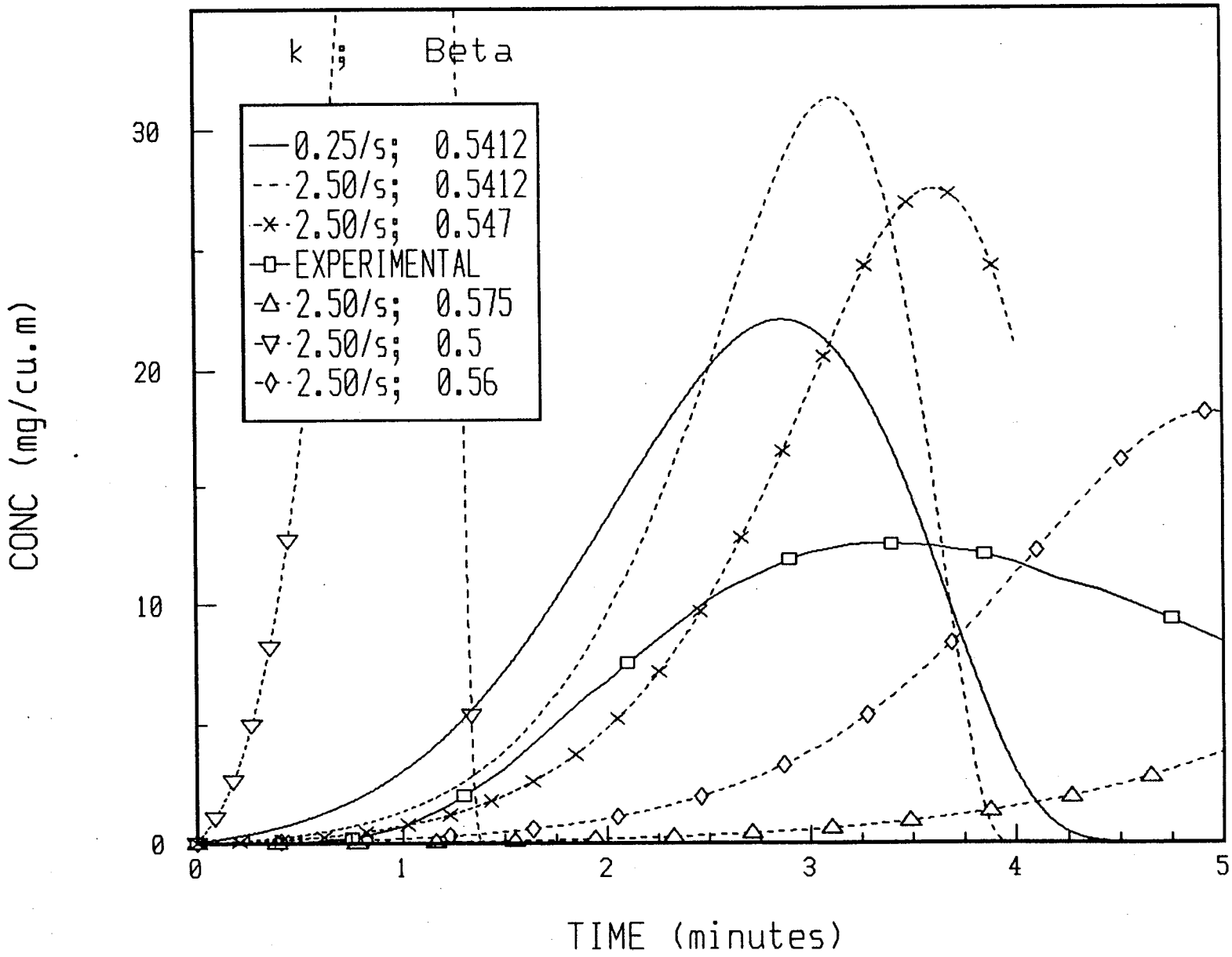


Fig.7: Effect of "$k_{co}$" and "$\beta_o$" on the predicted ethane pulse response curves through ASC carbon-filled C2 canisters

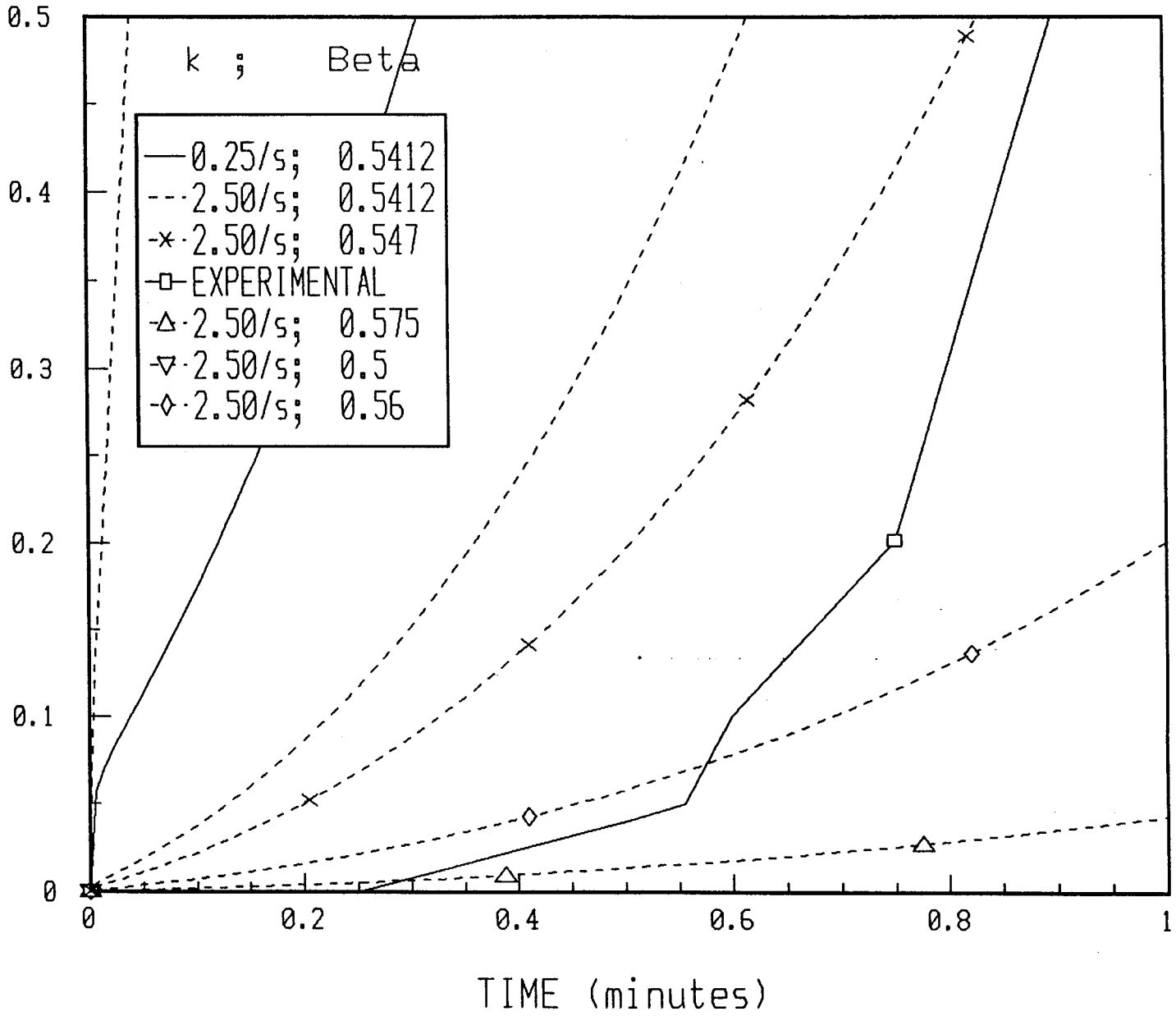


Fig.8: Effect of "$k_{co}$" and "$\beta_o$" on the predicted ethane pulse response curves through ASC carbon-filled C2 canisters

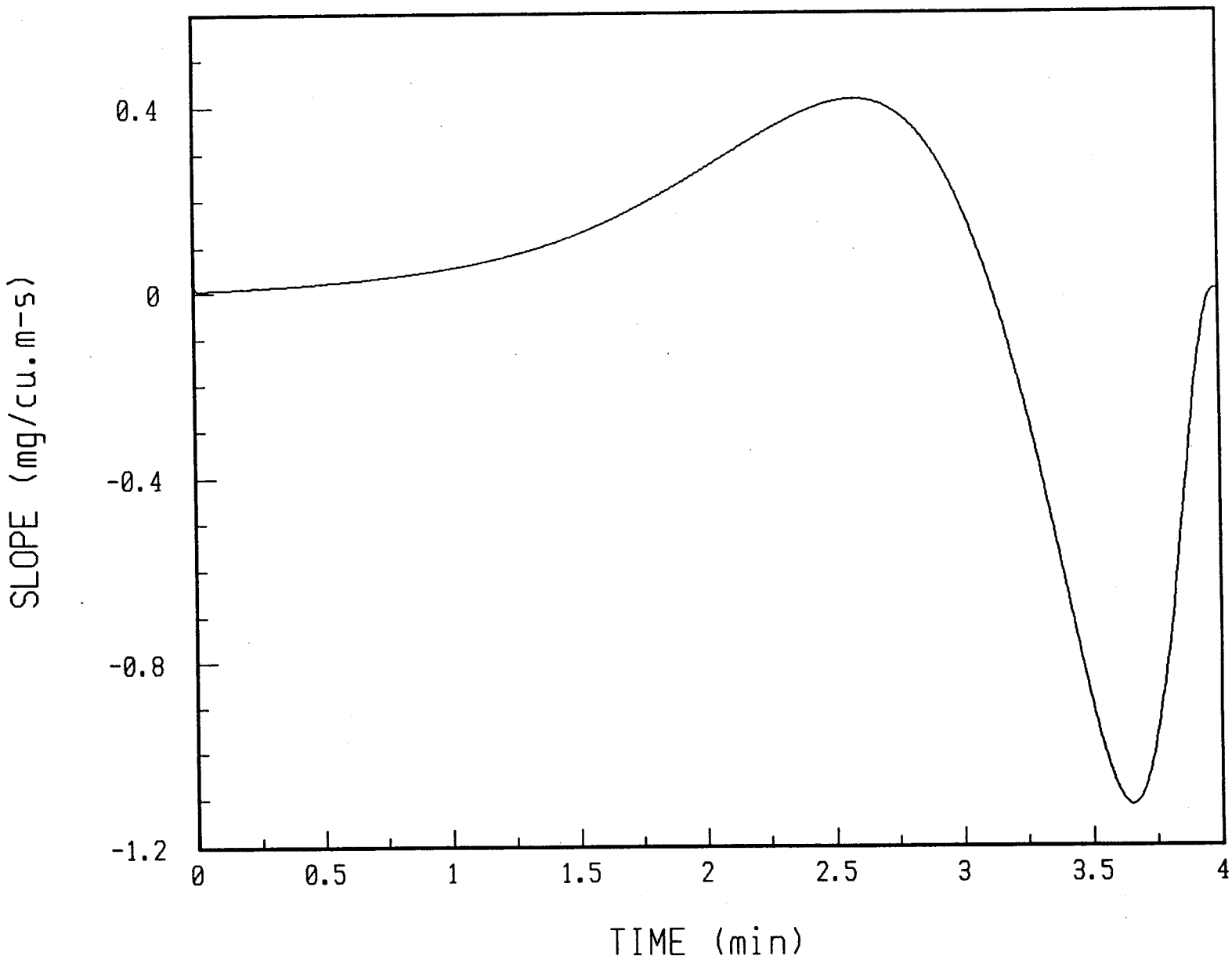


Fig. 9: Slope of the ethane pulse response curve through ASC ASC carbon-filled C2 canister

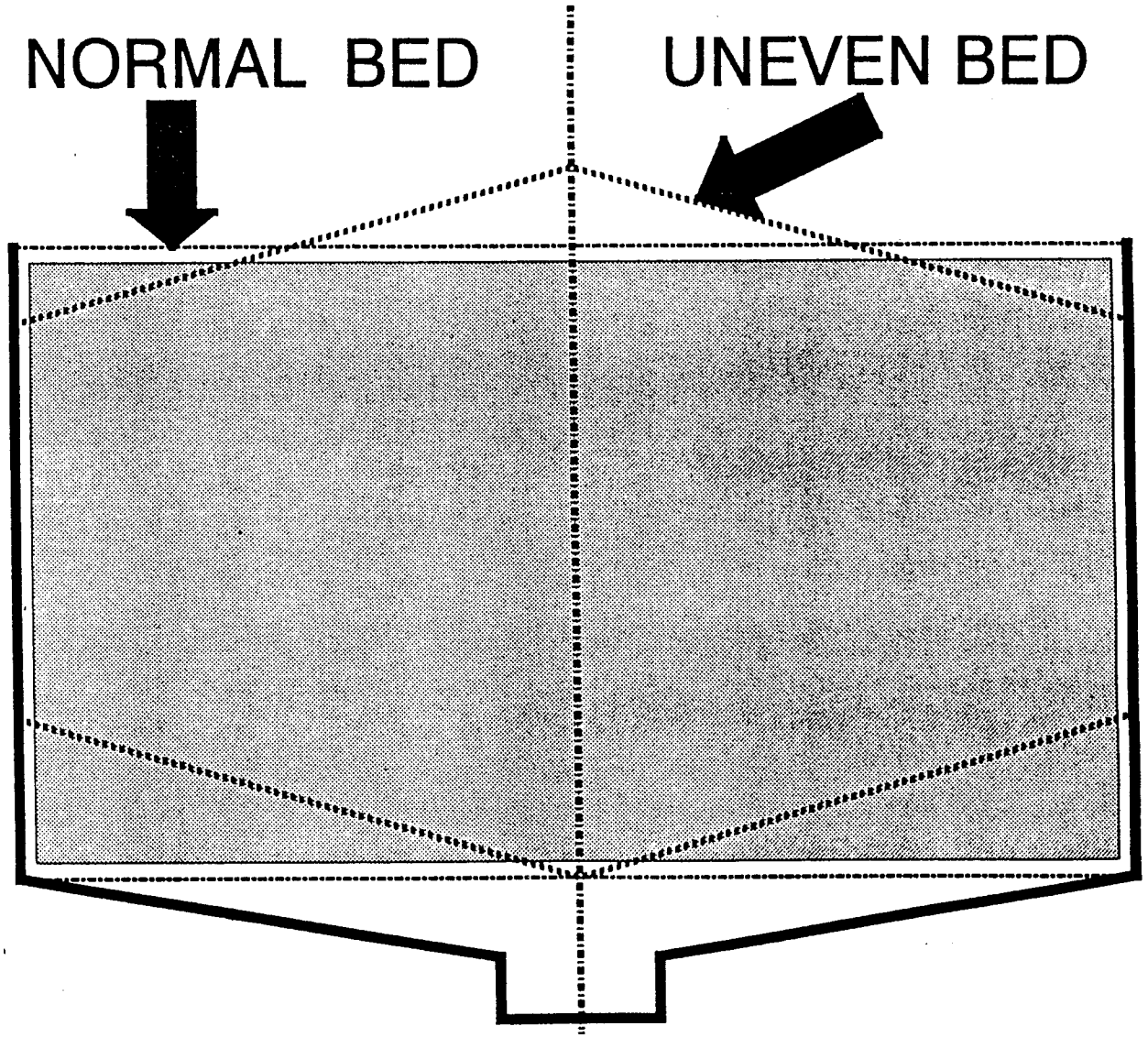


Fig.10: Schematic representation of "Unevenness of the Bed" in a C2 canister

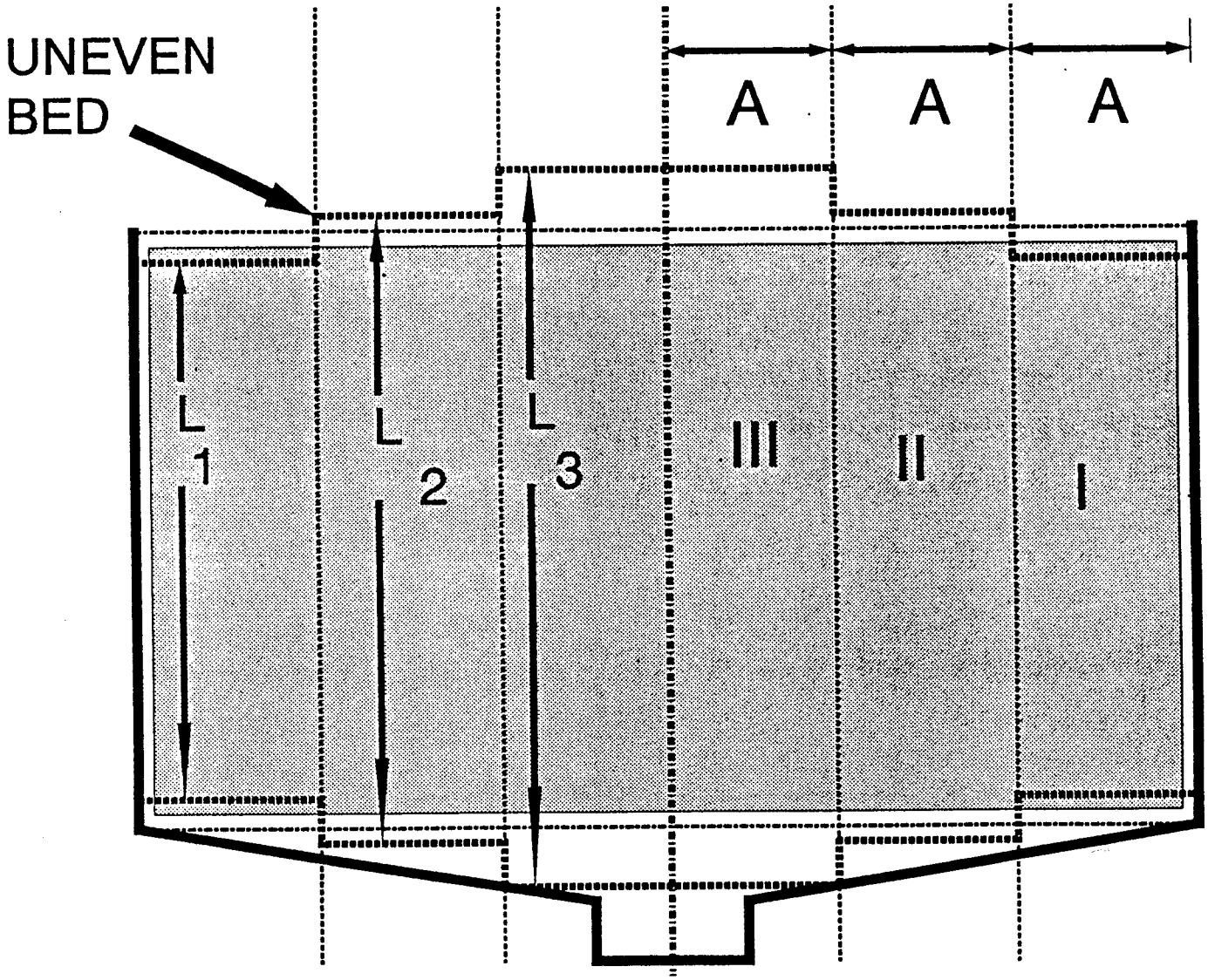


Fig.11: Schematic diagram of a simulated "Uneven" bed in a C2 canister

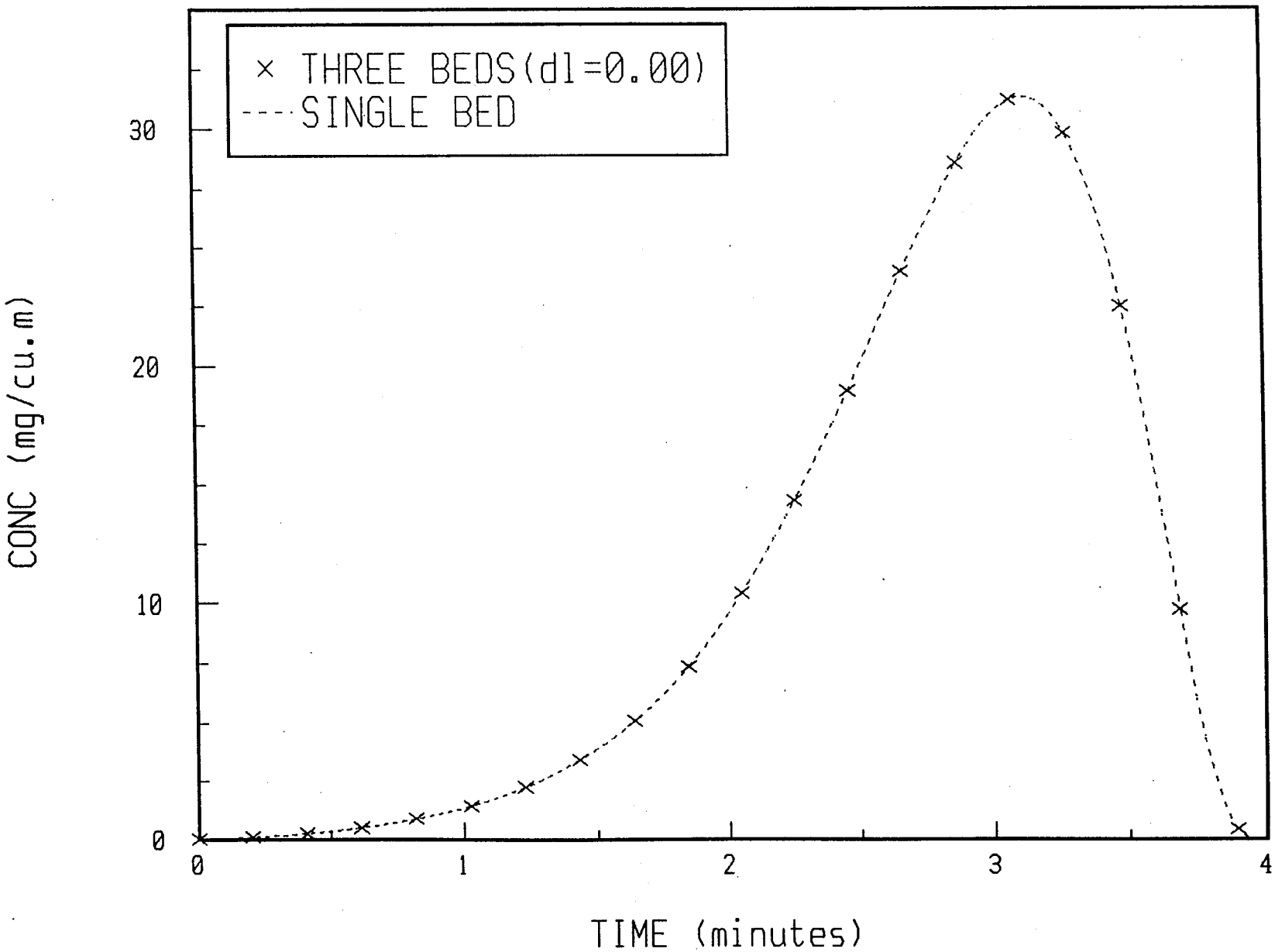


Fig.12: Comparison of predicted ethane pulse response data from single even and uneven beds with L=0.0

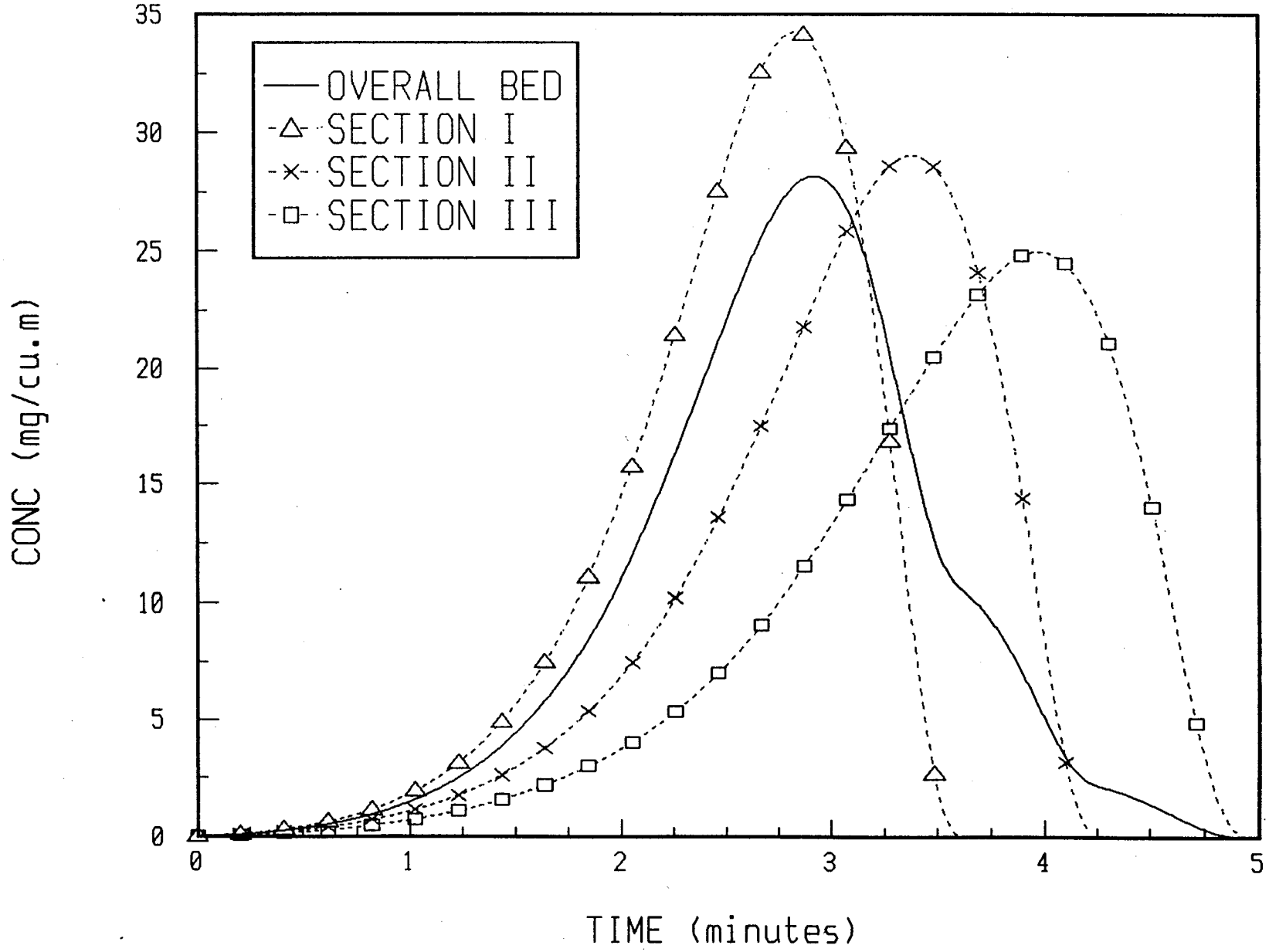


Fig.13: Dry ethane pulse response data from ASC carbon-filled C2 canister with an uneven bed ( L= 0.1 cm)

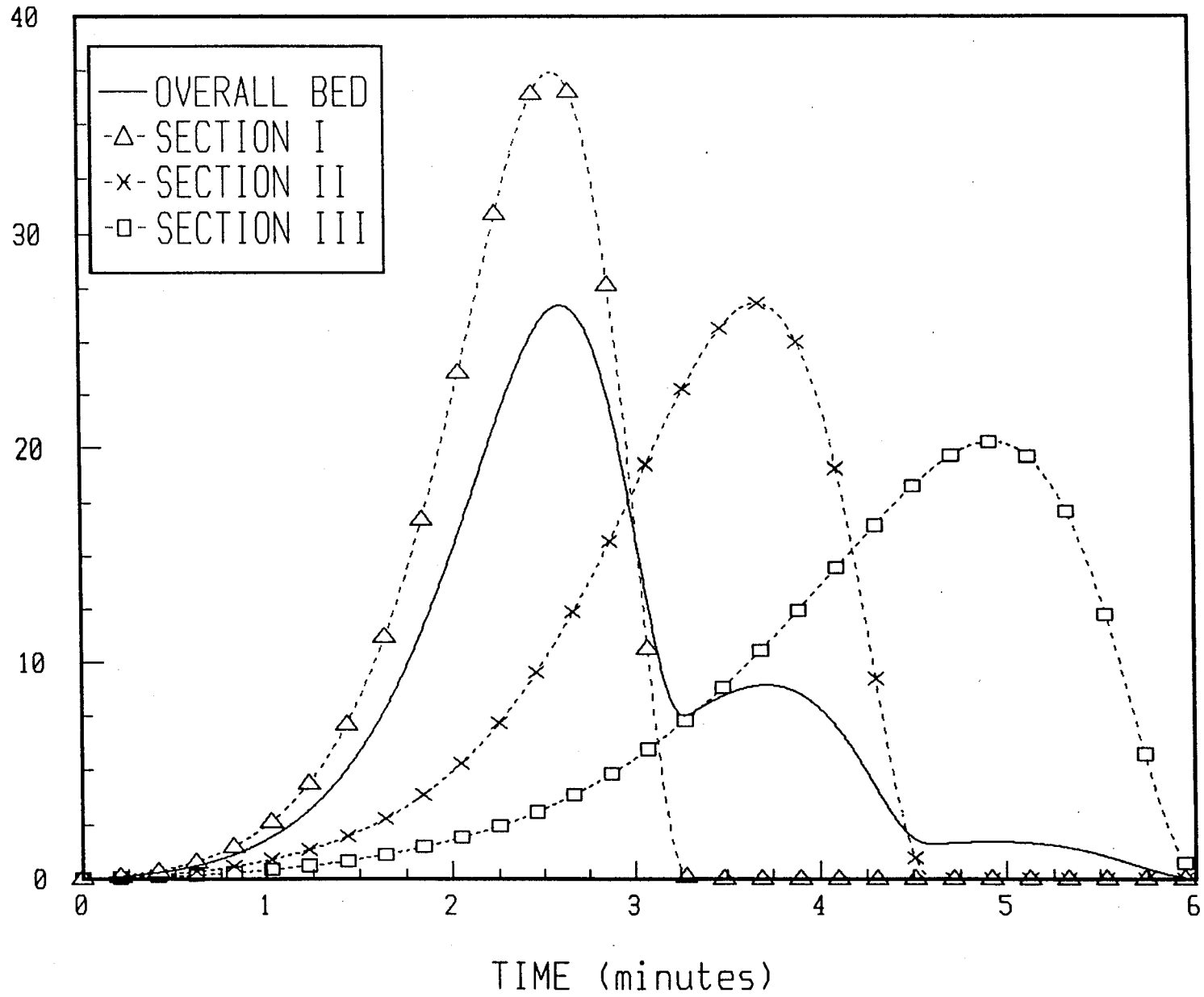


Fig.14: Dry ethane pulse response data from ASC carbon-filled C2 canister with an uneven bed ( L= 0.2 cm)

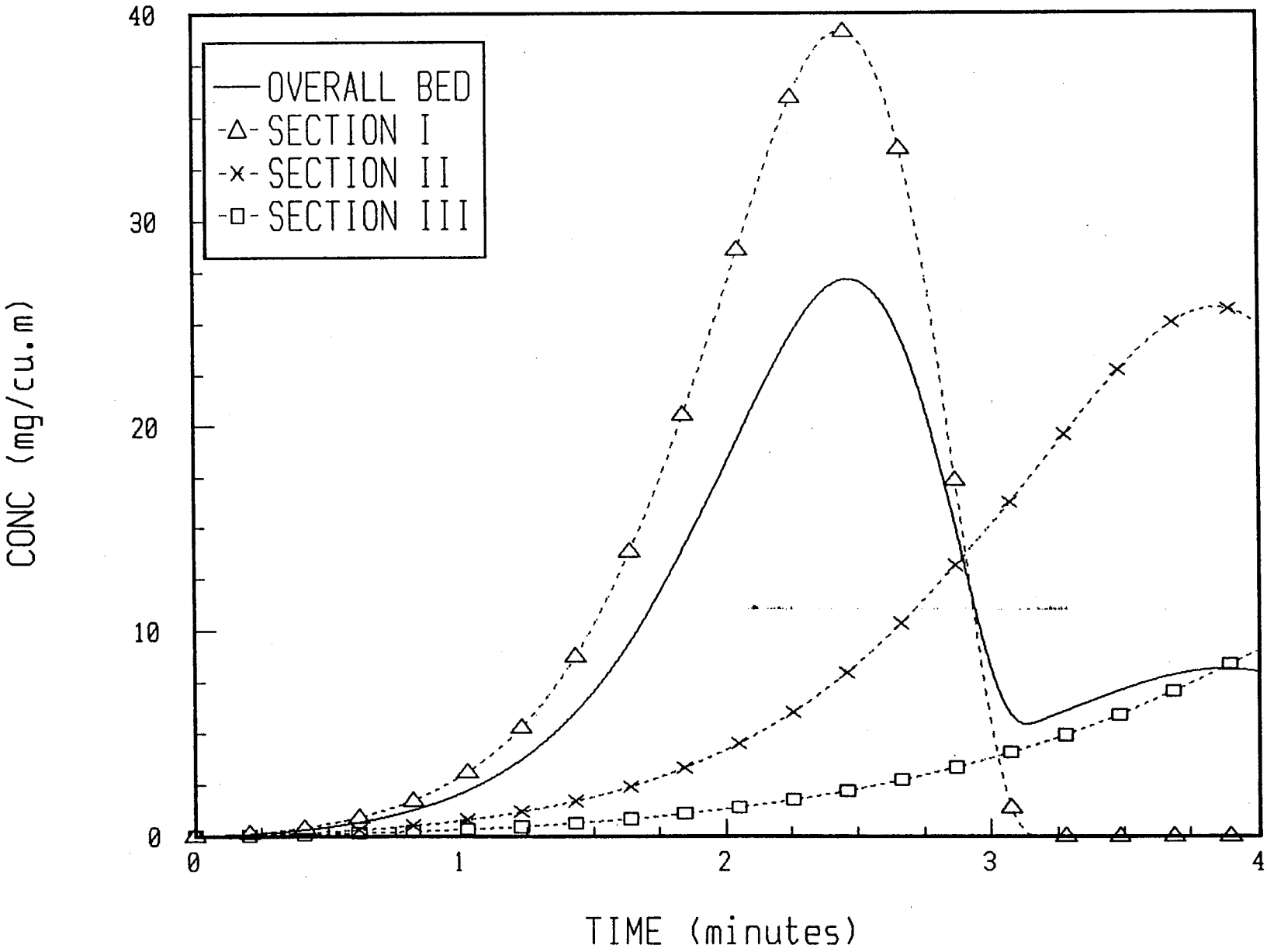


Fig.15: Dry ethane pulse response data from ASC carbon-filled C2 canister with an uneven bed ( L= 0.25 cm)

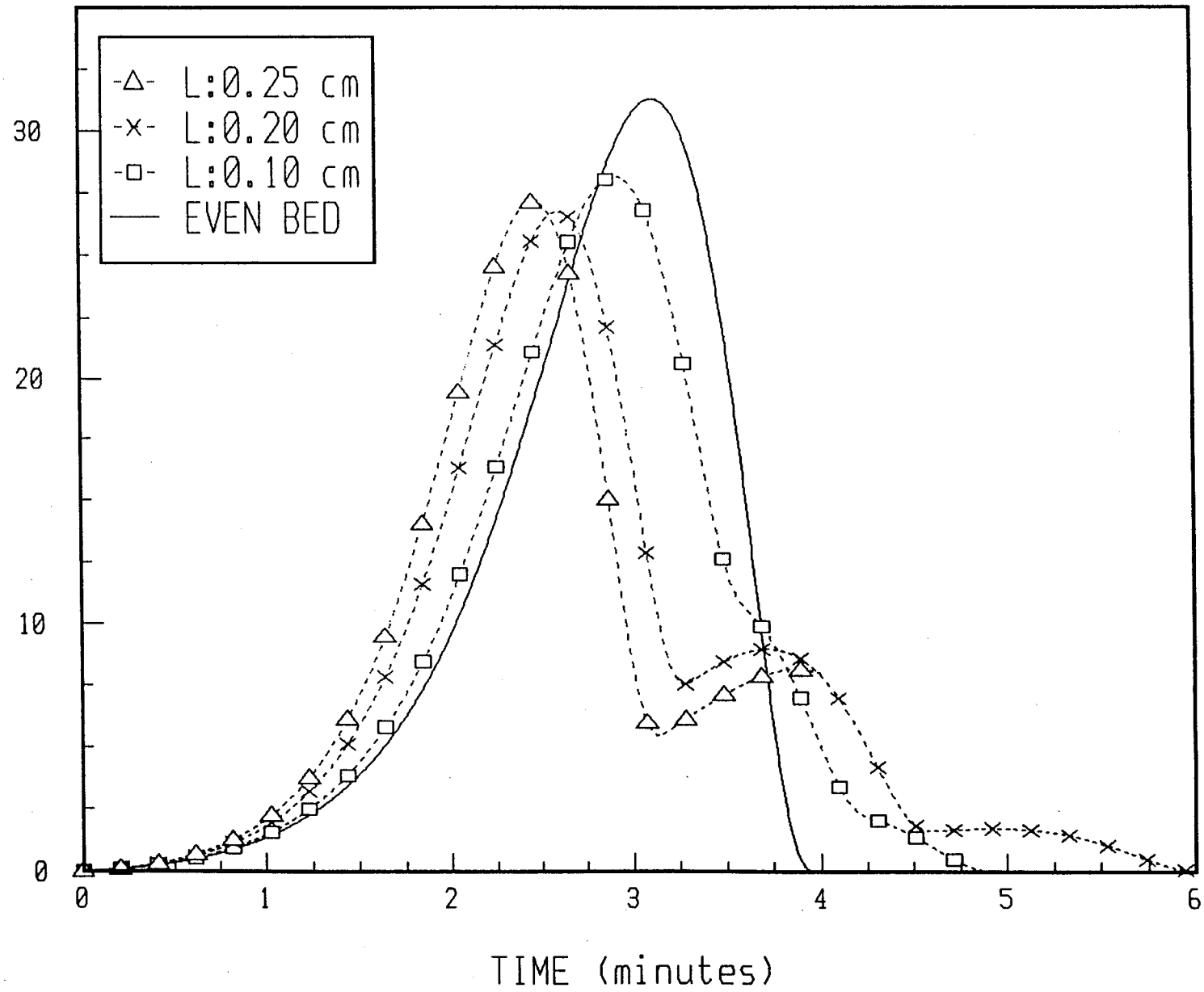


Fig.16: Dry ethane pulse response data from ASC carbon-filled C2 canister: Effect of "Degree of Unevenness"

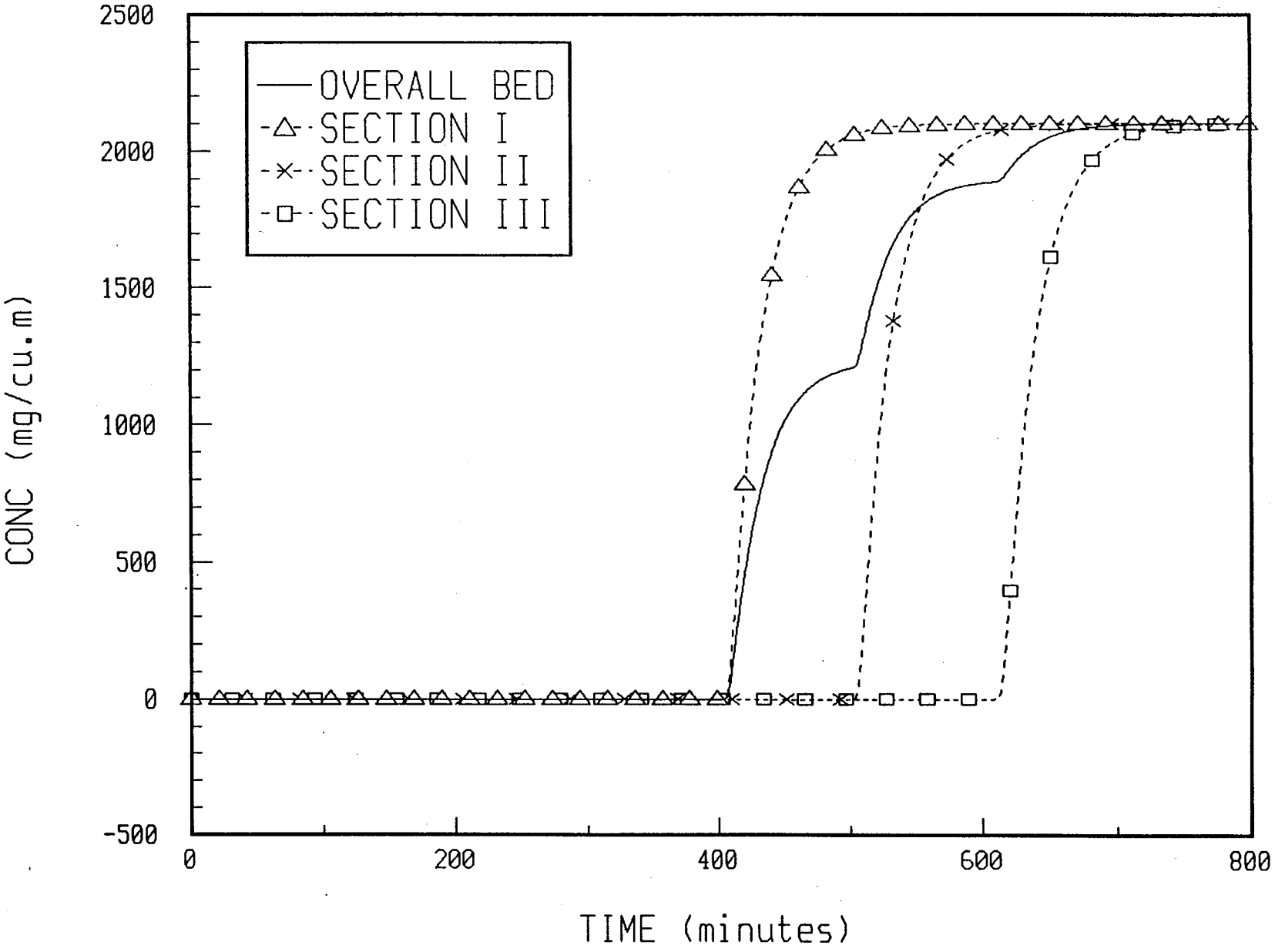


Fig.17: Dry n-octane step response data from ASC carbon-filled C2 canister with an uneven bed ( L= 0.1 cm)

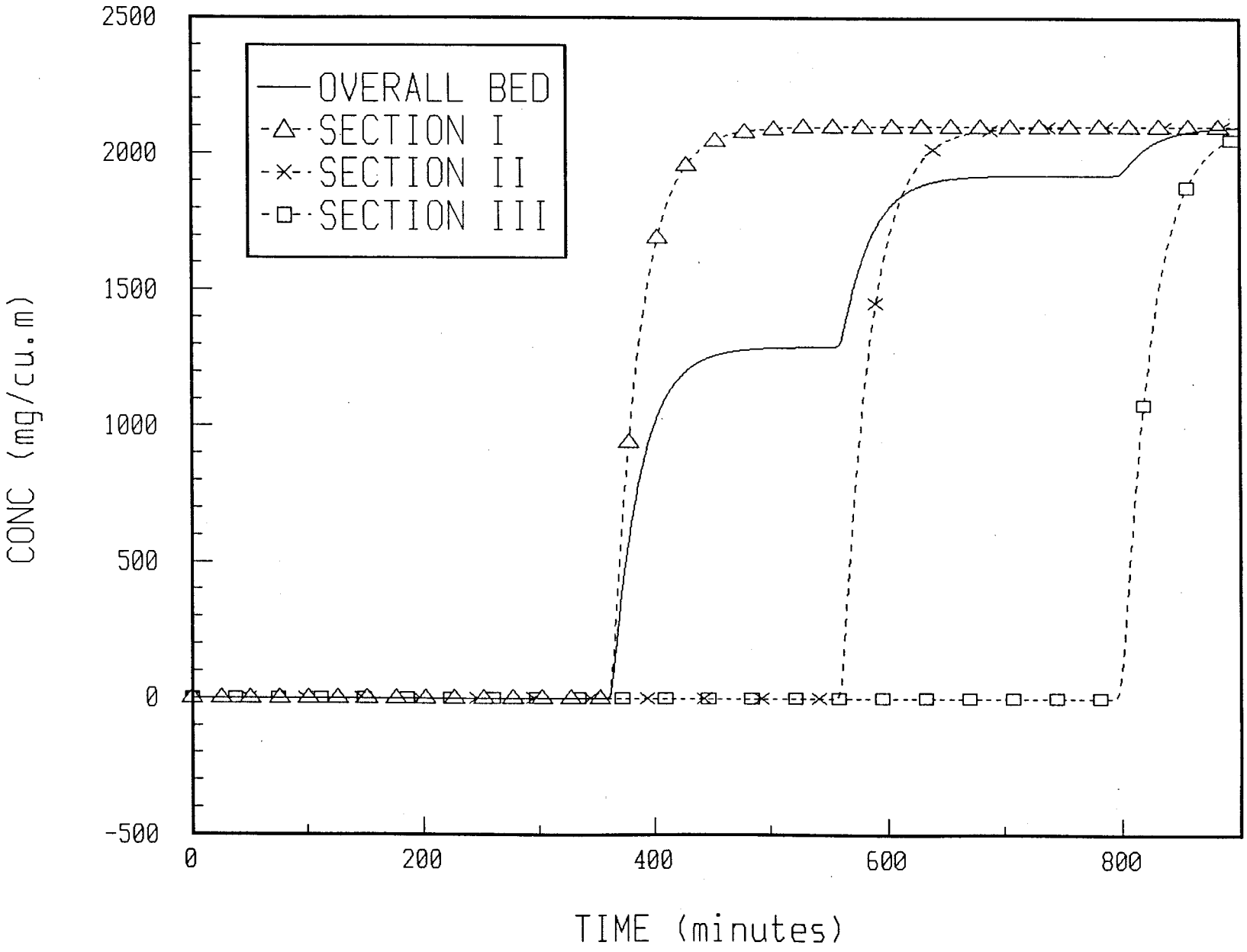


Fig.18: Dry n-octane step response data from ASC carbon-filled C2 canister with an uneven bed ( L= 0.2 cm)

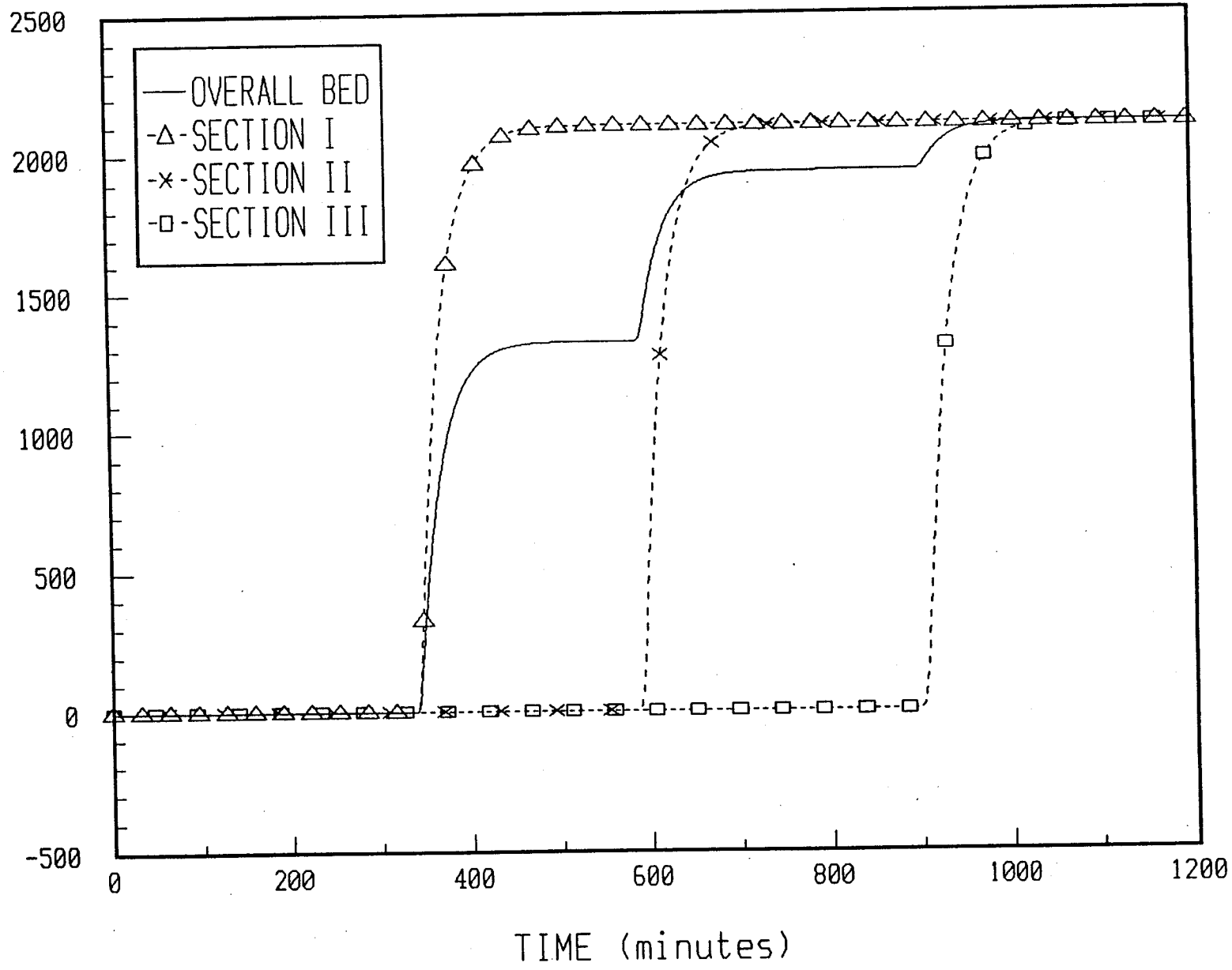


Fig.19: Dry n-octane step response data from ASC carbon-filled C2 canister with an uneven bed ( L= 0.25 cm)

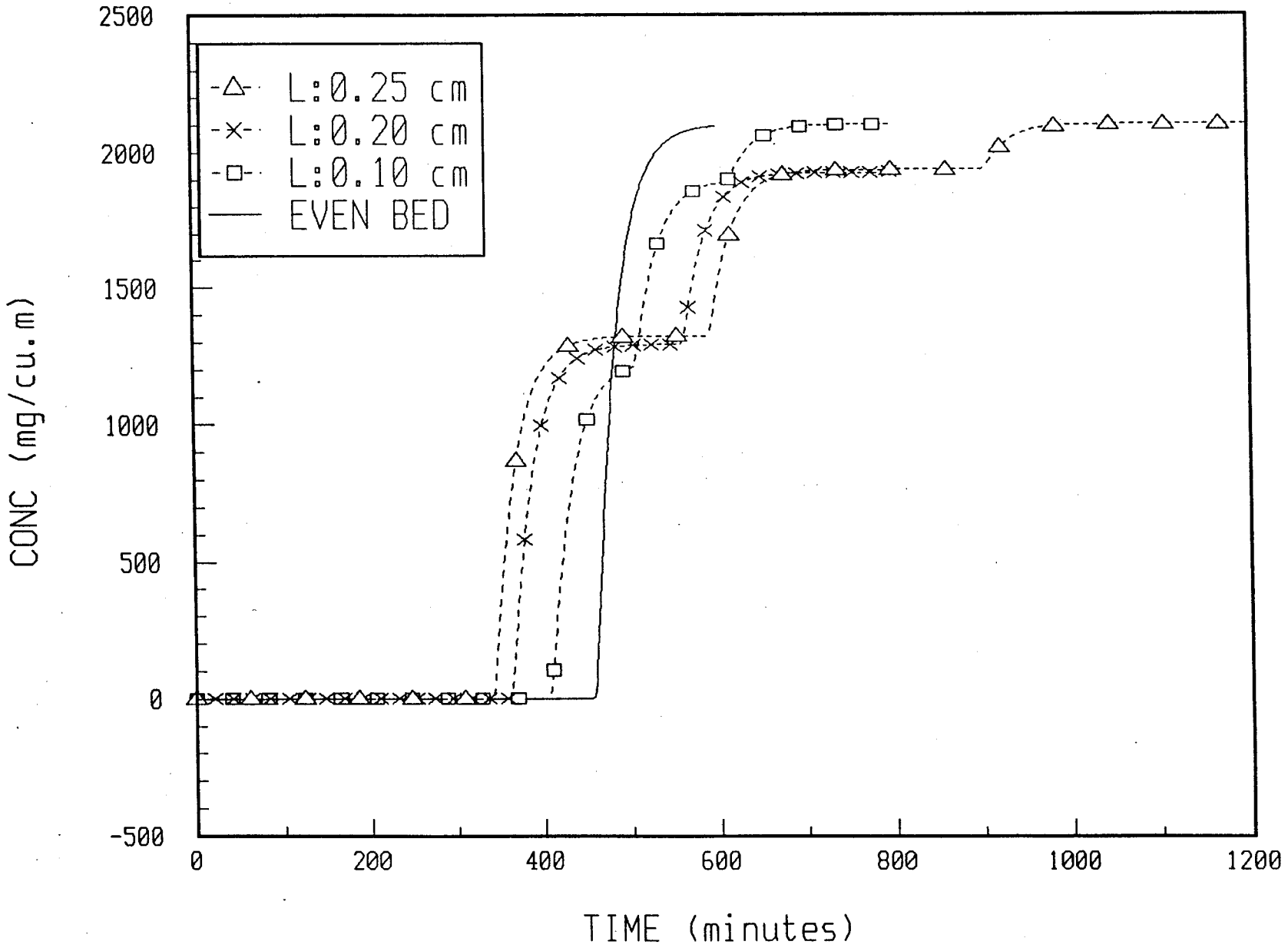


Fig.20: DRY n-octane step response data from ASC carbon-filled C2 canister : Effect of "Degree of Unevenness"

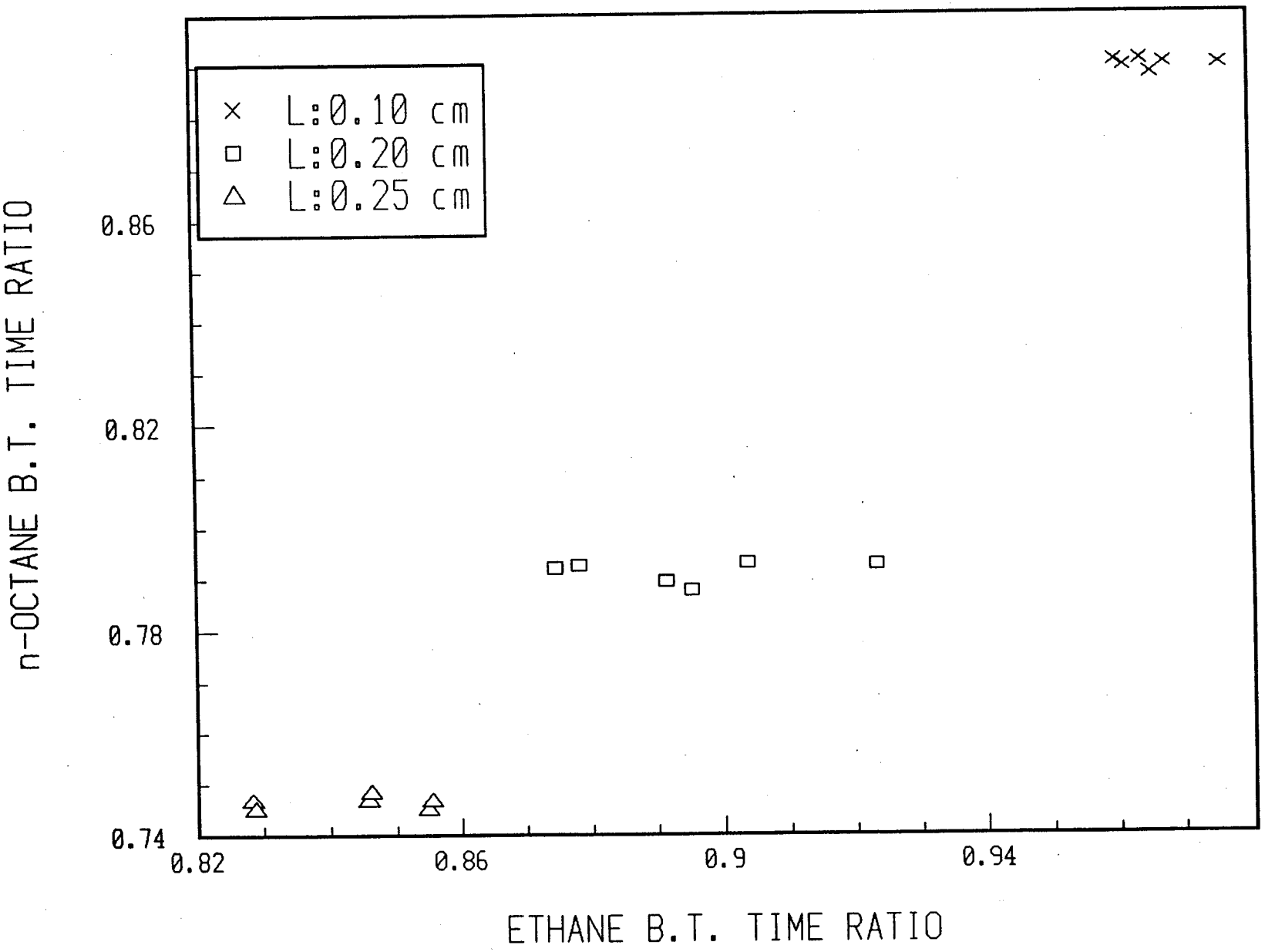


Fig.21: Comparison of ratios of breakthrough times of ethane (pulse) and n-octane (step) for an uneven bed

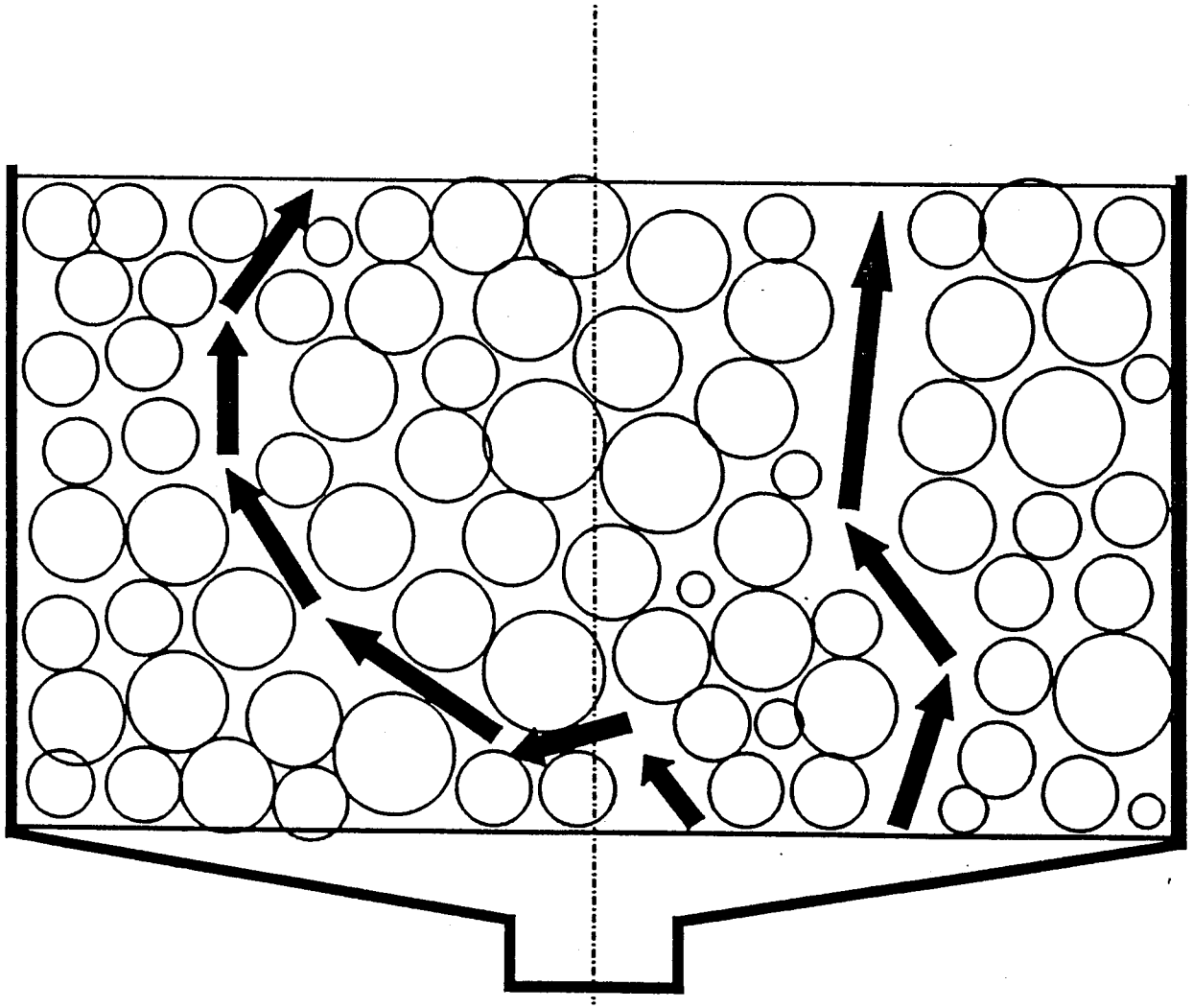

Fig.22: Schematic representation of "Non-uniformity of the Bed" in a C2 canister

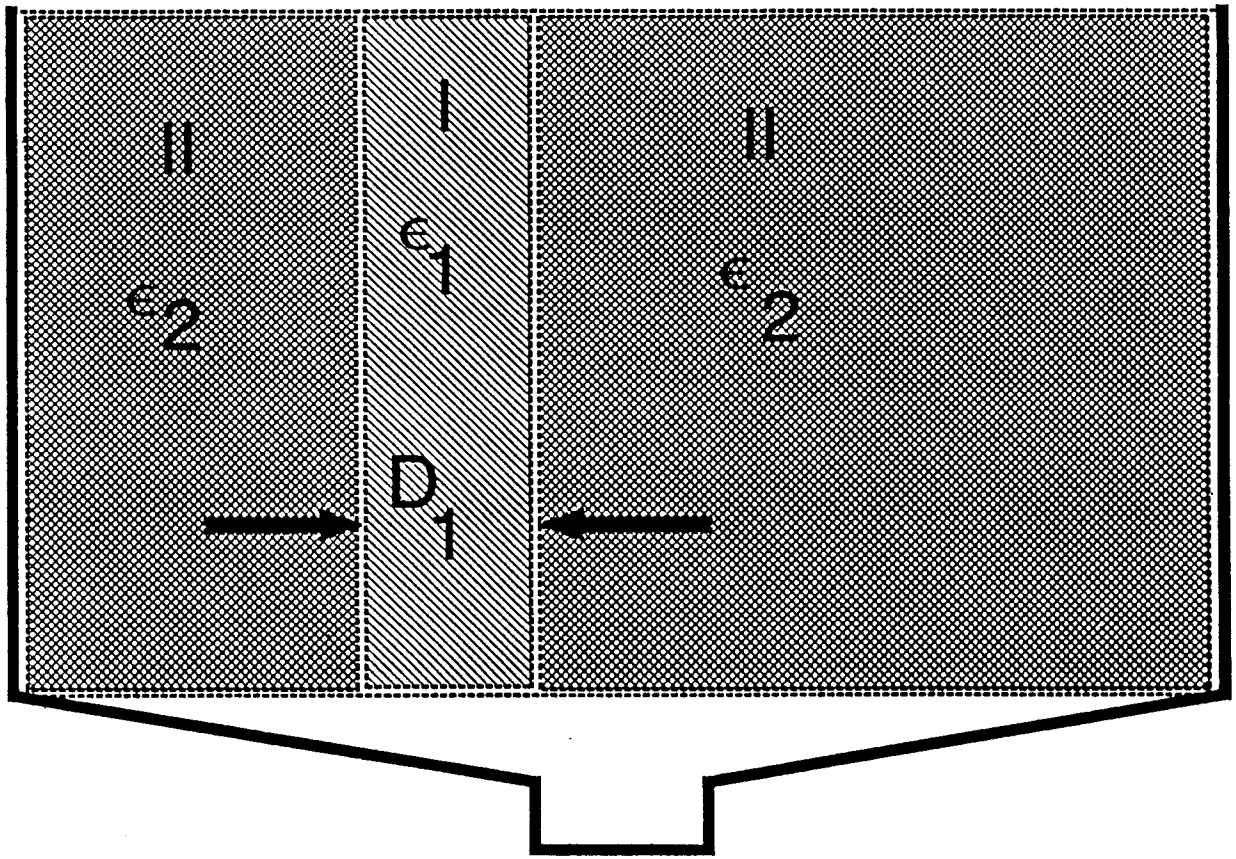


Fig.23: Schematic diagram of a simulated "Non-uniform" bed in a C2 canister

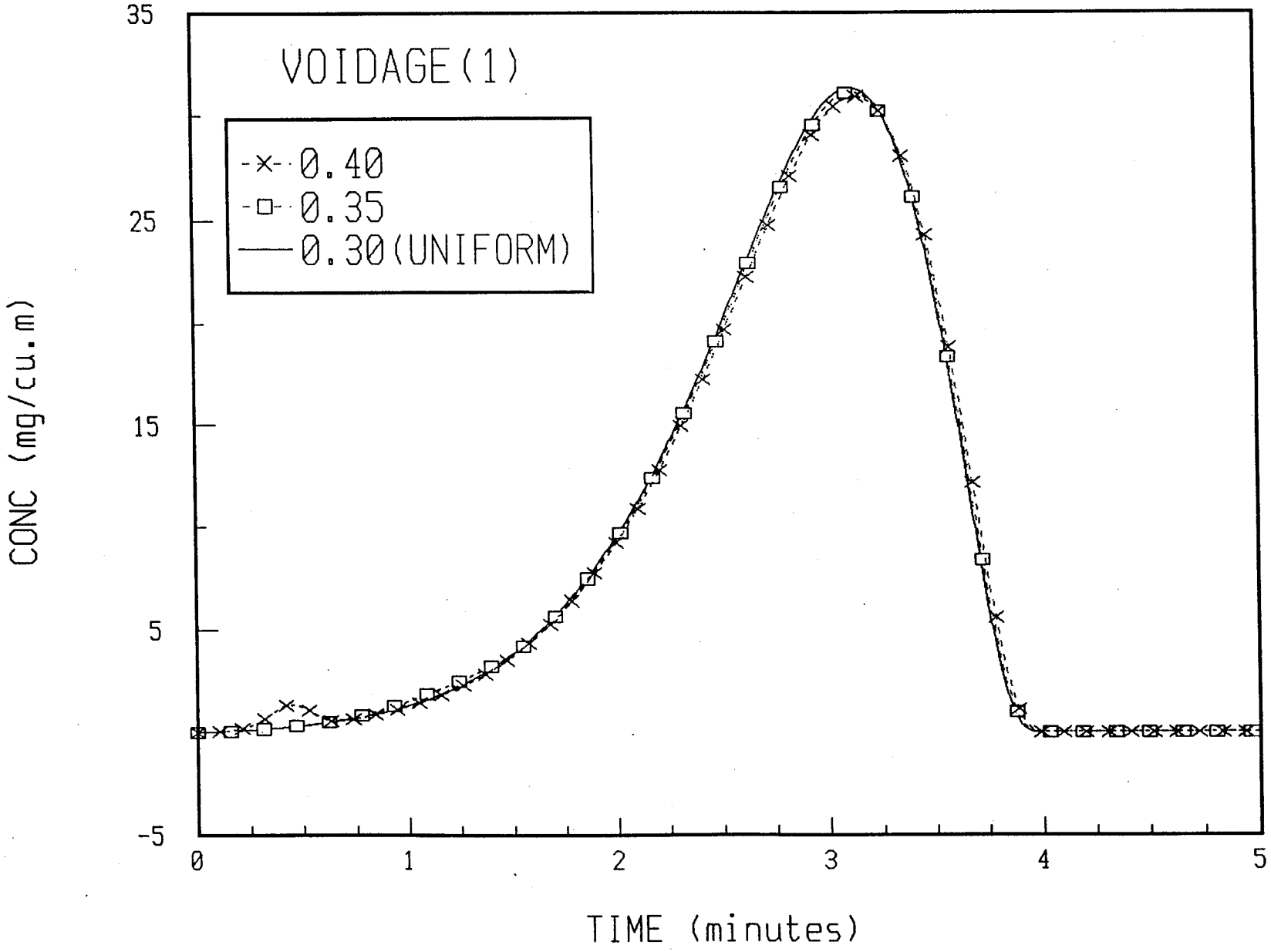


Fig.24: Dry ethane pulse response data through an ASC carbon filled C2 canister with a non-uniform bed (d1:0.5 cm)

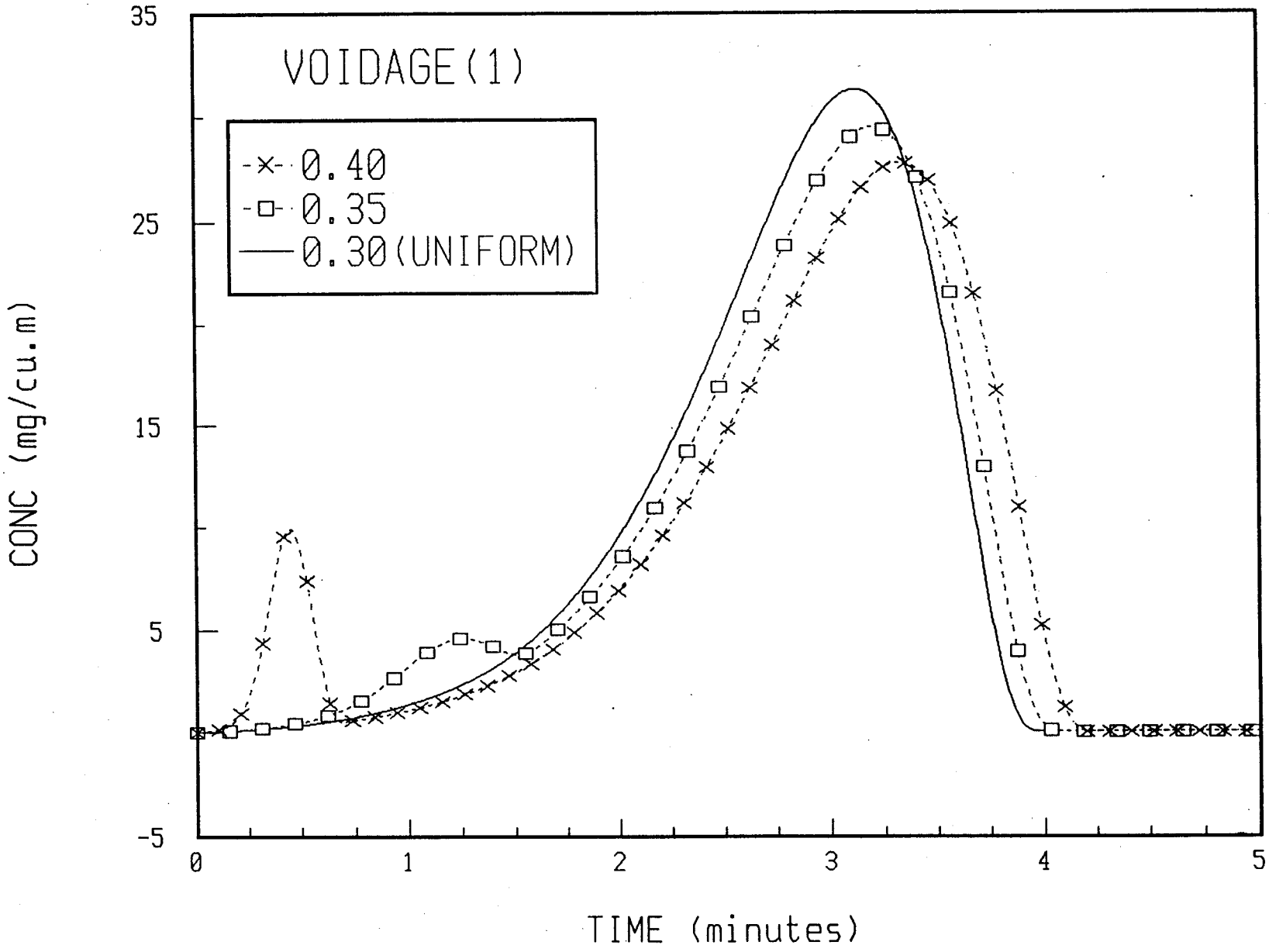


Fig.25: Dry ethane pulse response data through an ASC carbon-filled C2 canister with a non-uniform bed (d1:1.5 cm)

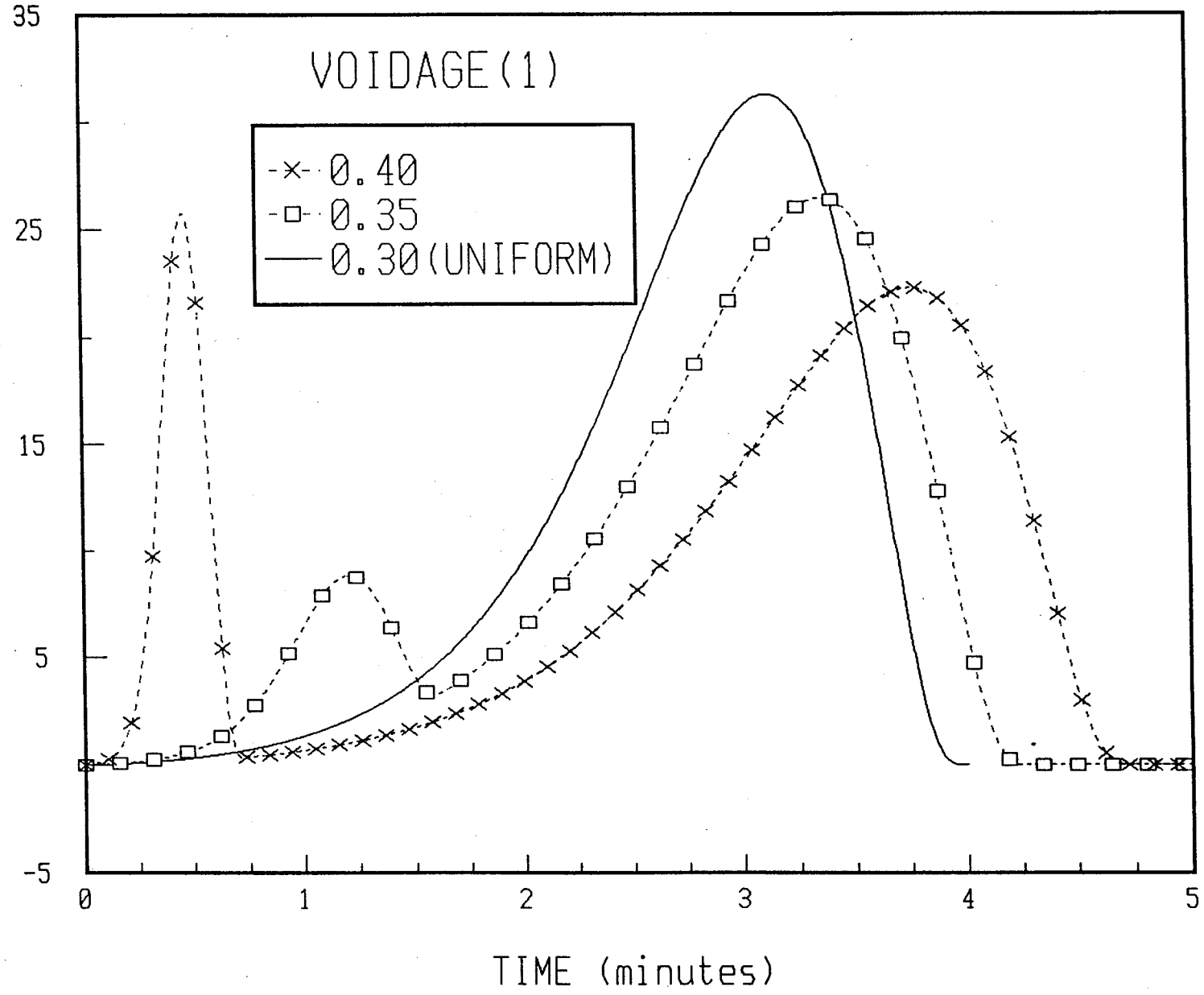


Fig.26: Dry ethane pulse response data through an ASC carbon-filled C2 canister with a non-uniform bed (d1:2.5 cm)

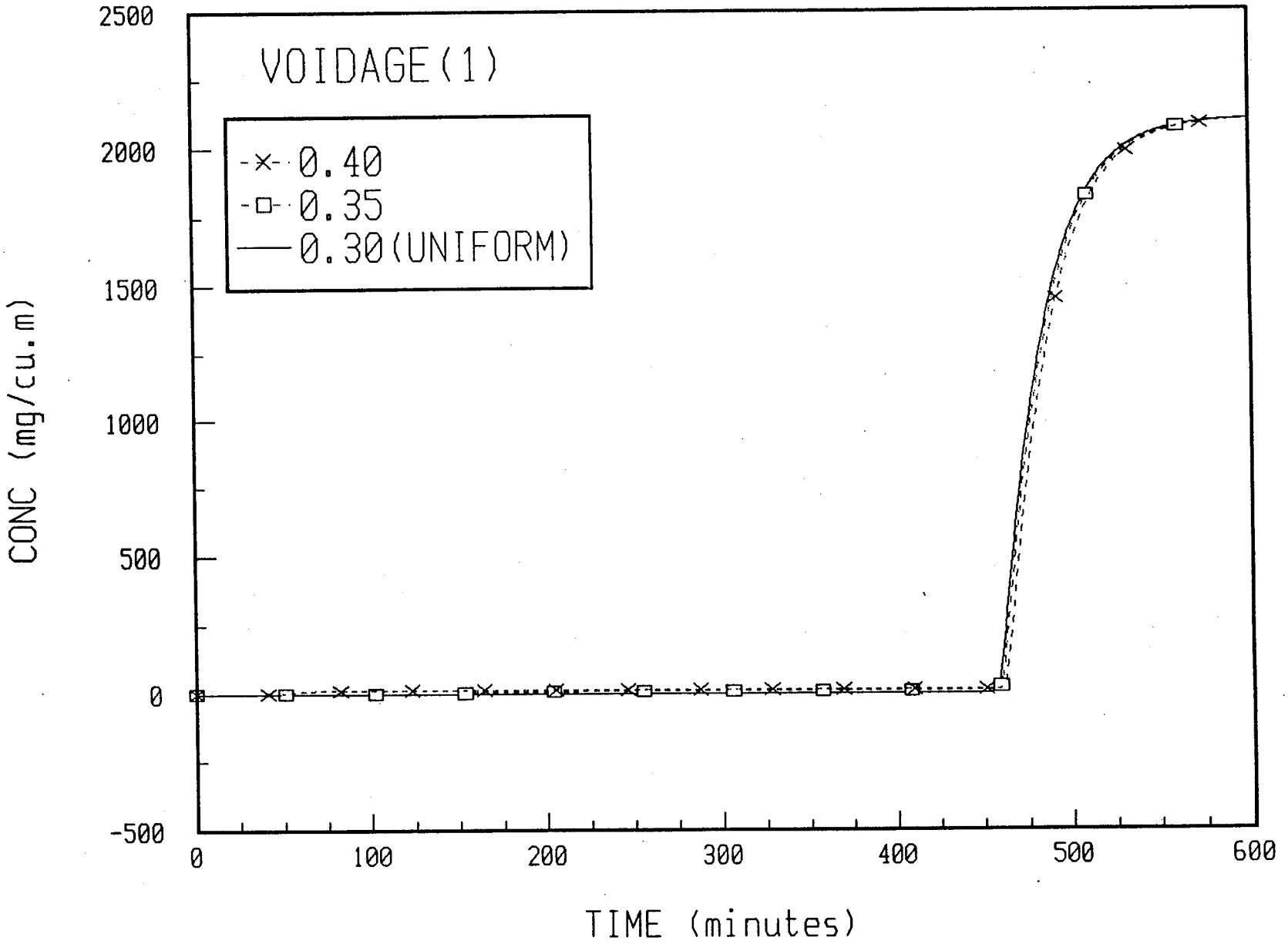


Fig.27: Dry n-octane step response data for an ASC carbon-filled C2 canister with a non-uniform bed (d1:0.5 cm)

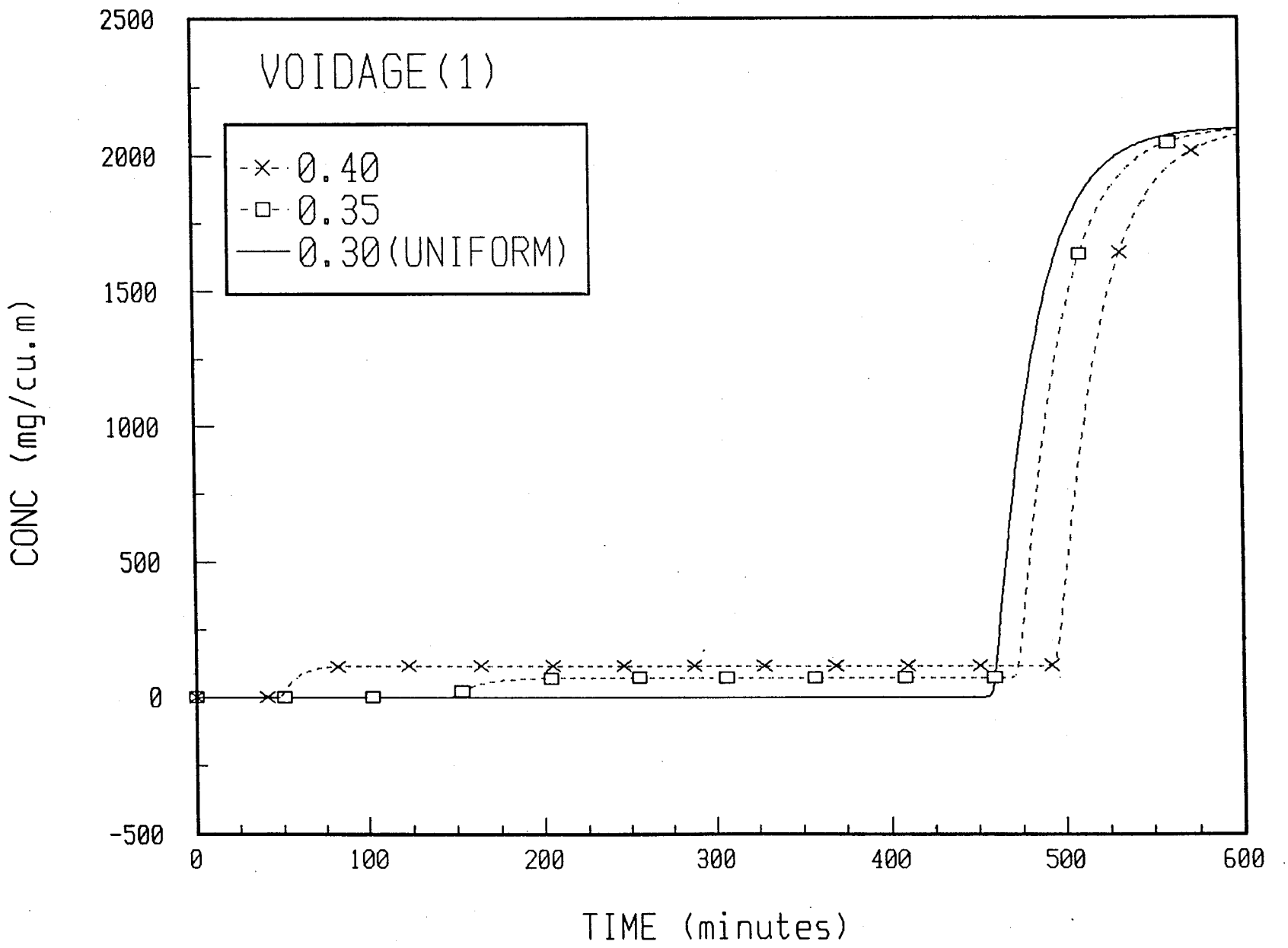


Fig.28: Dry n-octane step response data for an ASC carbon-filled C2 canister with a non-uniform bed (d1:1.5 cm)

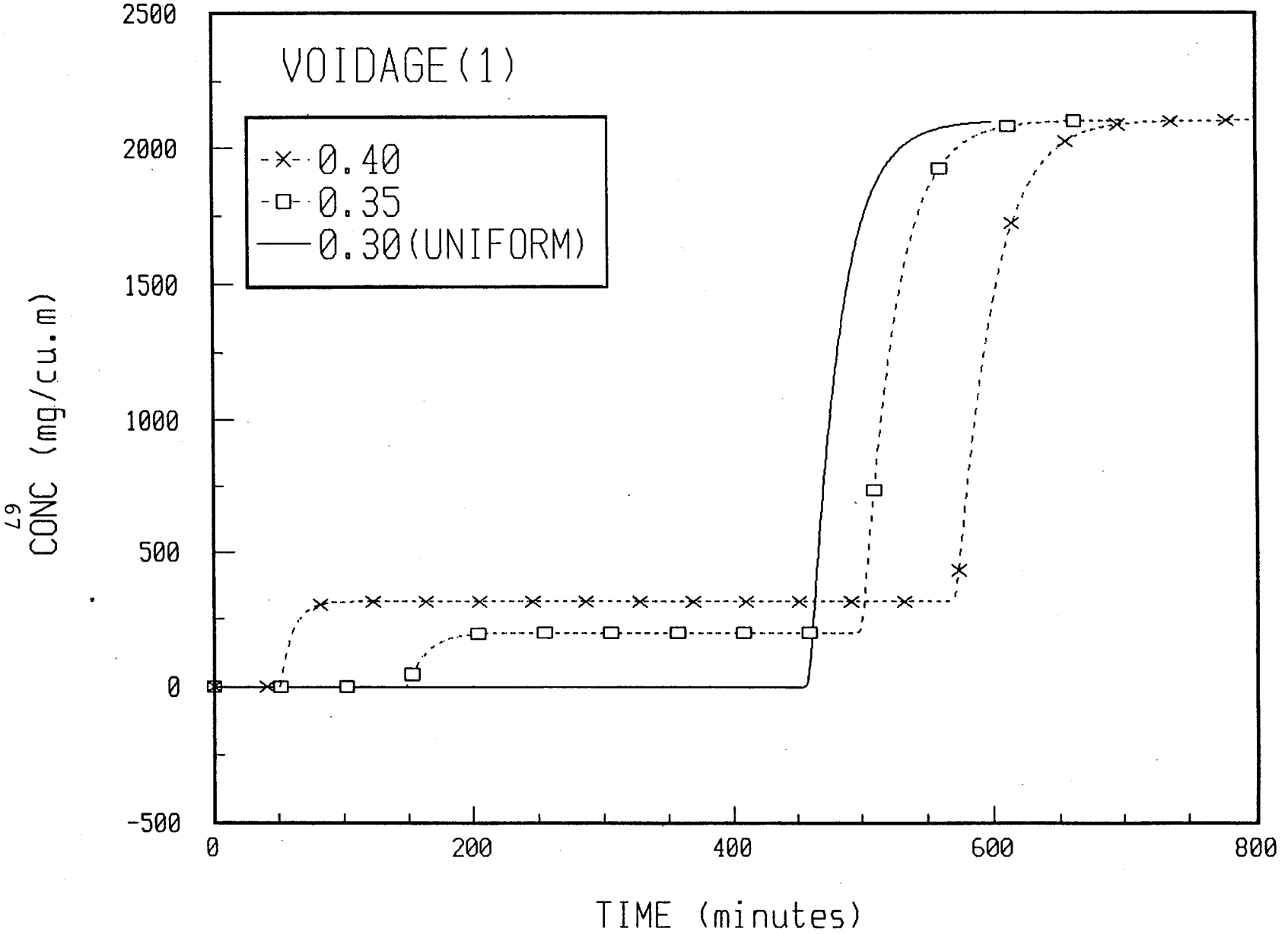


Fig.29: Dry n-octane step response data for an ASC carbon-filled C2 canister with a non-uniform bed (d1:2.5 cm)

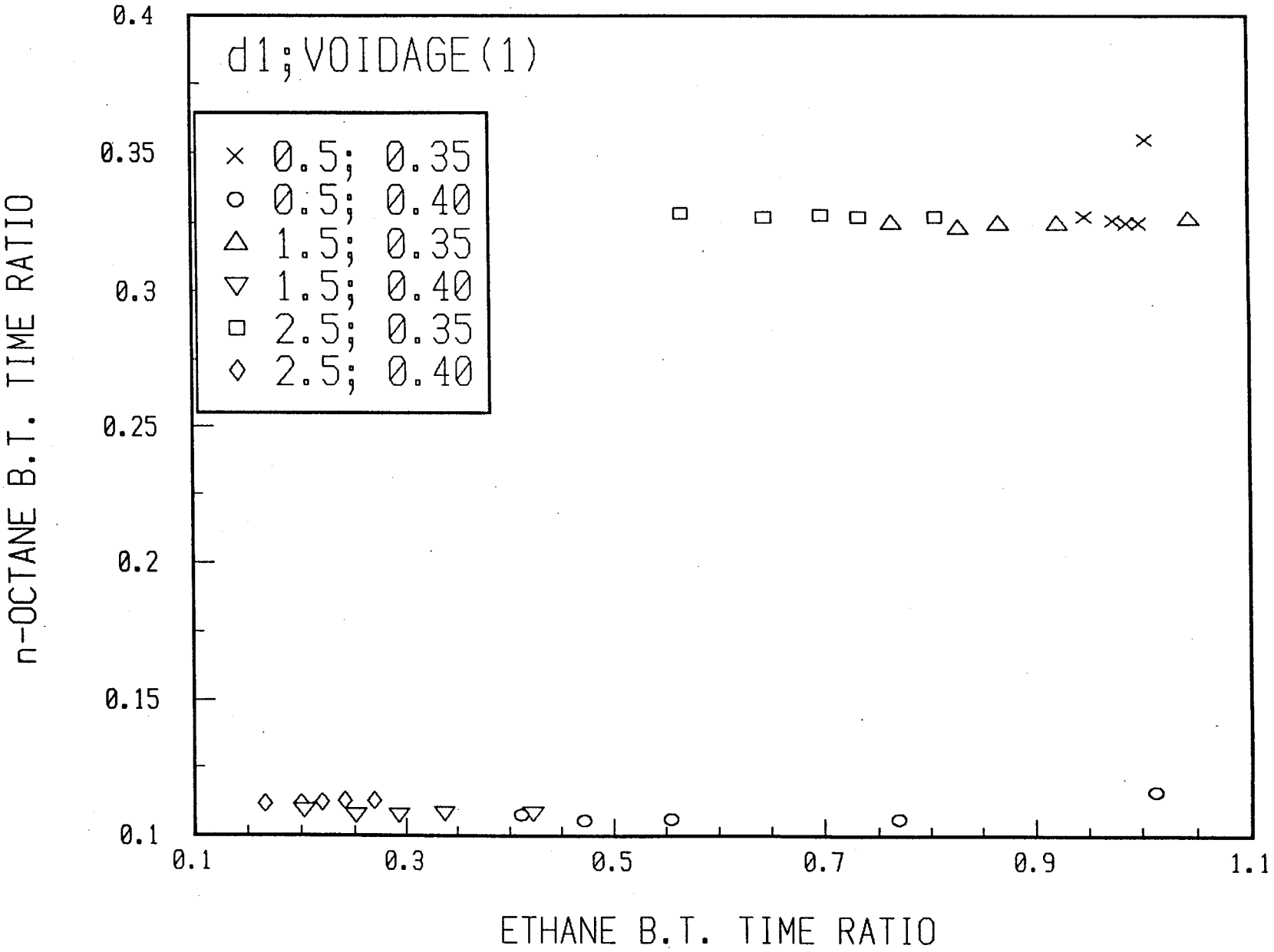


Fig.30: Comparison of ratios of breakthrough times of ethane (pulse) and n-octane (step) for a non-uniform bed

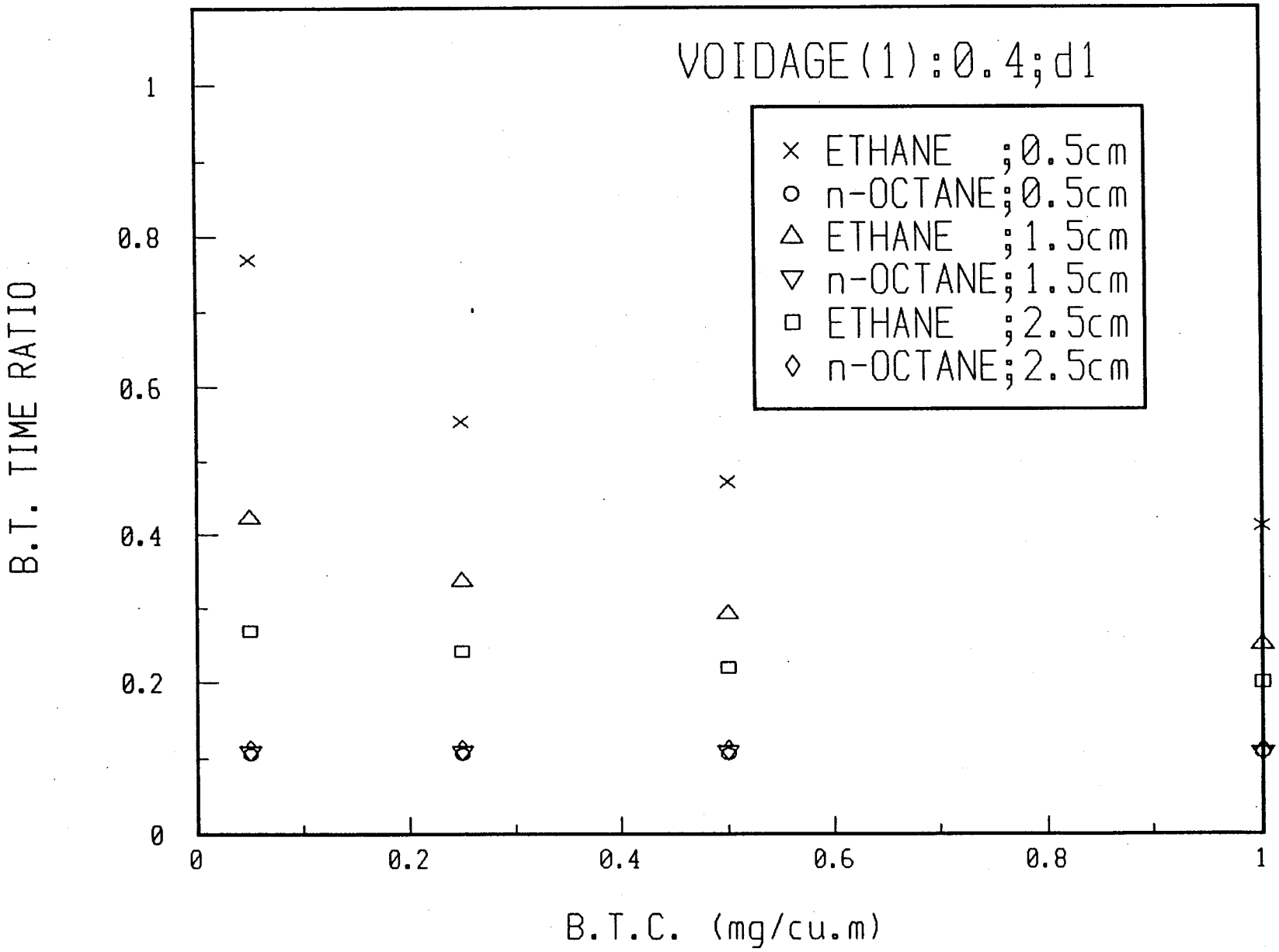


Fig.31: Ratio of breakthrough times of ethane and n-octane for an ASC carbon-filled C2 canister with a non-uniform bed

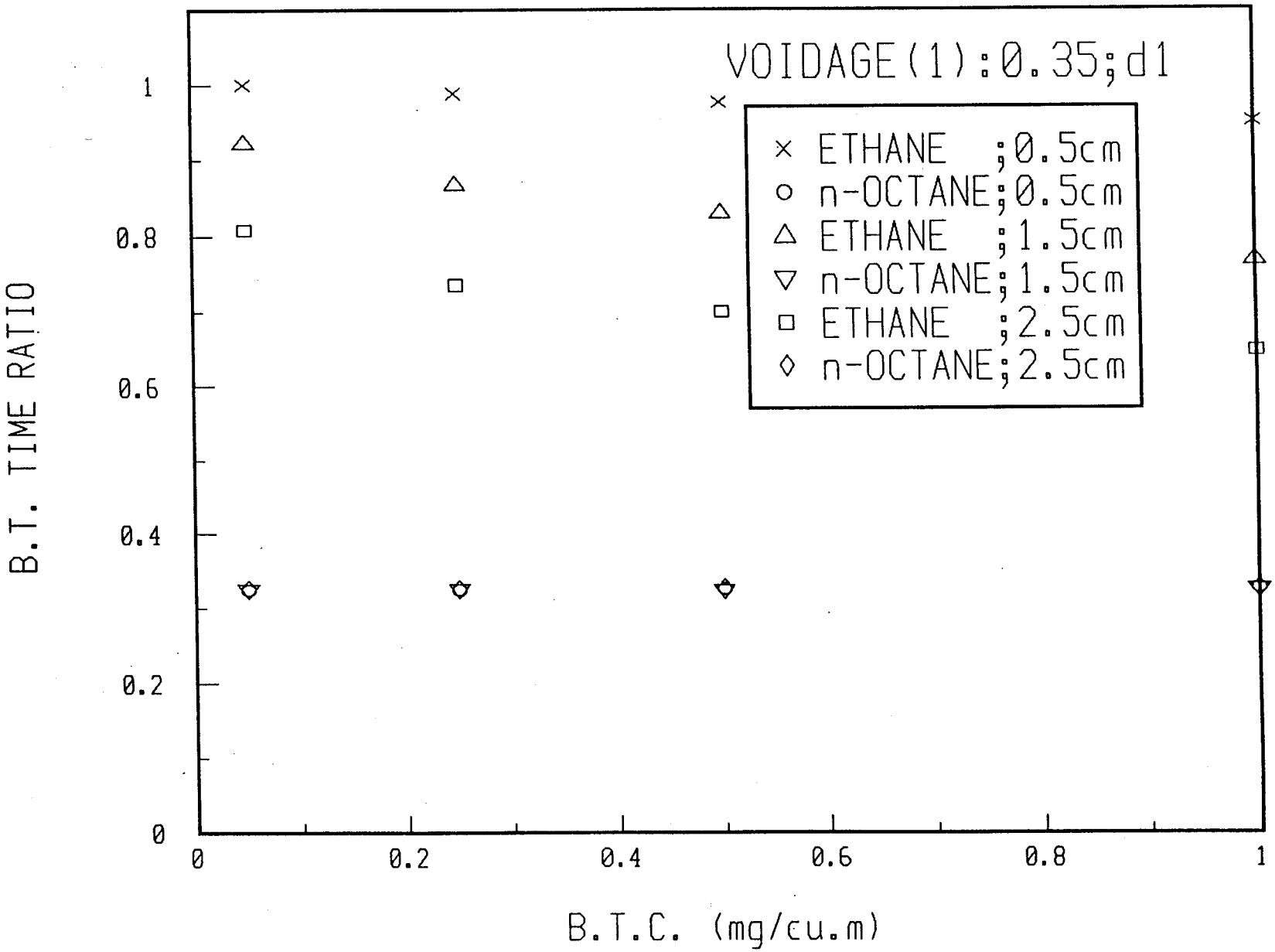


Fig.32: Ratio of breakthrough times of ethane and n-octane for an ASC carbon-filled C2 canister with a non-uniform bed

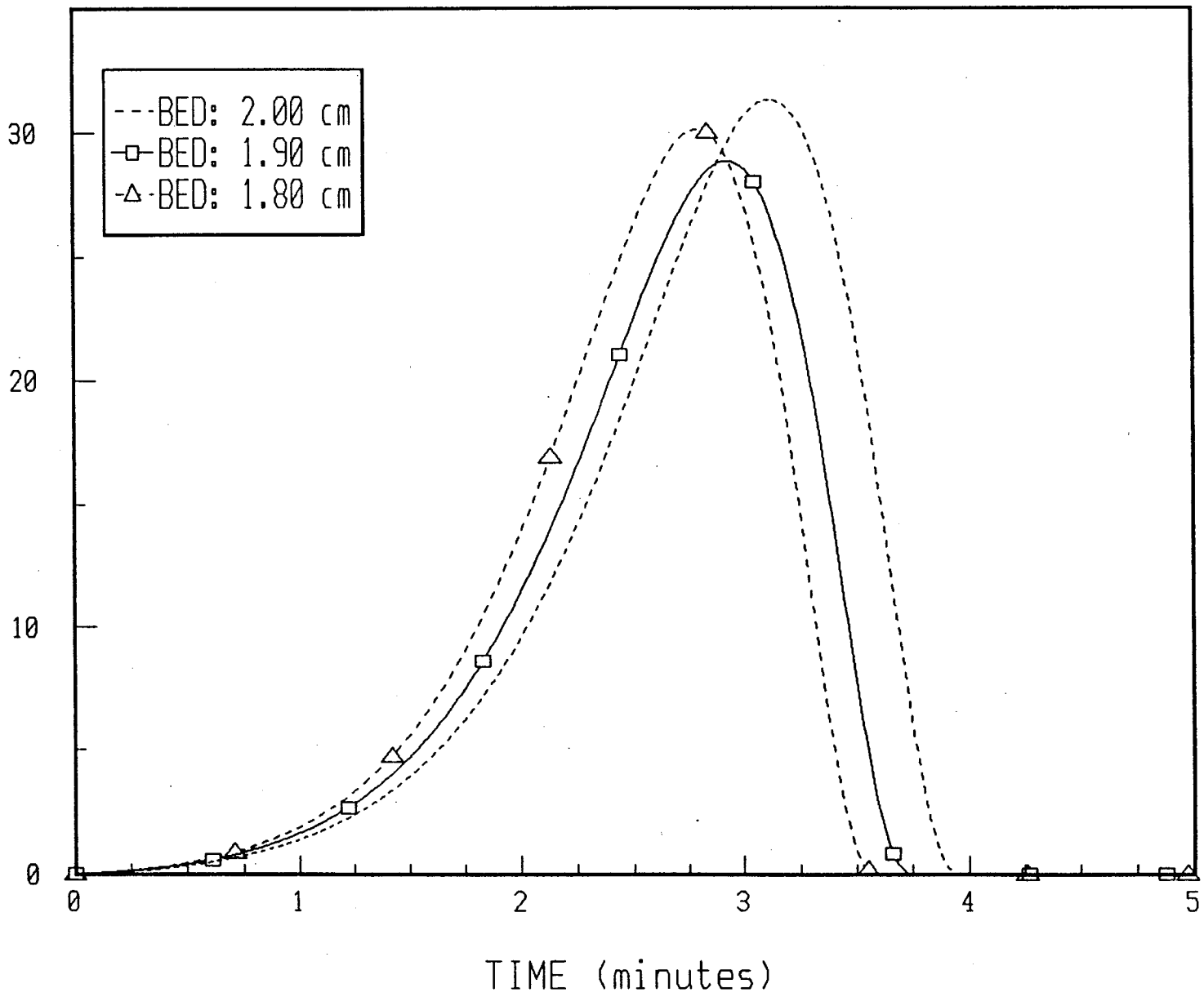


Fig.33: Dry ethane pulse response data for an ASC carbon-filled C2 canister : "Effect of bed depth"

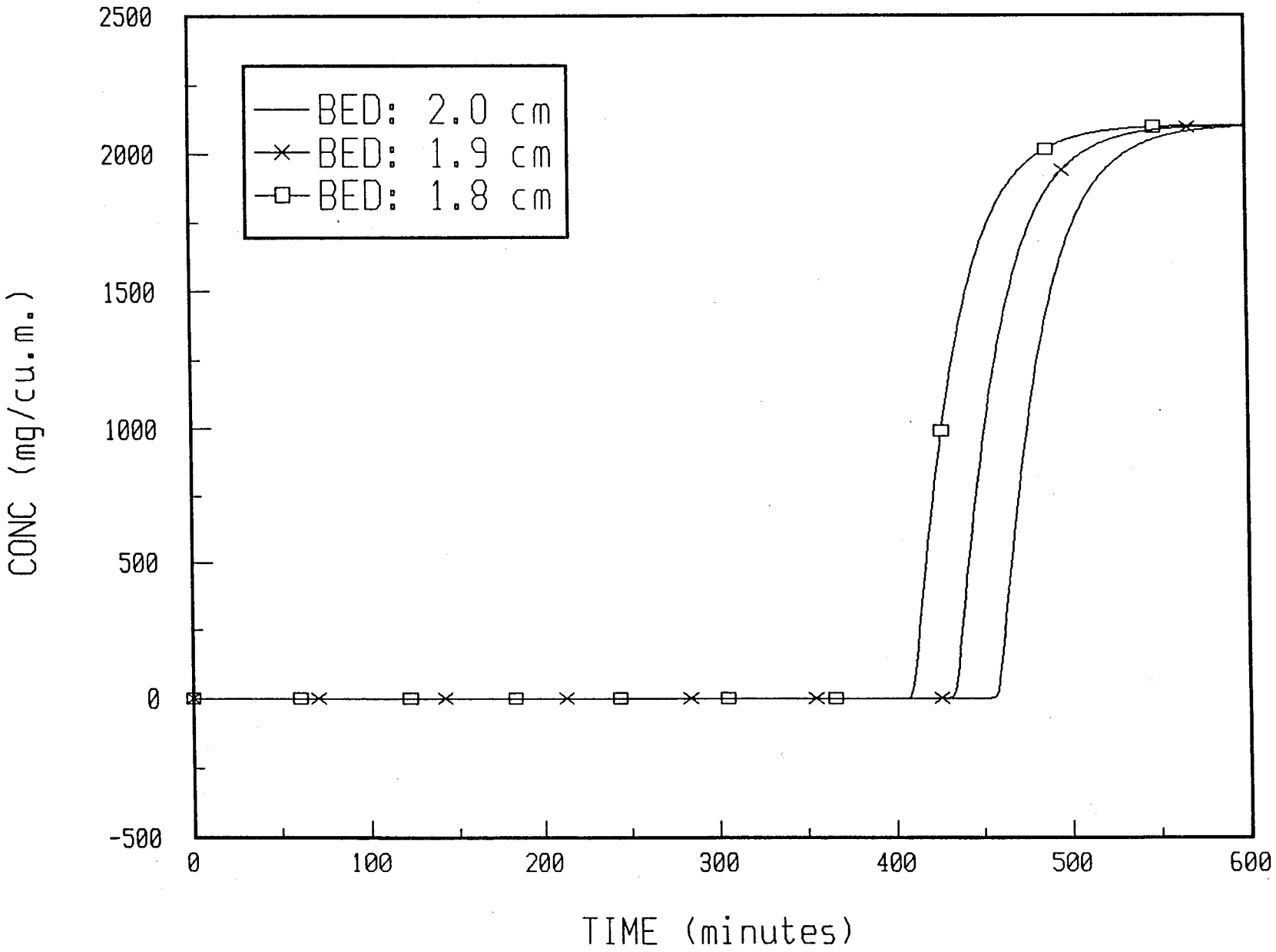


Fig.34: Dry n-octane pulse response data for an ASC carbon-filled C2 canister: "Effect of bed depth"

## APPENDIX A

### Velocity and Flow Distribution through an Uneven Bed

Calculation of Lengths and Volumes of Sections I, II and III :

As described in Section "Production Problems - Uneven Bed" the non-uniformity of the bed, generated due to improper filling of the activated carbon particles in the canister, is schematically represented in Fig. 11 as a bed made up of three sections of different lengths and volumes. The diameter of a nominal C2 canister (10.5 cm) is divided into three equal parts to give the following equations.

$$D_3 = \frac{D}{3} \tag{3}$$

$$D_2 = \frac{2D}{3} \tag{4}$$

$$D_1 = D \tag{5}$$

D represents the diameter of the normal, even C2 canister (10.5 cm) in cm. $D_1$, $D_2$ and $D_3$ represent the outer diameters, in cm, of the sections I, II and III respectively.

Representing the step size in the lengths of the sections II and III by $\Delta L$ cm, the lengths and volumes of the three sections can be represented by the following equations.

$$L_2 = L_1 + 2\Delta L \tag{6}$$

$$L_3 = L_2 + 2\Delta L = L_1 + 4\Delta L \tag{7}$$

$$V_1 = \frac{\pi}{4} [D_1^2 - D_2^2] L_1 = [\frac{\pi}{4} D^2] \frac{5}{9} L_1 \tag{8}$$

$$V_2 = \frac{\pi}{4}[D_2^2 - D_3^2]L_2 = [\frac{\pi}{4}D^2]\frac{3}{9}(L_1 + 2\Delta L) \quad (9)$$

$$V_3 = \frac{\pi}{4}[D_3^2]L_3 = [\frac{\pi}{4}D^2]\frac{1}{9}(L_1 + 4\Delta L) \quad (10)$$

$L_1$, $L_2$ and $L_3$ represent the lengths, in cm, of the three sections I, II and III respectively. $V_1$, $V_2$ and $V_3$ represent the volumes, in $cm^3$, of the three sections I, II and III respectively.

Assuming that the volume of the normal, even C2 canister (170 $cm^3$), represented by V, is kept constant, the volume balance equation can be written as follows.

$$V = V_1 + V_2 + V_3 \quad (11)$$

Equations 6-8 are substituted in the above equation to give the following.

$$V = [\frac{\pi}{4}D^2]\frac{5}{9}L_1 + [\frac{\pi}{4}D^2]\frac{3}{9}(L_1 + 2\Delta L) + [\frac{\pi}{4}D^2]\frac{1}{9}(L_1 + 4\Delta L) \quad (12)$$

Representing the cross-sectional area of the normal, even C2 canister as A ($= \pi D^2/4$), in $cm^2$, Equation 10 can be modified as follows.

$$V = AL_1 + \frac{10}{9}[A\Delta L] \quad (13)$$

which can be used to calculate $L_1$ as follows.

$$L_1 = \frac{V}{A} - \frac{10}{9}\Delta L \quad (14)$$

Equations 4 and 5 can then be used to calculate the values of $L_2$ and $L_3$ respectively.

The values of $L_1$, $L_2$, $L_3$, $V_1$, $V_2$ and $V_3$ were calculated from the equations given above for a normal, even C2 canister of volume 170 $cm^3$ and diameter 10.5 cm. The results are given in Table 3.

Calculation of Superficial Velocities and Flow Rates through Sections I, II and III :

The following assumptions were made in calculating the distribution of the superficial velocities and the volumetric flow rates through the three sections.

a. Ergun equation [7], used to calculate the pressure drop for the axial flow of a gas through a packed bed, can also be used to calculate the pressure drop for the axial flow of the carrier gas through the annular packed bed.

b. The pressure drop across each section is the same.

c. The properties of the carrier gas and the particle diameter of activated carbon are the same in each section.

d. The contribution of the pressure drop due to the turbulent flow of the carrier gas to the total pressure drop is negligible.

As per the Ergun's equation the pressure drop for the axial flow of the carrier gas is given by the following equation.

$$\Delta P = 150 \frac{(1-\epsilon)^2}{\epsilon^3} \frac{\mu L v}{D_p^2} + 1.75 \frac{(1-\epsilon)}{\epsilon^3} \frac{\rho L v^2}{D_p} \qquad (15)$$

where $\Delta L$ represents the pressure drop for the axial flow of a gas, of density $\rho$, in $g/cm^3$, and viscosity $\mu$, in g/cm-s, across a bed of length L cm. The superficial velocity of the gas is denoted by v; and $D_p$ and $\epsilon$ represent the diameter of the solid particles, in cm, and the voidage of the bed respectively. Neglecting the contribution of the second term in Equation 13, the pressure drop for the axial flow of the carrier gas through the sections I, II and III can be written as follows.

$$\Delta P = kL_1 v_{pb1} = kL_2 v_{pb2} = kL_3 v_{pb3} \qquad (16)$$

where k is a constant.

The mass balance equation for the total volumetric flow rate Q of the carrier gas through the canister gives the following.

$$Q = A_1 v_{pb1} + A_2 v_{pb2} + A_3 v_{pb3} \qquad (17)$$

where $A_1$, $A_2$ and $A_3$ represent the cross-sectional areas of the sections I, II and III, in $cm^2$, respectively. The procedure to calculate $A_1$, $A_2$ and $A_3$ has already been described in the section above. On substituting Equation 14 in the above equation and simplifying the resulting equation we get the following equation

$$v_{pb1} = \frac{Q}{A_1 + \frac{L_1}{L_2} A_2 + \frac{L_1}{L_3} A_3} \tag{18}$$

which can be used to calculate $v_{pb1}$. $v_{pb2}$ and $v_{pb3}$ can be calculated using Equation 15. The volumetric flow rates, $Q_1$, $Q_2$ and $Q_3$, through sections I, II and III can be calculated from the following equations.

$$Q_1 = A_1 v_{pb1} \tag{19}$$

$$Q_2 = A_2 v_{pb2} \tag{20}$$

$$Q_3 = A_3 v_{pb3} \tag{21}$$

The values of the superficial velocity and the volumetric flow rates through the sections I, II and III for the total flow rate of 500 $cm^3/s$ of the carrier gas through a normal, even bed of diameter 10.5 cm for different values of $\Delta L$ are given in Section "Production Problems - Uneven Bed".

## APPENDIX B

### Velocity and Flow Distribution through a Non-uniform Bed

Calculation of the Voidage in Section II :

As described in Section "Production Problem - Channels or Voids in the Bed", the non-uniformity of the bed, due to the presence of sections of different voidages in the bed, is schematically represented in Fig. 23. The bed is assumed to be made up of two sections, I and II, of different diameters and voidages. The first step is to calculate the voidage of section II when the diameter and voidage of the section I, the size of the normal, uniform bed and the amount of the activated carbon in the normal bed are given. Assuming that the apparent density of the activated carbon particles, $\rho_{app}$ in g/cm$^3$, remains constant, the bulk density of the particles in section I is given by the following equation.

$$\rho_{b1} = (1-\epsilon_1)\,\rho_{app} \qquad (1)$$

where $\rho_{b1}$ and $\epsilon_1$ represent the bulk density, in g/cm$^3$, and the voidage in section I. The amount of activated carbon in the section I, denoted as $M_1$ in g, can then be calculated from

$$M_1 = \rho_{b1}\left[\frac{\pi D_1^2}{4} L\right] = (1-\epsilon_1)\,\rho_{app} V \frac{D_1^2}{D^2} \qquad (2)$$

where D, L and V represent the diameter and length, in cm, and volume, in cm$^3$, of the normal, uniform C2 canister respectively. $D_1$ represents the diameter, in cm, of the section I. The amount of the activated carbon in the section II, denoted as $M_2$ in g, can be calculated as the difference in the amounts of the carbon in the total bed and the section I. It is, therefore, given by the following equation.

$$M_2 = \rho_b V - \left[(1-\epsilon_1)\,\rho_{app} V \frac{D_1^2}{D^2}\right] \qquad (3)$$

where $\rho_b$, the bulk density of the normal, uniform bed in g/cm$^3$, is given by

$$\rho_b = (1-\epsilon)\,\rho_{app} \qquad (4)$$

where $\epsilon$ represents the voidage of the normal, uniform bed in the C2 canister. The bulk density of the activated carbon in the section II, denoted as $\rho_{b2}$ in $g/cm^3$, can be calculated from its volume and the amount of carbon present as follows.

$$\rho_{b2} = \frac{V\rho_{app}\left[(1-\epsilon) - (1-\epsilon_1)\frac{D_1^2}{D^2}\right]}{L\left[\frac{\pi}{4}(D^2 - D_1^2)\right]} \qquad (5)$$

The voidage in the section II, denoted as $\epsilon_2$, can then be calculated from $\rho_2$ and $\rho_{app}$ as follows.

$$\epsilon_2 = 1 - \frac{\rho_{b2}}{\rho_{app}} \qquad (6)$$

which on substitution from Equation 5 gives

$$\epsilon_2 = 1 - \frac{(1-\epsilon) - (1-\epsilon_1)\frac{D_1^2}{D^2}}{1 - \frac{D_1^2}{D^2}} \qquad (7)$$

Calculation of the Distribution of the Superficial Velocity and the Volumetric Flow Rates :

The flow of carrier gas through the arrangement of the two sections, as schematically shown in Fig. 23, can be considered equivalent to the flow of a gas through a system of two packed beds in parallel. Assuming the validity of Ergun's equation to predict the pressure drop for the flow across the two sections, equality of properties such as $\mu$, $\rho$ and $D_p$ for both sections and the equality of pressure drop across them, the following equation can be written.

$$k_3 v_{pb1} + k_4 v_{pb1}^2 = k_5 v_{pb2} + k_6 v_{pb2}^2 \qquad (8)$$

where $v_{pb1}$ and $v_{pb2}$ represent the superficial velocities, in cm/s, of the carrier gas through the sections I and II respectively; and

$$k_3 = 150\frac{(1-\epsilon_1)^2}{\epsilon_1^3}\frac{\mu L}{D_p^2}$$

$$k_4 = 1.75 \frac{(1-\epsilon_1)}{\epsilon_1^3} \frac{\rho L}{D_p}$$

$$k_5 = 150 \frac{(1-\epsilon_2)^2}{\epsilon_2^3} \frac{\mu L}{D_p^2}$$

$$k_6 = 1.75 \frac{(1-\epsilon_2)}{\epsilon_2^3} \frac{\rho L}{D_p}$$

where L represents the length of the bed in cm; and $\epsilon_1$ and $\epsilon_2$ represent the voidages in sections I and II respectively.

The mass balance equation for the flow of the carrier gas across the canister can be written as follows.

$$A_1 V_{pb1} + A_2 V_{pb2} = AV \qquad (9)$$

where A, $A_1$ and $A_2$ represent the total cross-sectional area of the C2 canister and the cross-sectional areas of the sections I and II in $cm^2$ respectively. The superficial velocity of the carrier gas through the normal, uniform C2 canister is denoted by v in cm/s. Obviously

$$A = A_1 + A_2 \qquad (10)$$

which can be substituted in Equation 9 and simplified to give the following equation.

$$V_{pb1} = \frac{VA}{A_1} - \left(\frac{A}{A_1} - 1\right) V_{pb2} \qquad (11)$$

The value of v can be calculated from the total volumetric flow rate of the carrier gas (500 $cm^3/s$) and the diameter of the C2 canister (10.5 cm).

The superficial velocities $v_{pb1}$ and $v_{pb2}$ can be calculated by solving simultaneous Equations 1 and 11. The substitution of Equation 11 in Equation 1 results in a quadratic equation with only one unknown variable as given below.

$$k_7 v_{pb2}^2 + k_8 v_{pb2} + k_9 = 0 \quad (12)$$

where

$$k_7 = k_4 k_2^2 - k_6$$

$$k_8 = k_3 k_2 + 2 k_4 k_1 k_2 - k_5$$

$$k_9 = k_3 k_1 + k_4 k_1^2$$

$$k_1 = \frac{vA}{A_1}$$

$$k_2 = 1 - \frac{A}{A_1}$$

Knowing the values of the superficial velocities through the sections I and II the volumetric flow rates can be calculated from the following equations.

$$Q_1 = \left(\frac{\pi}{4} D_1^2\right) v_{pb1} \quad (13)$$

$$Q_2 = \left[\frac{\pi}{4} (D^2 - D_1^2)\right] v_{pb2} \quad (14)$$

where $Q_1$ and $Q_2$ represent the volumetric flow rates, in $cm^3/s$, of the carrier gas through the sections I and II respectively. $D_1$ and D represent the diameters, in cm, of the section I and the normal, uniform C2 canister respectively.

## DOCUMENT CONTROL DATA

(Security classification of title, body of abstract and indexing annotation must be entered when the overall document is classified)

1. ORIGINATOR (the name and address of the organization preparing the document. Organizations for whom the document was prepared, e.g. Establishment sponsoring a contractor's report, or tasking agency, are entered in section 8.)

DEFENCE RESEARCH ESTABLISHMENT OTTAWA
National Defence
Ottawa, Ontario K1A 0Z4

2. SECURITY CLASSIFICATION (overall security classification of the document including special warning terms if applicable)

UNCLASSIFIED

3. TITLE (the complete document title as indicated on the title page. Its classification should be indicated by the appropriate abbreviation (S,C or U) in parentheses after the title.)

THEORETICAL ASSESSMENT OF A NON-DESTRUCTIVE ETHANE GAS TEST FOR PRODUCTION CONTROL OF MILITARY CANISTERS (U)

4. AUTHORS (Last name, first name, middle initial)

NARAYAN, Shankar B. and HARRISON, Brian H.

5. DATE OF PUBLICATION (month and year of publication of document)

JANUARY 1994

6a. NO. OF PAGES (total containing information. Include Annexes, Appendices, etc.)

85

6b. NO. OF REFS (total cited in document)

7

7. DESCRIPTIVE NOTES (the category of the document, e.g. technical report, technical note or memorandum. If appropriate, enter the type of report, e.g. interim, progress, summary, annual or final. Give the inclusive dates when a specific reporting period is covered.)

REPORT

8. SPONSORING ACTIVITY (the name of the department project office or laboratory sponsoring the research and development. Include the address.)

DEFENCE RESEARCH ESTABLISHMENT OTTAWA
National Defence
Ottawa, Ontario K1A 0Z4

9a. PROJECT OR GRANT NO. (if appropriate, the applicable research and development project or grant number under which the document was written. Please specify whether project or grant)

051LB

9b. CONTRACT NO. (if appropriate, the applicable number under which the document was written)

10a. ORIGINATOR'S DOCUMENT NUMBER (the official document number by which the document is identified by the originating activity. This number must be unique to this document.)

DREO REPORT 1231

10b. OTHER DOCUMENT NOS. (Any other numbers which may be assigned this document either by the originator or by the sponsor)

11. DOCUMENT AVAILABILITY (any limitations on further dissemination of the document, other than those imposed by security classification)

(X) Unlimited distribution
( ) Distribution limited to defence departments and defence contractors; further distribution only as approved
( ) Distribution limited to defence departments and Canadian defence contractors; further distribution only as approved
( ) Distribution limited to government departments and agencies; further distribution only as approved
( ) Distribution limited to defence departments; further distribution only as approved
( ) Other (please specify):

12. DOCUMENT ANNOUNCEMENT (any limitation to the bibliographic announcement of this document. This will normally correspond to the Document Availabilty (11). However, where further distribution (beyond the audience specified in 11) is possible, a wider announcement audience may be selected.)

UNCLASSIFIED

SECURITY CLASSIFICATION OF FORM

13. ABSTRACT ( a brief and factual summary of the document. It may also appear elsewhere in the body of the document itself. It is highly desirable that the abstract of classified documents be unclassified. Each paragraph of the abstract shall begin with an indication of the security classification of the information in the paragraph (unless the document itself is unclassified) represented as (S), (C), or (U). It is not necessary to include here abstracts in both offical languages unless the text is bilingual).

A non-destructive vapour test, involving an ethane pulse challenge, that measures the integrity of the activated carbon bed in military canisters is presently under development at the Defence Research Establishment Ottawa. The effectiveness of the test has been theoretically assessed in this report by modelling the effect of the presence of defects in the carbon bed on its performance. The model has been modified to successfully predict the adsorption behaviour of a dry ethane pulse- or a dry n-octane step-challenge on uneven, non-uniform or short beds. It has been found that the behaviour for the non-uniform beds is different from uneven beds and that care must be taken in selecting the breakthrough concentration for the ethane test. Whilst the sensitivity of the ethane pulse test to identify the defects is not as good as the n-octane step test, the time required for the ethane test is much shorter. It has been shown that this reduced sensitivity is more than compensated for by the ability to test 100% of the canisters with the ethane pulse challenge test.

14. KEYWORDS, DESCRIPTORS or IDENTIFIERS (technically meaningful terms or short phrases that characterize a document and could be helpful in cataloguing the document. They should be selected so that no security classification is required. Identifiers, such as equipment model designation, trade name, military project code name, geographic location may also be included. If possible keywords should be selected from a published thesaurus. e.g. Thesaurus of Engineering and Scientific Terms (TEST) and that thesaurus-identified. If it is not possible to select indexing terms which are Unclassified, the classification of each should be indicated as with the title.)

ACTIVATED CARBON
CANISTERS
NBC DEFENCE
NON-DESTRUCTIVE GAS TEST